CANADIAN THESIS

THESES CANADIENNES

CARMICHAEL, JONATHAN BLOIS
LOCALIZATION OF CORE RNAI
PROTEINS AND THEIR ROLES IN ...

ISBN 0-494-08617-3
NR-08617

1 of 3

University of Alberta

Localization of core RNAi proteins and their roles in cell cycle regulation

by

Jonathan Blois Carmichael ©

A thesis submitted to the Faculty of Graduate Studies and Research in partial fulfillment of the

requirements for the degree of *Doctor of Philosophy*

Department of *Cell Biology*

Edmonton, Alberta
Fall 2005

Library and
Archives Canada

Published Heritage
Branch

395 Wellington Street
Ottawa ON K1A 0N4
Canada

Bibliothèque et
Archives Canada

Direction du
Patrimoine de l'édition

395, rue Wellington
Ottawa ON K1A 0N4
Canada

0-494-08617-3

Your file Votre référence
ISBN:
Our file Notre reference
ISBN:

NOTICE:
The author has granted a non-exclusive license allowing Library and Archives Canada to reproduce, publish, archive, preserve, conserve, communicate to the public by telecommunication or on the Internet, loan, distribute and sell theses worldwide, for commercial or non-commercial purposes, in microform, paper, electronic and/or any other formats.

The author retains copyright ownership and moral rights in this thesis. Neither the thesis nor substantial extracts from it may be printed or otherwise reproduced without the author's permission.

AVIS:
L'auteur a accordé une licence non exclusive permettant à la Bibliothèque et Archives Canada de reproduire, publier, archiver, sauvegarder, conserver, transmettre au public par télécommunication ou par l'Internet, prêter, distribuer et vendre des thèses partout dans le monde, à des fins commerciales ou autres, sur support microforme, papier, électronique et/ou autres formats.

L'auteur conserve la propriété du droit d'auteur et des droits moraux qui protège cette thèse. Ni la thèse ni des extraits substantiels de celle-ci ne doivent être imprimés ou autrement reproduits sans son autorisation.

In compliance with the Canadian Privacy Act some supporting forms may have been removed from this thesis.

While these forms may be included in the document page count, their removal does not represent any loss of content from the thesis.

Conformément à la loi canadienne sur la protection de la vie privée, quelques formulaires secondaires ont été enlevés de cette thèse.

Bien que ces formulaires aient inclus dans la pagination, il n'y aura aucun contenu manquant.

Canada

ABSTRACT

Ago1, Dcr1 and Rdp1 are the core components of the RNA interference machinery in the fission yeast, *Schizosaccaromyces pombe*. In addition to their functions in two distinct RNAi-related pathways that direct homology-dependent degradation of mRNA and chromatin modification, Ago1 and Dcr1 are required for regulated tyrosine-15 phosphorylation of Cdc2 when encountering genotoxic insults. My results suggest that Cdc2 phosphorylation regulated by Ago1 and Dcr1 is independent of small interfering RNAs. In addition, hAgo2, a human homologue associated with the endonuclease activity of RISC, compensates for the loss of *ago1*$^{+}$ function in *S. pombe* suggesting that PPD proteins may be important for regulation of cell cycle events in humans.

Functioning of the RNAi apparatus in these divergent pathways presumably requires differential localization of Ago1, Dcr1 and Rdp1. The localizations of chimeric HA- and GFP-Ago1, Dcr1 and Rdp1 were studied by fluorescence and immunoelectron microscopy. The results indicate that Rdp1 is predominantly localized to the nucleus where it is thought to function in siRNA generation. In contrast, Ago1 and Dcr1 are predominantly associated with large cytoplasmic complexes. However in the absence of Ago1, or when cells are arrested in S- or M-phases, nuclear localization of Dcr1 was evident. In addition, conditions that arrested cell cycle progression in G_1 resulted in nuclear accumulation of both Ago1 and Dcr1. These results suggest that the roles Ago1 and Dcr1 perform in genome stability require dynamic localizations of these proteins.

ACKNOWLEDGEMENTS

I would like to express my gratitude to Dr. Tom C. Hobman for his patience, understanding, friendship and of course guidance and mentoring in all things pertaining to life within and without of the academic arena. It has been a taxing time and I am very certain that your encouragement has been the deciding factor in my ability to complete the first stage of the job, Thank you Tom.

Dr. Henry Parker, you will never know how important our early morning discussions about science and life were to my ability to finish. From your critical reading of manuscripts to timely advice, your input was always sought.

We have had a tremendous turnover of students in the lab during my time here and it seems that everyone has added a very integral and needed personality to our group dynamic. I would like to thank the past and present people of the Hobman Lab, Dr. Tracey Hunt, Dr. John Law, Dr. Nasser Tobaz, Cezar, Jason, Kasia, Carolina, Justin, Matt, Ahn, Eileen, Vilaria, Darren and Margaret for the excellent atmosphere they created for work and at times, play.

I would like to thank my committee members, Drs. Richard Wozniak and Paul Melançon, for their ideas and criticisms. Without your support and 'small chats' I would not be at this point today. In addition thanks to Dr Paul Young and Dr. Alan Underhill for the time spent on my defense committee.

To my mother and father, who through their love and guidance instilled in me the importance of hard work and honesty, tempered with humor. Finally to my friends who never lost step with me through my time in Edmonton though the road has been rocky at times.

TABLE OF CONTENTS

CHAPTER 1: INTRODUCTION 1

1-1 Overview 2

1-2 Core RNAi proteins 5

- 1-2-1 PPD proteins 5
  - 1-2-1-1 PPD protein superfamily 5
  - 1-2-1-2 PPD proteins and development 7
- 1-2-2 Dicer family of proteins 10
  - 1-2-2-1 RNase III enzyme family 10
  - 1-2-2-2 Functional diversification and characteristics of Dicer proteins 10
- 1-2-3 RNA-dependent RNA polymerase family 12

1-3 RNA interference 13

- 1-3-1 Interactions between Dicer and dsRNA binding proteins 13
- 1-3-2 Protein components of RISC 15
- 1-3-3 PPD proteins in siRNA and miRNA mediated pathways 17

1-4 RNA-induced initiation of transcriptional gene-silencing 19

- 1-4-1 RITS-dependent heterochromatin formation 19

1-5 *S. pombe* cell cycle regulation 22

- 1-5-1 Cell cycle regulatory pathway 22
- 1-5-2 DNA replication and DNA damage checkpoints 25
  - 1-5-2-1 Histone methylation in DNA damage responses 26
  - 1-5-2-2 DNA damage response proteins and signal transduction 27

1-5-2-3 Cell cycle regulators as targets of DNA damage checkpoints 27

1-5-3 Core RNAi proteins and the cell cycle 29

1-5-4 Stress-activated protein kinase family 31

1-5-4-1SAPK regulatory proteins 31

1-5-4-2 SAPKs and cell cycle regulation 33

1-6 Objectives 36

CHAPTER 2: MATERIALS AND METHODS **38**

2-1 Reagents and materials 39

2-2 Commonly used buffers, media and drugs 41

2-3 Antibodies 42

2-4 Oligonucleotides 42

2-5 Plasmids 43

2-6 *Schizosaccharomyces pombe* strains used in this study 44

2-7 DNA analysis and modification 44

2-7-1 Isolation of plasmid DNA from *E. coli* 44

2-7-2 Isolation of yeast genomic DNA 45

2-7-3 Isolation of plasmid DNA from yeast 46

2-7-4 Polymerase chain reaction 46

2-7-5 Restriction endonuclease digestion 47

2-7-6 Dephosphorylation of 5', 3' or blunt ended linearized vectors 47

2-7-7 Filling-in of 5' overhangs 47

2-7-8 Ligation of DNA 47

2-8 Transformation with plasmid DNA 48

2-8-1 Transformation of *E. coli* 48

2-8-1-1 Transformation of chemical competent *E. coli* 48

2-8-1-1 Transformation of electrocompetent *E. coli* 49

2-8-2 Transformation of *S. pombe* strains 49

2-8-2-1 Large-scale transformation 49

2-8-2-2 Small-scale ttransformations 50

2-9 Isolation of *S. pombe* RNA 50

2-10 Reverse transcriptase-polymerase chain reaction (RTPCR) 51

2-11 Agarose gel electrophoresis 52

2-11-1 DNA agarose gel electrophoresis 52

2-11-2 RNA agarose gel electrophoresis 52

2-12 Southern blot analyses 52

2-12-1 Transfer of DNA fragments to nitrocellulose membranes 52

2-12-2 ^{32}P-labelled probe production 53

2-12-3 Southern blot hybridization 53

2-13 Construction of cDNAs encoding tagged RNAi effector proteins 54

2-13-1 GFP-Ago1 construction 54

2-13-2 EGFP-Rdp1 construction 54

2-13-3 Dcr1-EGFP construction 55

2-13-4 HA-Ago1 and HA-Rdp1 construction 55

2-14 Automated DNA sequencing 56

2-15 Protein gel electrophoresis and detection 56

- 2-15-1 Sodium dodecyl-sulphate gel electrophoresis (SDS-PAGE) 56
- 2-15-2 Western blot analyses 56
  - 2-15-2-1 Protein transfer 56
  - 2-15-2-2 Immunoblotting 57
- 2-15-3 Protein preparations 57
  - 2-15-3-1 Whole cell extracts 57
  - 2-15-3-2 Subcellular fractionation 58
- 2-15-4 Immunoprecipitation assay 58
- 2-16 Microscopy 59
- 2-16-1 Fluorescence microscopy 59
  - 2-16-1-1 Live cell imaging 59
  - 2-16-1-2 Immunofluorescence microscopy 60
- 2-16-2 Differential interference contrast microscopy 60
- 2-16-3 Immunoelectron microscopy 61

2-17 Flow cytometry 62

2-18 Yeast techniques 62

- 2-18-1 One-step gene replacement 62
- 2-18-2 Mating assays 63
- 2-18-3 Tetrad analysis 63
- 2-18-4 Determination of growth rates 63
- 2-18-5 Functionality assay 64
- 2-18-6 Septation analyses 64

2-18-7 UV irradiation survival assay 63

2-19 Drug-induced cell cycle arrest 65

2-19-1 Survival assay 65

2-19-2 Cdc2 phosphorylation analysis 65

CHAPTER 3: Ago1 and Dcr1 RNAi-independent cell cycle regulation **66**

3-1 Overview 67

3-2 *ago1*$^+$ and *dcr1*$^+$ null mutants are delayed in cytokinesis 67

3-3 *ago1*$^+$ and *dcr1*$^+$, but not *rdp1*$^+$ are required for G_1-arrest and mating in response to nitrogen starvation 74

3-4 *ago1*$^+$ and *dcr1*$^+$ null mutants fail to enact and/or maintain the S-M checkpoint 77

3-5 *ago1*$^+$ and *dcr1*$^+$ null mutants are defective for the DNA damage checkpoint 87

3-6 Ago1 may function downstream of Dcr1 to regulate cell cycle events 90

3-7 Ago1 and Dcr1 functionally diverge from Rdp1 and RNAi to regulate cell cycle events 93

CHAPTER 4: Localizations and interactions of core RNAi proteins **98**

4-1 Overview 99

4-2 Ago1 and Dcr1 associate with large cytoplasmic complexes 100

4-3 Interactions among RNAi effector proteins 103

4-4 Analyses of RNAi effector proteins by fluorescence microscopy 109

4-5 Localization of HA-tagged Ago1 and Dcr1 chimeras by immunoelectron microscopy 115

4-6 Ago1 and Dcr1 are not excluded from the nucleus in G_1-arrested cells 118

4-7 Localization of Ago1 and Dcr1 in S- and M-phase arrested cells 121

4-8 Ago1 is required for cytoplasmic retention of Dcr1 124

4-9 Conclusion 124

CHAPTER 5: DISCUSSION **133**

5-1 Overview 134

5-2 Ago1 and Dcr1 function to regulate cell cycle events 136

- 5-2-1 Ago1 and Dcr1 are required to couple completion of mitosis to cytokinesis 136
- 5-2-2 Ago1 and Dcr1 function independently of Rdp1 and the RNAi pathway for conjugation in a nitrogen-dependent manner 137
- 5-2-3 Ago1 and Dcr1 are required for enactment of replication and DNA damage checkpoints through regulated tyrosine-15 phosphorylation of Cdc2 in an siRNA-independent manner 140
- 5-2-4 Convergence of Ago1 and Dcr1 RNAi-independent functions with the stress-activated MAP kinase pathway 142

5-3 Interactions between Ago1, Dcr1 and Rdp1 146

5-4 Localizations of Ago1, Dcr1 and Rdp1 148

- 5-4-1 Rdp1 is largely confined to nuclei in *S. pombe* 148
- 5-4-2 Ago1 is largely confined to the cytoplasm in *S. pombe* 150

5-4-3 Dcr1 cytoplasmic retention is cell cycle-regulated and Ago1-dependent 154

5-4-4 The RNAi pathway converges with cell cycle regulation 156

5-5 Concluding Remarks and future directions 150

REFERENCES **162**

LIST OF TABLES

Table 2.1 Reagents 39

Table 2.2 Multi-component systems 40

Table 2.3 DNA modifying enzymes 40

Table 2.4 Radiochemicals 40

Table 2.5 Detection systems 40

Table 2.6 Molecular size standards 40

Table 2.7 Commonly used buffers and solutions 41

Table 2.8 Yeast media 41

Table 2.9 Drugs and antibiotics 41

Table 2.10 Primary antibodies 42

Table 2.11 Secondary antibodies 42

Table 2.12 Primers used in this study 42

Table 2.13 Plasmids used in this study 43

Table 2.14 Strains 44

LIST OF FIGURES

Figure 1-1. Overview of RNAi-dependent gene-silencing pathways 4

Figure 1-2. Basic structures of PAZ PIWI domain (PPD), Dicer and RdRP proteins 6

Figure 1-3. Schematic of the mitotic cell cycle and proteins involved in DNA checkpoint arrest 24

Figure 1-4. Schematic representation of the SAPK pathway in *S. pombe* 35

Figure 3-1. Deletion of the *ago1*$^+$ open reading frame 70

Figure 3-2. Morphology and growth of Δ*ago1* cells 73

Figure 3-3. ***ago1***$^+$ and *dcr1*$^+$ are both required for normal cytokinesis 76

Figure 3-4. ***ago1***$^+$ and *dcr1*$^+$ mutants are defective for G_1-arrest and mating following nitrogen limitation 79 –80

Figure 3-5. ***ago1***$^+$ null mutants fail to activate the S-M DNA replication checkpoint 83

Figure 3-6. ***ago1***$^+$ and *dcr1*$^+$ are both required for hyper-phosphorylation of Cdc2 and enactment of the replication checkpoint 86

Figure 3-7. ***ago1***$^+$ and *dcr1*$^+$ are both required for enactment of the DNA damage checkpoint 89

Figure 3-8. ***ago1***$^+$ functions downstream of *dcr1*$^+$ to regulate cell cycle events 92

Figure 3-9. Model for RNAi and RNAi-independent functions of Ago1 and Dcr1 97

Figure 4-1. Ago1 and Dcr1 co-purify with large cytoplasmic structures 102

Figure 4-2. Construction of functional epitope-tagged RNAi effector proteins 105

Figure 4-3. Assays to address the functionality of GFP- and HA-fusion proteins 108

Figure 4-4. Binding interactions among RNAi proteins 111

Figure 4-5. Localization of GFP-tagged core RNAi proteins 114

Figure 4-6. Localization of HA-tagged core RNAi proteins 117

Figure 4-7. Ago1 and Dcr1 are associated with large cytoplasmic complexes 120

Figure 4-8. Localization of GFP-Ago1 and Dcr1-GFP following nitrogen-starvation 123

Figure 4-9. Distribution of core RNAi proteins subjected to S- and M-phase arrest 126-128

Figure 4-10. Ago1-dependent localization of Dcr1 131

Figure 5-1 Convergence of the RNAi, SAPK and cell cycle regulatory pathways in the maintenance of genome integrity 145

Figure 5-2 RNAi-dependent and independent processes are mediated by the localizations of the core RNAi proteins 159

CHAPTER 1

INTRODUCTION

Portions of this chapter have been published in " Katarzyna Jaronczyk, Jon B. Carmichael and Tom C. Hobman (2005). Exploring the functions of RNA interference pathway proteins: some functions are more RISCy than others? Biochem. J., 387, 561-571".

1-1 Overview

Control of eukaryotic gene expression at the transcriptional and post-transcriptional level is in part mediated by a process called RNA interference (RNAi) (Hannon, 2002). In its original context, RNAi is thought to have evolved as a genome immune system that functioned to maintain the integrity of eukaryotic genomes. For example, in fungi and plants, components of the RNAi apparatus are required for transposon silencing, resistance to viruses and maintenance of chromosome stability (Liu et al., 2004b; Mochizuki et al., 2002; Mochizuki and Gorovsky, 2004; Nolan et al., 2005).

The canonical RNAi pathway has been divided into two stages: initiation and effector (Figure 1-1). The initiation stage involves the recognition and processing of long dsRNA into small interfering RNAs (siRNAs) of 21-26 base pairs (Hamilton et al., 2002; Lagos-Quintana et al., 2001; Lau et al., 2001; Lee and Ambros, 2001), or the processing of endogenously encoded hairpin precursor RNA transcripts into micro RNAs (miRNAs) (Park et al., 2002; Reinhart et al., 2002). Cleavage of dsRNA into si/miRNAs is mediated by the RNase III enzyme Dicer (Bernstein et al., 2001) (Figure 1-2). The effector stage requires the transfer of the si/miRNAs to ribonucleoprotein complexes known as RNA induced silencing complexes (RISC) (Hammond et al., 2000). Proteins containing both PAZ and PIWI domains (PPD) (Caudy et al., 2002; Hammond et al., 2001; Hutvagner and Zamore, 2002; Mourelatos et al., 2002) are essential components of RISC and, in the context of the complex, are guided by the si/miRNAs to specific mRNA targets or genomic loci. Gene-silencing

Figure 1-1. Overview of RNAi-dependent gene-silencing pathways. Briefly, exogenous or endogenous dsRNA is detected and cleaved by Dicer into siRNAs or miRNAs, respectively. It is unknown if siRNA processing occurs exclusively in the cytoplasm. The si/miRNA is incorporated into a RISC or RITS complex, which is then targeted to homologous mRNA or DNA in the cytoplasm and/or nucleus. RNA-directed RNA polymerase complex (RDRC) activity is required for RNAi in fungi, plants and nematodes but it is not known if amplification of dsRNA used in RISC-dependent mRNA degradation occurs in the cytoplasm or requires export of dsRNA to cytoplasmic Dicer (Adapted from Hannon, 2002).

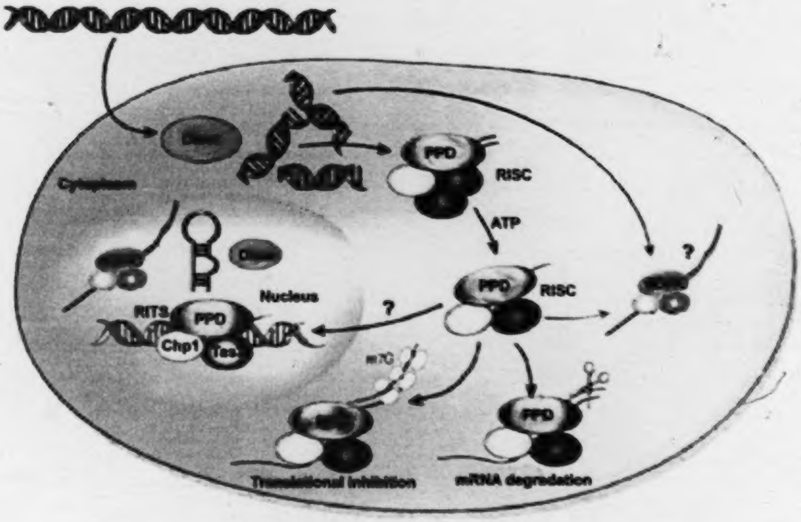
Cytoplasm
PPD
RISC
ATP
?
PPD
RISC
?
Nucleus
RITS
PPD
Chp1
Tas
?
m7G
PPD
Translational inhibition
mRNA degradation

by RISC is accomplished by homology-dependent mRNA degradation (Hamilton and Baulcombe, 1999; Tuschl et al., 1999; Zamore et al., 2000) or translational repression (Grishok et al., 2001). RNAi-mediated transcriptional gene-silencing (TGS) requires a RISC-like PPD-containing complex called RNA induced initiation of transcriptional silencing (RITS) complex (Ekwall, 2004; Hall et al., 2002; Pal-Bhadra et al., 2002; Volpe et al., 2002). Another core component of the RNAi pathway, RNA dependent RNA polymerase (RdRP), is utilized by a number of eukaryotes, including fission yeast and nematodes (Dalmay et al., 2000; Hall et al., 2002; Volpe et al., 2002), to amplify siRNAs and possibly miRNAs. Interestingly, this enzyme is not encoded for in the mammalian or *Drosophila melanogaster* genomes, yet it is critical for RISC and RITS functioning in yeast (Catalanotto et al., 2002; Motamedi et al., 2004; Sigova et al., 2004; Sugiyama et al., 2005).

1-2 Core RNAi proteins

1-2-1 *PPD proteins*

1-2-1-1 PPD protein superfamily

The PPD superfamily is comprised of highly conserved proteins found in diverse organisms ranging from archaebacteria to humans. Family members are divided into two sub-families, Argonaute and Piwi, depending on the level of sequence similarity to these two founding members (Bohmert et al., 1998; Cox et al., 1998). PPD proteins contain two signature domains, a centrally located PAZ domain and a carboxyl-terminally located PIWI domain (Cerutti et al., 2000) (Figure 1-2).

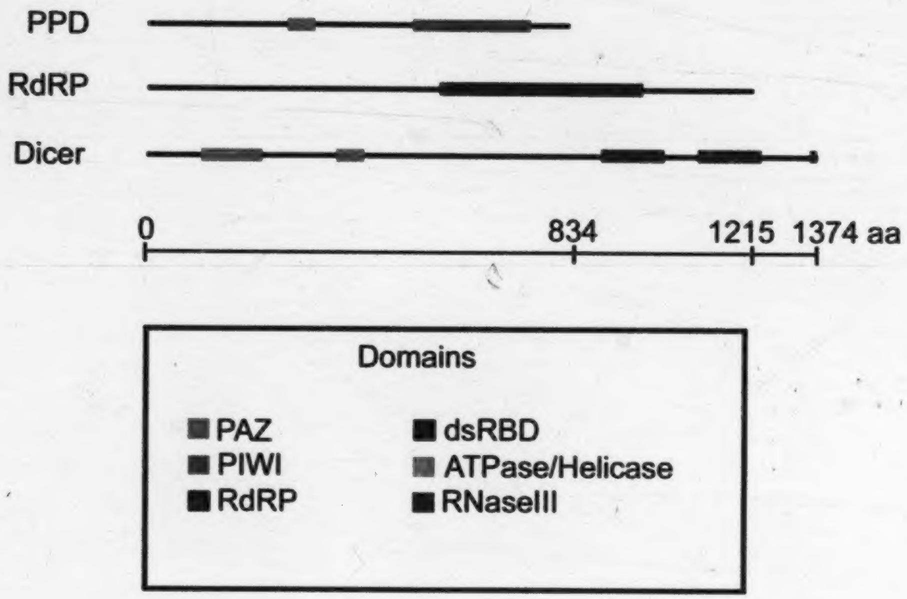

Figure 1-2. Basic structures of PAZ PIWI domain (PPD), Dicer and RdRP proteins. The domain and their proposed functions are as follows: PAZ domain: binding of 2-base 3' overhangs of siRNAs. PIWI domain: Dicer binding site and putative RNase H domain required for cleavage of RNA. RdRP domain: required for amplification of si/miRNAs. Helicase/ATPase domain: ATP binding, nucleic acid unwinding. RNase III domain: endonucleolytic cleavage of dsRNA. dsRBD: double-stranded RNA-binding domain. The scale represents the numbers of amino acids comprising the *S. pombe* PPD, Dicer and RdRP proteins. It should be noted that not all Dicer proteins contain a PAZ domain.

The 100 amino acid PAZ domain anchors the guide siRNA into the effector complex through binding of the 2-nucleotide 3'-overhang of the siRNA duplex (Ma et al., 2004). The 300 amino acid residue PIWI domain mediates the interaction with the initiator RNase III protein, Dicer (Doi et al., 2003; Tahbaz et al., 2004), as well as providing the endonuclease activity required for mRNA cleavage (Liu et al., 2004a; Parker et al., 2004; Rand et al., 2004; Song et al., 2004).

1-2-1-2 PPD proteins and development

Genetic studies first pointed to the importance of PPD proteins in developmental pathways both in plants and animals (Bohmert et al., 1998; Cox et al., 1998; Kataoka et al., 2001; Moussian et al., 1998). For example, AGO1 and ZWILLE are required for leaf development in *A. thaliana*, whereas Piwi and *d*Ago1 are essential for normal development of gametes and nervous system tissues, respectively in *D. melanogaster* (Cox et al., 1998; Kataoka et al., 2001). PPD protein activity is also required for maintaining undifferentiated stem cells in the shoot apical meristems of plants (Lynn et al., 1999; Moussian et al., 1998). Loss of Piwi expression results in differentiation and ultimately the depletion of germline stem cell populations in *D. melanogaster* (Cox et al., 1998), whereas overexpression of Piwi leads to increased proliferation of these cell types (Cox et al., 2000).

In vertebrates, members of the PPD family appear to be important for regulating multiple developmental pathways. Members of the Piwi subfamily in particular, are often highly expressed in undifferentiated cells and germline tissues. For example, levels of Hiwi mRNA expression are high in Cdc34+ hematopoietic progenitor bone marrow stem cells, but as these cells differentiate, Hiwi expression levels decrease dramatically (Sharma et al., 2001). Similarly, Mili is essential for spermatogenesis in mice. Null strains of mice are sterile due to arrest of spermatogenesis at the spermatocyte stage (Kuramochi-Miyagawa et al., 2001). Mili associates with MVH, the mammalian homolog of Vasa, which is an ATP-dependent DEAD-box RNA helicase. MVH was previously found to co-localize with the PPD protein Aub in nuage, which are germline specific granules (Findley et al., 2003), and in a ribonucleoprotein complex that has RISC-like properties (Caudy et al., 2002). Finally, mouse Ago2 was recently demonstrated to play a critical role in embryogenesis. Targeted disruption of the *ago2* gene results in a defect in neural tube closure and cardiac failure (Liu et al., 2004a). Taken together, these data suggest that it is not only the level of expression and/or activity of PPD family members, but also their tissue-specific localization that dictates various developmental processes.

Bioinformatic analysis has revealed that many of the miRNA targets in plants are transcription factors (Rhoades et al., 2002; Wang et al., 2004). In addition, stem cell division in *D. melanogaster* is controlled through the miRNA pathway (Hatfield et al., 2005). Thus, it is quite possible that many of the developmental defects exhibited by PPD mutants are due to aberrant expression of transcription factors that determine cell fate. Indeed, upon the loss of a functioning RNAi pathway in *S. pombe*, genes under the control of the stress-activated pathway transcription factor Atf1 are significantly upregulated (Hansen et al., 2005). It is not known if these genes are direct targets of siRNA-dependent silencing or if the observed upregulation of Atf1-dependent genes occurs in a compensatory role to combat the loss of $ago^{+}1$, *dcr1*$^+$ or *rdp1*$^+$. However, it is important to consider the possibility that at least some of the developmental roles of PPD proteins are unrelated to gene-silencing.

In *A. thaliana*, some allelic mutants of *ago1*$^+$ are defective for RNAi, but are developmentally normal (Morel et al., 2002). This indicates that the gene-silencing functions of PPD proteins can be genetically uncoupled from their developmental roles. There is evidence from studies in *D. melanogaster* that PPD proteins function in signaling pathways that control cell fate and developmental patterning. For example, *dAGO1* was isolated in a genetic screen for dominant activators of the Wingless signal transduction pathway (Kataoka et al., 2001). Moreover, the phenotypes of *PIWI* mutants can be rescued by over-expression of Hedgehog, a secreted signaling protein that is not implicated in RNAi (Barnes et al., 2001; King et al., 2001; Roy and Ingham, 2002; Tabata and Kornberg, 1994). Mammalian Sonic hedgehog is implicated in regulating the passage of cells through mitosis by its indirect action on Cyclin B1 (Barnes et al., 2001). Of course, these results do not discount the possibility that Wingless and Hedgehog function downstream of *d*Ago1 and Piwi respectively. Rather, over-expression of Wingless or Hedgehog may bypass the need for PPD proteins in an upstream miRNA-dependent pathway, although as of yet there is no evidence that Piwi associates with miRNAs (Liu et al., 2005). Finally, in *S. pombe* Ago1 and Dcr1 have been shown to function independently of siRNAs in regulating cell cycle checkpoints (Carmichael et al., 2004) suggesting that PPD proteins can function outside of the canonical RNAi pathway.

1-2-2 *Dicer family of proteins*

1-2-2-1 RNase III enzyme family

Dicer was the first member of the RNase III family of enzymes shown to be involved with the initiation stage of RNAi (Bernstein et al., 2001; Lamontagne et al., 2001). This family is divided into three structural classes. Class I includes enzymes from bacteria and fungi. These proteins are required for maturation of ribosomal RNAs, tRNAs and mRNAs. Proteins of this class contain one catalytic endonuclease domain and a dsRNA-binding domain (dsRBD) (Nicholson, 1999). The nuclear enzyme Drosha represents the second class of RNase III proteins. These enzymes are comprised of two catalytic endonuclease domains, a dsRBD, and long amino termini that is rich in proline, serine and arginine residues (Kay et al., 2000). The latter region is presumably involved in protein-protein interactions. Drosha enzymes, encoded in the *D. melanogaster, C. elegans*, mouse and human genomes (Filippov et al., 2000; Fortin et al., 2002; Wu et al., 2000), are responsible for the nuclear processing of primary miRNAs into the stem-loop pre-miRNAs (Lee et al., 2003). Dicer belongs to the third class of RNase III enzymes. Class III enzymes contain an amino-terminal DEXH-box RNA helicase/ATPase domain, a domain of unknown function (named DUF283), two catalytic endonuclease domains and a dsRBD (Hammond et al., 2001). Most Dicer proteins also contain PAZ domains but it is conspicuously absent from *S. pombe* Dcr1 (Figure 1-2).

1-2-2-2 Functional diversification and characteristics of Dicer proteins

C. elegans, S. pombe and vertebrates each encode only one Dicer protein (Bernstein et al., 2003; Grishok et al., 2001; Hutvagner et al., 2001; Ketting et al., 2001; Knight and Bass, 2001; Volpe et al., 2002; Wienholds et al., 2003). In contrast, *Neurospora crassa* expresses two Dicer proteins that are functionally redundant (Catalanotto et al., 2004). *D. melanogaster* also has two Dicer paralogs, DCR-1 and DCR-2. The former enzyme, which is essential for miRNA processing and miRNA-directed translational repression (Lee et al., 2004), contains a PAZ domain, but lacks a functional helicase domain. Surprisingly, a complex that includes DCR-1 and DCR-2 is required for siRNA-directed mRNA degradation (Lee et al., 2004). The *A. thaliana* genome encodes four Dicer homologues, at least three of which have unique functions: DCL1 processes miRNA precursors (Park et al., 2002; Reinhart and Bartel, 2002; Schauer et al., 2002); DCL2 is required for processing virus-specific dsRNA (Xie et al., 2004), and DCL3 processes endogenous siRNAs (Xie et al., 2004). Interestingly, DCL1 and DCL4 have one or more predicted nuclear localization signals (NLS) (Schauer et al., 2002). *D. melanogaster* DCR-1, and the mouse and human Dicers each contain a predicted NLS (Schauer et al., 2002). However, to date, these proteins have not been detected in the nucleus. In contrast, the NLS of DCL1 was shown to be required for nuclear localization of a GFP-DCL1 chimera (Papp et al., 2003). Interestingly, DCL1 mRNA is subject to negative feedback regulation by the RNAi pathway through a miR162-dependent mechanism (Xie et al., 2003).

Recently, Dicer enzymes were found to be essential for the normal development of zebrafish (Wienholds et al., 2003) and mice (Bernstein et al., 2003), as well as for the formation of heterochromatin in vertebrate cells (Fukagawa et al., 2004). Whereas *C. elegans* and *D. melanogaster* Dicer activities are stimulated by ATP (Bernstein et al., 2003; Ketting et al., 2001; Liu et al., 2003; Nykanen et al., 2004), mammalian Dicer enzymes do not require ATP for activity, and are instead strongly stimulated by limited proteolysis *in vitro* (Zhang et al., 2002).

1-2-3 *RNA-dependent RNA polymerase (RdRp) family*

The RdRp family is present in fungi, plant and nematodes but is conspicuously absent in *D. melanogaster* and human genomes (Chan et al., 2004; Cogoni and Macino, 1999; Mourrain et al., 2000; Smardon et al., 2000; Volpe et al., 2002) (Figure 1-2). These proteins are thought to enhance siRNA-dependent cleavage of mRNA through amplification of the dsRNA siRNA precursor (Sijen et al., 2001). However, evidence suggests that this amplification step is not required in *D. melanogaster* or vertebrates (Schwarz et al., 2002; Stein et al., 2003). In *S. pombe, N. crassa*, and *A. thaliana*, the RdRP proteins Rdp1, Qde1 and SGS2/SDE1, respectively, are required for mRNA degradation (Catalanotto et al., 2002; Dalmay et al., 2000; Mourrain et al., 2000; Sigova et al., 2004). Interestingly, in the absence of *SGS2/SDE1*, transgenes were not silenced and recovered transgenic sequences were in a non-methylated form (Dalmay et al., 2000; Mourrain et al., 2000). This suggests that the RNAi pathway, or members of the pathway are also involved in DNA methylation.

In *S. pombe*, transcriptional silencing is in part enacted through the targeting of factors required for histone H3 lysine 9 methylation by siRNAs derived from Rdp1-amplified centromeric dsRNA (Hall et al., 2002; Motamedi et al., 2004; Sugiyama et al., 2005; Volpe et al., 2002). Surprisingly, in *N. crassa*, Qde1 is dispensable for this process, although a similar process, transposon silencing, requires Qde1 function (Chicas et al., 2004; Chicas et al., 2005). Where once it was thought that Rdp1 was simply an enhancer of RNAi, it is now suggested that Rdp1 plays a more integral role as both the amplifier of dsRNA and as an adapter/scaffold for RITS-targeted DNA-association (Motamedi et al., 2004).

1-3 RNA interference

1-3-1 *Interactions between Dicer and dsRNA binding proteins*

In nematodes, flies and plants several dsRNA binding proteins (RDE-4, R2D2, Pasha, Loquacious and HYL1) are known to associate with Dicer isoforms (Denli et al., 2004; Forstemann et al., 2005; Liu et al., 2003; Parrish and Fire, 2001; Saito et al., 2005; Tabara et al., 2002; Vazquez et al., 2004). These proteins may function as physical links between the initiation and effector stages of RNAi. The R2D2 protein was identified as a 36 kilodalton dsRNA-binding protein that co-fractionated with dsRNA processing activity from *D. melanogaster* S2 cell extracts (Liu et al., 2003). R2D2 forms a stable complex with DCR-2 (which lacks a PAZ domain) and dsRNA. In the absence of R2D2, DCR-2 fails to bind detectable amounts of dsRNA (Liu et al., 2003). Maximum stimulation of dsRNA-initiated RISC activity was observed in the presence of DCR-2/R2D2 complexes and was abolished when the dsRNA binding domains of R2D2 were altered by site-directed mutagenesis (Liu et al., 2003). Similar results were obtained when pre-cleaved siRNAs were used to trigger RISC activity, indicating that R2D2 is needed for RISC to efficiently utilize siRNAs. Finally, the DCR-2/R2D2 complex is required for efficient siRNA transfer and binding to *d*Ago2 in *D. melanogaster* RISC (Liu et al., 2003).

Recently it was recognized that Drosha and DCR-1 also function with the aid of dsRNA binding proteins Pasha and Loquacious respectively (Denli et al., 2004; Forstemann et al., 2005; Saito et al., 2005). Loss of *Loqs* results in accumulation of pre-miRNAs in *D. melanogaster* S2 cells (Saito et al., 2005) suggesting that DCR-1 requires Loqs for cleavage of pre-miRNAs (Forstemann et al., 2005; Saito et al., 2005). Similarly, suppression of Pasha in *C. elegans* or *D. melanogaster* is coincident with an accumulation of pri-miRNAs and decrease in the production of mature miRNAs (Denli et al., 2004).

The pairing of a specific dsRNA binding protein with a Dicer isoform is also the case in *A. thaliana*. For example, the nuclear dsRNA binding protein HYL1 is required for miRNA accumulation and development but not for post-transcriptional transgene silencing in *A. thaliana* (Vazquez et al., 2004). The developmental defects of *hyl1* mutants overlap with those of *dcl1*. Specifically both exhibit a decrease in miRNA accumulation and a concomitant reduction in targeted mRNA cleavage. In addition, the reported nuclear localization of HYL1 and the predicted nuclear localization of DCR1 are consistent with the possibility that these proteins function together as a complex in the nucleus (Vazquez et al., 2004).

In *C. elegans* the dsRNA binding protein RDE-4 interacts with Dicer, RDE-1 (a PPD protein) and Dicer-Related Helicase-1 (DRH-1), a DEXH-box helicase (Tabara et al., 2002). RDE-4 was first identified as a protein necessary for the initiation step of RNAi in *C. elegans* (Grishok et al., 2000; Tabara et al., 1999), but its activity is not required for miRNA processing or development (Tabara et al., 1999; Tabara et al., 2002). The protein binds to long dsRNA molecules, but not to double or single stranded siRNAs (Tabara et al., 2002). Interestingly, RDE-1, whose activity was previously shown to be required for the effector stage of RNAi (Parrish and Fire, 2001), is necessary for the accumulation of long dsRNAs, which are then bound by RDE-4 (Tabara et al., 2002). Thus, the recognition of long dsRNAs by RDE-4 in concert with RDE-1 likely mediates the transfer of dsRNAs to DCR-1 for processing into siRNAs. The helicase activity of DRH-1 may be required to unwind dsRNA to facilitate the movement of the RDE-4/DCR-1/RDE-1 complex along the molecule. Alternatively, DRH-1 may required for the transfer of dsRNA from RDE-4 to DCR-1 (Tabara et al., 2002). In *S. pombe* no dsRNA binding partner(s) has been identified for Dcr1 but it is probable that a similar mechanism operates to mediate the transfer of Rdp1-amplified dsRNA to sites of Dcr1-cleavage activity in the cytoplasm and/or nucleus.

1-3-2 *Protein components of RISC*

The earliest identified protein component of RISCs were PPD proteins, specifically *D. melanogaster* Ago2 (Hammond et al., 2001; Nykanen et al., 2001) and human Ago1 and Ago2 (Martinez et al., 2002). There is still controversy regarding the remaining components of RISC as purified complexes range in size from 160 kilodaltons (Martinez et al., 2002) to 500 kilodaltons (Hammond et al., 2000; Hammond et al., 2001; Nykanen et al., 2001). One common thread between all of these studies was that the RISC-like complexes always purified with 21 to 25 nt long RNAs. The fact that nuclease activity is associated with all of the complexes suggests that different RISC-associated proteins impart specificity to the RNAi process, perhaps by altering the cellular localization of the complex and/or targeting to specific mRNAs.

Additional RISC components are still being identified, a situation that makes the precise determination of RISC composition difficult at the present time. Two putative RNA-binding proteins, the *D. melanogaster* homolog of the fragile X mental retardation protein (FMRP), dFXR, and Vasa intronic gene protein (VIG) were recently identified as components of RISC (Caudy et al., 2002). However, the precise roles of these proteins in RISC function are not known. The dFXR ribonucleoprotein complex also contains the ribosomal proteins L5 and L11, as well as 5S RNA, dAgo2, and p68 RNA helicase (Dmp68) (Ishizuka et al., 2002). Furthermore, the dFXR protein was found to associate with Dicer, and Dmp68, a protein that is important for RNAi in *D. melanogaster* (Ishizuka et al., 2002). Since one of the functions of dFMR1 is to repress translation of the microtubule-associated protein Futsch mRNA, it is possible that different dFMR-containing complexes function in siRNA- and miRNA-initiated pathways (Ishizuka et al., 2002).

A miRNA-containing ribonucleoprotein complex (miRNP) was found to contain components similar to those in RISC (Mourelatos et al., 2002; Schwarz et al., 2002). The 15S miRNP complex isolated from HeLa cells contains hAgo2, Gemin3, a DEAD-box helicase, Gemin 4, and is associated with multiple miRNAs (Mourelatos et al., 2002). In human retinoblastoma Weri cells, the let7b-containing miRNP complex binds to the 3' untranslated region (3'UTR) of its lin28 mRNA target in polyribosome-containing fractions. The level of reporter protein, but not the corresponding mRNA containing the lin28 3'UTR, was significantly lowered in the presence of let7b-miRNP, suggesting that the miRNP functions through translational suppression (Nelson et al., 2004). In contrast, human let-7 programmed RISC was shown to be a multiple turnover enzyme complex, capable of catalyzing the cleavage of more than 10 target mRNA molecules (Hutvagner and Zamore, 2002). These findings are not surprising since miRNAs that are perfectly complementary to mRNAs can mediate targeted mRNA degradation, similar to siRNAs and *vice versa* (Doench et al., ; Zeng et al., 2003). In general, perfect complementarity between a miRNA and its target mRNA results in degradation of the target as opposed to translational repression (Doench et al., 2003).

1-3-3 *PPD Proteins in siRNA and miRNA mediated pathways*

A. thaliana AGO1 and ZWILLE were the first PPD proteins to be characterized. Prior to the discovery that PPD proteins are RNAi effectors, AGO1 and ZWILLE were shown to have overlapping functions in plant development (Bohmert et al., 1998; Lynn et al., 1999). Although it has yet to be shown that ZWILLE has RNAi-related functions, it is well documented that AGO1 is integral to gene-silencing (Boutet et al., 2003; Fagard et al., 2000; Vaucheret et al., 2004).

The *C. elegans* genome encodes 27 PPD proteins compared to eight found in humans. It appears that in nematodes at least, PPD proteins perform highly specialized functions within the RNAi pathway. For example, the PPD proteins RDE-1 and PPW-1, are required for efficient siRNA-mediated mRNA cleavage (Fagard et al., 2000; Tabara et al., 1999; Tijsterman et al., 2002), whereas ALG-1 and ALG-2 function in maturation and translational inhibition activities of lin-4 and let-7 miRNAs in developmental timing pathways (Grishok et al., 2001).

In *D. melanogaster*, *d*Ago2 is required for loading siRNAs into RISC and the subsequent targeting of homologous mRNAs for destruction (Okamura et al., 2004). In the absence of *d*Ago2 activity, fly embryos are defective for siRNA-targeted mRNA cleavage. In contrast, *d*Ago1 is required for miRNA biogenesis but not siRNA-mediated RISC activities (Okamura et al., 2004). In humans, four PPD proteins (Argonautes1-4) were shown to bind miRNAs, but only hAgo2 is associated with the catalytic activity required for mRNA cleavage (Meister et al., 2004). Thus the roles PPD proteins perform within RNAi-related context are isoform-specific. These roles are probably dictated by the less conserved amino-terminal domain in combination with the ability of the PIWI domain to exhibit endonuclease activity.

Recently the *S. pombe* PPD protein, Ago1, was shown to be required for siRNA-directed mRNA degradation (Sigova et al., 2004). Interestingly, whereas there appear to be PPD isoform-specific functions within the si/miRNA pathways of metazoans, Ago1 functions in at least two distinct RNAi-dependent complexes that presumably reside in the cytoplasm and the nucleus of fission yeast. In addition to the cytoplasmic mRNA degradation pathway which presumably occurs at sites of mRNA degradation known as P-bodies (Liu et al., 2005; Sen and Blau, 2005), *S. pombe* Ago1 and other PPD proteins have been shown to be involved in siRNA-targeted silencing of pericentric chromatin and for accurate chromosome segregation during mitosis and meiosis (Ekwall, 2004; Hall et al., 2003; Hall et al., 2002; Volpe et al., 2003; Volpe et al., 2002).

1-4 RNA-induced initiation of transcriptional gene-silencing

1-4-1 *RITS-dependent heterochromatin formation*

Analysis of the RNAi components in *S. pombe* using chromatin immunoprecipitation revealed that both Rdp1 and Ago1 are associated with centromeric chromatin (Noma et al., 2004; Volpe et al., 2002). Ago1 also associates with chromatin derived from telomeric and mating type loci (Noma et al., 2004; Volpe et al., 2002). Moreover, pools of tagged Ago1 and Chp1 have been localized to the nuclei of *S. pombe* cells (Noma et al., 2004). In contrast, Dcr1, although integral to chromatin silencing, was not shown to associate with any of the heterochromatic region assayed (Volpe et al., 2002). Early genetic and biochemical studies suggested that PPD proteins and Dcr1 homologues are present in the nucleus (Hall et al., 2003; Hall et al., 2002; Pal-Bhadra et al., 2004; Verdel et al., 2004; Volpe et al., 2003; Volpe et al., 2002) however, the evidence to support the notion that the initiation and/or effector stages of RISC or RITS-dependent RNAi take place in the nucleus emerged only recently.

The discovery of Drosha offered a plausible mechanism to account for nucleus-restricted processing of pri-miRNAs to pre-miRNAs (Lee et al., 2003). In addition, studies in *A. thaliana* documenting the localization of DCL-1-GFP fusion protein provide evidence for nuclear production of siRNAs and miRNAs from precursor molecules in plants (Papp et al., 2003). It is not only Dicer family members that localize to the nucleus, in fact the *D. melanogaster* nuclear protein, Piwi, has been shown to be required for RNA silencing of *gypsy* by inhibiting transcription (Sarot et al., 2004). Indeed, human miRNA and siRNA-mediated RISC activities reportedly localize to the nucleus (Meister et al., 2004; Robb et al., 2005). This suggests that cytoplasmic miRNA and siRNA–associated RISCs may be able to translocate to the nucleus or that there is a stable nuclear pool of RISC. In support of these possibilities, several studies demonstrate the involvement of RDR2, DCL-3, AGO4, and HEN-1 in chromatin modification events in *A. thaliana* (Xie et al., 2004). In subsequent investigations, DCL-3-GFP, HEN-1-GFP, and GFP-AGO4 protein were detected exclusively in nuclei (Xie et al., 2004).

Recently, the importance of RNAi in nuclear events such as genome rearrangement (Janetopoulos et al., 1999; Mochizuki et al., 2002; Mochizuki and Gorovsky, 2004)}, chromatin silencing (Hall et al., 2002; Pal-Bhadra et al., 2004; Volpe et al., 2003; Volpe et al., 2002; Zilberman et al., 2003) and chromosome segregation (Hall et al., 2003; Provost et al., 2002b) has come to light. The latter process is dependent upon the assembly of centromeric heterochromatin (Grewal and Elgin, 2002) followed by cohesin mediated sister chromatid association (Ciosk et al., 1998; Guacci et al., 1997; Lee and Orr-Weaver, 2001; Michaelis et al., 1997). The binding of the cohesin complex to silent centromeric sites requires the chromodomain-containing protein, Swi6 (Bernard et al., 2001; Nonaka et al., 2002). Histone H3 lysine-9 methylation-dependent Swi6 localization to centromeric, telomeric and silent mating-type loci is partially dependent on the three core components of the RNAi pathway in *S. pombe* (Ago1, Dcr1 and Rdp1) and *D. melanogaster* (Piwi, Aub and Homeless) (Hall et al., 2002; Pal-Bhadra et al., 2004; Volpe et al., 2002).

Targeting of Swi6 to sites of heterochromatin formation in the *S. pombe* genome is thought to be mediated by the RITS complex (Verdel et al., 2004). It is likely that targeting of the RITS complex requires the incorporation of siRNAs derived from centromeric transcripts (Reinhart and Bartel, 2002). Indeed, in *D. melanogaster* loss of function of one of the PPD proteins Piwi or Aub, results in mis-localization of heterochromatin protein 1 (HP1), a Swi6 homologue (Pal-Bhadra et al., 2004). Further, mutations in *A. thaliana ago4* results in decreased methylation of histones and an accumulation of siRNAs corresponding to the target sequence (Zilberman et al., 2003; Zilberman et al., 2004). Deletion of any one of the core RNAi genes, *ago1*$^+$, *dcr1*$^+$ or *rdp1*$^+$, or genes that encode the RITS-associated proteins Chp1 and Tas3, results in the reduction of histone H3 lysine-9 methylation and the absence of Swi6 from centromeric chromatin in *S. pombe* (Hall et al., 2003; Hall et al., 2002; Pal-Bhadra et al., 2004; Verdel et al., 2004; Volpe et al., 2003; Volpe et al., 2002), presumably due to the loss of correct targeting of the methyltransferase, Clr4. However, it was reported by Volpe *et al.* (2002) that in the absence of Ago1, Dcr1 or Rdp1 function, heterochromatin formation at silent centromeric sites still does occur. This suggests that there are redundant pathways that compensate or cooperate with the RNAi machinery in the formation of heterochromatin. Indeed, the SAPK pathway in *S. pombe* was recently shown to facilitate heterochromatin formation in RNAi-defective mutants (Jia et al., 2004). Only in the absence of both the RNAi pathway and SAPK pathway were histone methylation and heterochromatin formation completely abolished (Jia et al., 2004).

The merging of two distinct pathways in heterochromatin formation underscores the importance of heterochromatin nucleation in maintaining genome integrity. Indeed, it is now known that proteins required for efficient histone methylation and heterochromatin formation facilitate targeting of factors to sites of DNA damage (Garcia-Salcedo et al., 2003). Further, a prerequisite for enactment of the DNA damage checkpoint appears to require the nucleation of heterochromatin at sites of DNA damage and subsequent targeting of DNA damage repair proteins by BRCA1 (Abbott et al., 1999; Schlegel et al., 2003; Yamamoto et al., 2000). Interestingly, BRCA1 is the vertebrate homologue of *S. pombe* Cut5, which has also been shown to facilitate heterochromatin nucleation and recruitment of the Rad/Hus DNA damage response complex upon sensing DNA damage (Harris et al., 2003; Parrilla-Castellar and Karnitz, 2003; Saka et al., 1994a).

1-5 *S. pombe* cell cycle regulation

1-5-1 *Cell cycle regulatory pathway*

The coupling of replication to mitosis ensures that the genome is faithfully segregated to both mother and daughter cells with no DNA aberrations. A number of temporal and spatial controls have been established to facilitate the passage from G_1 through M phases. In the event of incomplete DNA replication or DNA damage, sensors transduce effector signals to cell cycle regulatory molecules to slow-down or halt the cycle. In *S. pombe*, progress through S- or M-phases is ultimately controlled by the cyclic activation and de-activation of a cyclin-dependent kinase, Cdc2 (Nurse, 1990; Nurse and Bissett, 1981; Nurse and Thuriaux, 1980) (Figure 1-3).

Figure 1-3. Schematic of the mitotic cell cycle and proteins involved in DNA checkpoint arrest. The left side of the schematic highlights the major players that control progression through S-M phase/G_2-M phase through inhibition or activation of Cdc2. Inhibitory tyrosine-15 phosphorylation of Cdc2 by Wee1 and/or Mik1 results in a delay in the cell cycle. Dephosphorylation of Cdc2 Y15 by the phosphatase Cdc25 results in progression through S and G_2 phases. The right side of the schematic, illustrated in the inhibitory configuration, depicts the proteins required for replication and DNA damage checkpoint arrest. *S. pombe* proteins are indicated with the mammalian homologues in parenthesis. Briefly, checkpoint enactment requires sensing and response to DNA abnormalities in a Cut5-dependent manner. Rad17-dependent loading of the 9-1-1 complex results in activation of Rad3 and subsequent Chk1-dependent activation of Wee1/Mik1 kinases and inhibition of Cdc25. Inhibitory phosphorylation of Cdc25 results in phosphatase inactivation and Cdc25 retention in the cytoplasm through 14-3-3 binding. The combined Chk1-dependent cell cycle regulation results in phosphorylation of Cdc2 Y15 and cell cycle arrest.

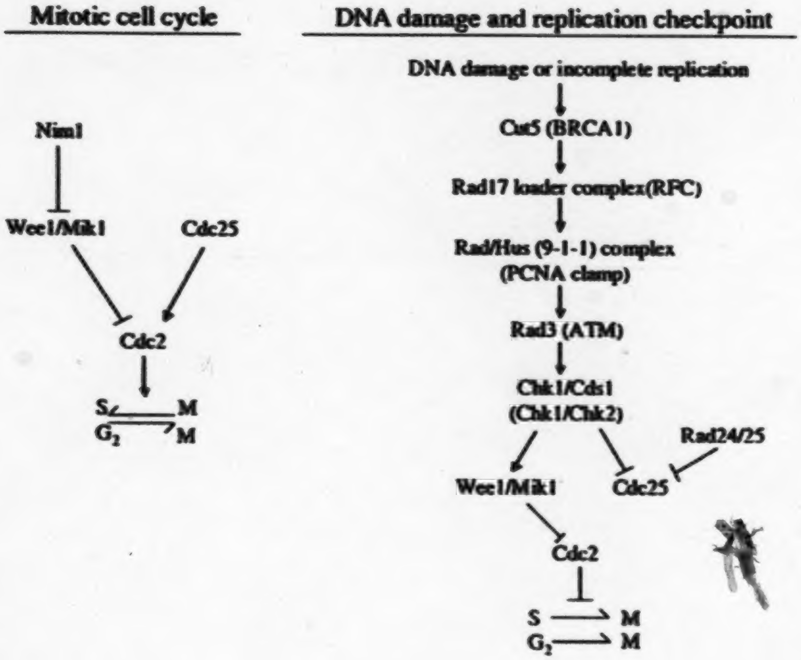

Mitotic cell cycle

DNA damage and replication checkpoint

In interphase, Cdc2 binds its regulatory cyclin partners, Cig2 and Cdc13 (Martin-Castellanos et al., 1996). The specific activities of these complexes are controlled in part through inhibitory phosphorylation of tyrosine-15 (Y15) by the Wee1 and Mik1 kinases (Lundgren et al., 1991). Interphase levels of Cdc2 activity are sufficient to allow passage through S-phase but not M-phase (Fisher and Nurse, 1996). Indeed, the level of Cdc2 activity in interphase is approximately 30% of that required to drive cells through mitosis (Borgne and Meijer, 1996). The triggering of mitosis is brought about by full activation of Cdc2 through the dephosphorylation of Cdc2 Y15 by the phosphatase Cdc25 (Millar et al., 1991).

Cdc2 regulators are also the targets of kinases that sense and respond to DNA damage. For instance, Cdc2 activity is decreased upon sensing genotoxic insults that cause incomplete replication or DNA damage by the activation of Wee1 and Mik1 coupled with the inactivation of Cdc25 (Furnari et al., 1997; Lundgren et al., 1991; Millar et al., 1991; Raleigh and O'Connell, 2000; Rhind et al., 1997; Rhind and Russell, 1998b).

1-5-2 *DNA-replication and DNA damage checkpoints*

The surveillance of genomes for efficacy in replication and segregation of genomic material is a task that falls to proteins involved in cell cycle arrest. It is also now evident that in order to ensure the coupling of complete replication to segregation of chromosomes that numerous pathways come to bear in this effort (Degols and Russell, 1997; Lee et al., 1998; Lee et al., 1999; Rhind and Russell, 1998a; Taricani et al., 2001).

The sensing of DNA damage and, indeed, the continued monitoring of the genome for imperfections appears to be the job of a multi-faceted protein called BRCA1 (Abbott et al., 1999; Peng et al., 2002). Like its mammalian counterpart, *S. pombe* Cut5 is crucial for sensing DNA abnormalities and coupling the recruitment of response proteins to checkpoint enactment and cell cycle arrest (Harris et al., 2003; Parrilla-Castellar and Karnitz, 2003; Saka et al., 1994b).

1-5-2-1 Histone methylation in DNA damage responses

Upon sensing DNA abnormalities BRCA1 is recruited to sites of damage potentially through an association with histone deacetylases (HDACs) (Yarden and Brody, 1999). Heterochromatin nucleation is thought to be an important factor in targeting and stabilizing repair proteins at sites of damage (Paull et al., 2000). Indeed, loss of Sir2 results in a decrease in H3-MeK9 levels and derepression of the silent mating locus in *S. pombe* (Shankaranarayana et al., 2003).

Histone methylation and subsequent heterochromatin formation is a requirement for accurate DNA segregation (Nonaka et al., 2002; Volpe et al., 2002). The abolishment of histone methylation results in DNA segregation defects in *S. pombe* as a result of incorrectly aligned sister chromatids and improper spindle attachment (Hall et al., 2003; Provost et al., 2002a). Recently RNAi-mediated HP1 localization and heterochromatin formation was linked to DNA damage response by the finding that Ku70 binds HP1α (Nonaka et al., 2002; Pal-Bhadra et al., 2004; Song et al., 2001). Ku70 localization to dsDNA breaks, presumably in an RNAi-dependent manner (Pal-Bhadra et al., 2004), and its subsequent binding to DNA ends results in activation of DNA-dependent kinases (Ouyang et al., 1997).

1-5-2-2 DNA damage response proteins and signal transduction

Cut5 and BRCA1 respond to DNA damage and replication inhibition by recruiting a highly conserved module of proteins (Harris et al., 2003; Parrilla-Castellar and Karnitz, 2003; Yamamoto et al., 2000). In *S. pombe*, the initial response of five proteins, Rad1, Rad3, Rad9, Rad17 and Hus1 is required for both replication and damage checkpoints (al-Khodairy and Carr, 1992; Enoch et al., 1992; Enoch and Nurse, 1990; Jimenez et al., 1992). Rad17 functions in a complex that is analogous to the proliferating cell nuclear antigen (PCNA) clamp-loading complex (Griffith et al., 2002; Majka and Burgers, 2003; Rauen et al., 2000; Shiomi et al., 2002; Venclovas and Thelen, 2000). The PCNA clamp-loading complex facilitates the binding of the sliding clamp Rad9/Rad1/Hus1 (9-1-1) complex onto DNA which is then used as a moving platform for DNA polymerases (Parrilla-Castellar and Karnitz, 2003; Toueille et al., 2004). The 9-1-1 complex is also an activator of Rad3, a homologue of ATR and ATM checkpoint activators (Bentley et al., 1996; Naito et al., 1998; Roos-Mattjus et al., 2003; Weiss et al., 2002). The phosphorylation of Rad3 results in Chk1-dependent cell cycle delay or arrest (Furnari et al., 1997; Weiss et al., 2002; Yarden et al., 2002).

1-5-2-3 Cell cycle regulators as targets of DNA damage checkpoints

The effector proteins involved in cell cycle progression, namely the kinases Wee1 and Mik1 and the phosphatase Cdc25, are integral for the response to incomplete DNA replication or DNA damage (Raleigh and O'Connell, 2000; Rhind et al., 1997). The activities of these cell cycle effectors are controlled by Cds1 and Chk1 in a Rad3-dependent manner (Furnari et al., 1997; Tanaka et al., 2001; Tanaka and Russell, 2004; Weiss et al., 2002; Yarden et al., 2002).

Chk1-dependent activation of Wee1 and Mik1 results in sustained inactivation of Cdc2 through inhibitory phosphorylation of Y15 (Baber-Furnari et al., 2000; O'Connell et al., 1997). Cdc25 is also a target of Chk1-dependent DNA damage regulation (Furnari et al., 1997). Chk1-dependent phosphorylation on Cdc25 serine residue 216 results in two distinct control responses. First, phosphorylation results in phosphatase inactivation whereas dephosphorylation of this residue results in activation of Cdc25 and mitotic entry through dephosphorylation of Y15 of Cdc2 (Furnari et al., 1997; Kumagai et al., 1998; Rhind et al., 1997). Further evidence suggests that the inactivation of Cdc25 is sufficient to enable prolonged checkpoint arrest (Chen et al., 1999; Lopez-Girona et al., 2001b). Secondly, phosphorylation of serine 216 on Cdc25 creates a binding site for 14-3-3 proteins (Chen et al., 1999; Kumagai and Dunphy, 1999; Kumagai et al., 1998; Lopez-Girona et al., 1999). 14-3-3 proteins comprise a conserved family of adapter proteins that recognize phosphoserine residues (Muslin et al., 1996). Two 14-3-3 proteins have been identified in *S. pombe*, Rad24 and Rad25. Rad24 appears to be more dominant during checkpoint arrest (Ford et al., 1994). During checkpoint arrest, 14-3-3 proteins bind phosphoserine 216 of Cdc25 and essentially tether or relocate Cdc25 to the cytoplasm and away from Cdc2 (Lopez-Girona et al., 1999; Zeng and Piwnica-Worms, 1999). Interestingly, although Chk1-dependent phosphorylation of Cdc25 mediates 14-3-3 binding to Cdc25, Chk1 nuclear accumulation is Rad24-dependent (Dunaway et al., 2005). During mitotic cell cycling, Cdc25 nuclear accumulation in late G_2 is dependent on the importin-β Sal3 (Chua et al., 2002). Loss of Sal3 function results in a cell cycle delay due to a failure in Cdc25 nuclear localization (Chua et al., 2002). This again suggests that by inhibiting nuclear import of Cdc25, and thus access to Cdc2, cell cycle arrest is initiated. However, nuclear exclusion of Cdc25 is not obligatory for Cdc2 inactivation (Lopez-Girona et al., 2001a) suggesting that cytoplasmic sequestration of Cdc25 in combination with inactivation of the phosphatase active center is required for complete inactivation of Cdc2.

Sequestration and inactivation may only be two means of regulating Cdc2 activity. The possibility exists that Cdc25 stability is also a factor in sustained checkpoint activation as indicated by the cyclic production and destruction of Cdc25 through the mitotic cycle (Ducommun et al., 1990). Thus, the importance of genome integrity and the necessity to arrest the cell cycle when DNA lesions are sensed requires a number of mechanisms to maintain Cdc2 in an inactive state. Interestingly, two core components of the RNAi pathway, as well as the stress-activated protein kinase (SAPK) pathway, have been implicated in the regulation of Cdc2 activity indicating that control of the cell cycle and genome integrity requires monitoring and activity of a number of conserved pathways (Carmichael et al., 2004; Lopez-Aviles et al., 2005; Smith et al., 2002).

1-5-3 *Core RNAi proteins and the cell cycle*

The heterochromatin defects associated with *ago1*$^+$, *dcr1*$^+$ and *rdp1*$^+$ mutants manifest in lagging DNA and chromosome loss as a direct result of incorrect sister chromatin orientation and kinetochore attachment to spindles (Hall et al., 2003; Provost et al., 2002b). This suggests that these proteins may be involved at many stages in the control of higher chromatin order and are central to cell cycle progression. Indeed in yeast and metazoans, the requirement for heterochromatin formation through siRNA-dependent silencing is also important for the recruitment of proteins that enact checkpoint arrests (Martin et al., 1999; Peng et al., 2002; Takeda et al., 2004).

Evidence is mounting to support the possibility that RNAi core proteins and related proteins have roles not directly related to gene-silencing (Morel et al., 2002; Provost et al., 1999). For example, in the budding yeast *Saccharommyces cerevisiae*, it was recently discovered that a type III RNase, Rnt1, functions in cell cycle regulation. Catala *et al.* (2004) demonstrated that the nuclear localization of catalytically dead Rnt1 mutants was sufficient for efficient cell cycle progression (Catala et al., 2004). Although the classical RNAi pathway is not present in *S. cerevisiae*, this result does support the notion of cell cycle-related functions for RNaseIII proteins that are independent of their nuclease activity. By extension, Dcr1 function in the *S. pombe* cell cycle may be independent of its ability to generate siRNAs.

In *S. pombe*, Ago1 and Dcr1, but not Rdp1, are required for regulated phosphorylation of Cdc2 Y15 when encountering insults that cause DNA damage or incomplete replication of DNA (Carmichael et al., 2004). In the presence of agents that interrupt DNA replication or cause DNA damage, *ago1*$^{+}$ and *dcr1*$^{+}$ mutants fail to block mitosis, presumably due to an inability to undergo regulated phosphorylation of Cdc2 Y15. These cells continue to divide unchecked, resulting in unequal division of genomic material between mother and daughter cells (Carmichael et al., 2004).

Interestingly, human Ago2 was shown to complement the *S. pombe ago1* mutant growth defect associated with replication inhibition (Carmichael et al., 2004). This suggests that in humans, the core catalytic subunit of RISC (Liu et al., 2004a) may play a role in cell cycle checkpoint regulation.

Recently it was reported that in the absence of siRNA-initiated heterochromatin formation, the SAPK pathway, and in particular Atf1 activation, was able to compensate for this loss by recruiting factors required for heterochromatin formation to the silent mating type locus (Jia et al., 2004). The link between these pathways appears even stronger when one considers that loss of the RNAi pathway results in upregulation of SAPK targeted genes such as *hsp16* (Hansen et al., 2005). Indeed, the SAPK activator Srk1 kinase has also been shown to function in cell cycle regulation (Lopez-Aviles et al., 2005; Smith et al., 2002).

1-5-4 *Stress-activated protein kinase family*

1-5-4-1 SAPK regulatory proteins

The SAPK pathway is a highly conserved pathway required for responses to environmental stimuli such as osmotic stress, nutritional limitation and DNA-damaging agents (Degols and Russell, 1997; Degols et al., 1996; Kato et al., 1996; Millar et al., 1995). In addition, this pathway is required for initiation of sexual differentiation and coordinating mitotic initiation with cell size (Degols et al., 1996; Shiozaki and Russell, 1995; Shiozaki and Russell, 1996). The mammalian homologues of the *S. pombe* SAPK pathway are the p38 and cJun stress-activated protein cascades (Kyriakis et al., 1994; Rouse et al., 1994; Saka et al., 1994a). Stress-activated pathways sense environmental alterations and transduce signals down a cascade of proteins via a series of phosphorylation events of active centers ultimately ending in the phosphorylation and activation of transcription factors (Gaits et al., 1998; Gupta et al., 1995; Kyriakis et al., 1994).

The manner by which plasma membrane bound sensors transmit signals to mitogen-activated protein kinase kinase kinase (MAPKKK) is currently unknown. However, three activators of the mitogen-activated protein kinase kinase (MAPKK), Wis1 have been identified in *S. pombe,* Mcs4, Wak1 and Win1. Indeed, it is now apparent that the stress-activated pathway regulators Mcs4 and Wak1 respond to similar environmental cues while Win1 in addition to responding to these same cues, is also responsible for sensing nutritional changes (Shieh et al., 1997; Shieh et al., 1998). Thus, the transmission to the conserved MAPKK-MAPK (mitogen-activated protein kinase) module is an integration of multiple upstream signaling molecules.

The MAPKK Wis1, represents the entry point into the SAPK pathway. Wis1 activation by MAPKKK requires the dual phosphorylation of serine 469 and threonine 473 within the catalytic domain by upstream activators (Samejima et al., 1998). Wis1 tyrosine phosphorylation and activation of the MAPK Spc1/Sty1 results in Sty1 nuclear translocation and activation of transcription factors (Degols and Russell, 1997; Degols et al., 1996; Gaits et al., 1998; Shiozaki and Russell, 1995). The cytoplasmic localization of Wis1 is necessary for Sty1 activation and nuclear localization (Nguyen et al., 2002) whereas nuclear retention and accumulation of Sty1 occurs in an Atf1-dependent manner (Gaits et al., 1998) (Figure 1-4).

1-5-4-2 SAPKs and cell cycle regulation

The initial observation that cells deleted of *wis1*, *sty1* or *atf1* were elongated and unable to arrest in G_1 when deprived of nitrogen led to investigation of the roles the SAPK pathway perform in cell cycle regulation (Kanoh et al., 1996; Warbrick and Fantes, 1991). Initially, Wis1 was shown to be a dose-dependent regulator of mitosis (Warbrick and Fantes, 1991). Indeed, like Cdc25, overexpression of Wis1 results in early entry into mitosis at decreased cell size (Warbrick and Fantes, 1991). It is possible that Wis1 overexpression causes activation and nuclear translocation of Sty1, activation of Atf1 and subsequent aberrant transcription of stress response genes that initiate cell cycle delay.

Nuclear localization of activated Sty1 may be the common thread for cellular responses to stress in *S. pombe*, but there are instances where survival responses do not necessitate transcriptional regulation (Smith et al., 2002). For example, Sty1-dependent activation of the MAPK Srk1 likely results in sequestration of Cdc25 in the cytoplasm and prolonged G_2 delay as suggested by overexpression studies of Srk1 (Smith et al., 2002). Srk1 inhibits Cdc25 by phosphorylating the same Chk1-targeted serine/threonine residues leading to 14-3-3 binding to Cdc25 and ultimately Cdc2 inactivation (Lopez-Aviles et al., 2005). Thus, Srk1 represents a direct link between the stress-activated pathway and cell cycle regulation.

Although Srk1 activity is independent of genotoxic insults, the SAPK pathway is implicated in response to DNA damage and incomplete replication.

Figure 1-4. Schematic representation of the SAPK pathway in *S. pombe*. Responses to stresses are detected by receptors resulting in a series of phosphorylation events from MAPKKK-MAPKK-MAPK. Sty1 activation and nuclear localization results in activation of the transcription factor Atf1. It is not known how the transcription factor Pap1 is activated. Stress signals result in a Pap1 cytoplasmic localization where it is activated in an Sty1-dependent manner. Pap1 relocalization to the nucleus is required for its transcriptional activity.

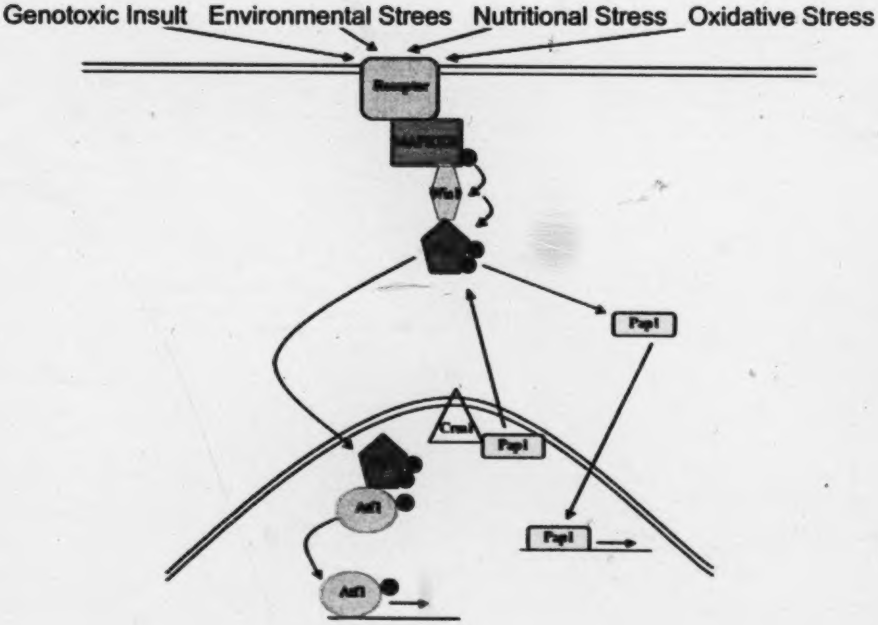
Genotoxic Insult
Environmental Strees
Nutritional Stress
Oxidative Stress
Receptor
Wis1
Pap1
Crm1
Pap1
Atf1
Pap1
Atf1

Recently it was reported that the SAPK pathway, acting through Atf1, results in compensatory action when *S. pombe* strains are defective in siRNA-mediated heterochromatin formation (Jia et al., 2004). Cell cycle arrest and subsequent repair responses to genome insult seems to require nucleation of heterochromatin (Martin et al., 1999; Mills et al., 1999). Further, in humans, ATF1 has been shown to interact with BRCA1, suggesting that this interaction may be important for regulating gene expression in response to DNA damage or incomplete replication (Houvras et al., 2000). Thus, the SAPK pathway, like the RNAi pathway, functions to exert control over cell cycle regulation and heterochromatin nucleation at two distinct levels.

1-6 Objectives

The goal of this thesis is to explore the potential roles that the core RNAi proteins Ago1, Dcr1 and Rdp1 perform in non-RNAi related pathways. Genetic evidence suggests that the roles core RNAi proteins perform in development can be uncoupled from gene-silencing. In addition, proteins involved in cell cycle regulation and response have been identified as having functional overlap with PPD proteins. In light of this ,I asked the question: if the cell cycle is impacted by the loss of Ago1, Dcr1 or Rdp1 is this effect due to loss of siRNA-mediated gene-silencing? Secondly, at what point is the cell cycle impacted? For instance, if cells are sensitive to genotoxins, are they unable to enact a checkpoint through Cdc2 inactivation, or are they able to undergo cell cycle arrest but unable to re-enter the cell cycle? Finally, I asked the question, what bearing does the cell cycle have on the localizations of Ago1, Dcr1 and Rdp1? As *S. pombe* encodes only one PPD, Dicer and RdRP family member, it seems likely that the localizations of these proteins in part dictate the particular functions they play in RNAi-dependent and independent pathways.

CHAPTER 2

MATERIALS AND METHODS

2-1 Reagents and Materials

Reagents and supplies were used as recommended by the manufacturer unless otherwise stated.

Table 2.1 Reagents

Reagents	Source
40% Acrylamide/Bis-acrylamide solution (29:1)	Bio-Rad
Glacial acetic acid	Fisher
Acid washed glass beads (425-600 micron)	Sigma
Adenine hemisulfate salt	Sigma
Agar	Difco
Agarose A, electrophoresis grade	Rose Scientific
Ammonium sulfate (enzyme grade)	Fisher
Ammonium persulphate	BDH
Ampicillin	Sigma
Bacto-tryptone	Difco
Bacto-yeast extract	Difco
Bovine serum albumin (BSA) fraction V	Sigma
Bromophenol blue	BDH
Complete^{TM} EDTA-free protease inhibitors	Roche
Complete synthetic media (CSM) drop out mixtures	Bio101 Systems
Coomassie Brilliant Blue	ICN
4',6-diamidino-2-phenylindole (DAPI)	Sigma
Diatomaceous earth	Sigma
Dimethyl sulphoxide (DMSO)	Sigma
Dithiothreitol (DTT)	Sigma
EMM	Stratagene, Bio 101 Systems
EPON resin (TAAB 812 resin)	Marivac
Ethanol	Commercial Alcohols
Ethylenediaminetetraacetic acid (EDTA)	Sigma
Formaldehyde, 37% (v/v)	Sigma
Glycerol	BDH
Glycine	EM Science
Guanidine hydrochloride	EM Science
HEPES	Invitrogen
L-Histadine	Sigma
Hydrochloric acid	Fisher
Isopropanol	Fisher
Kanamycin	Sigma
L-Lysine hydrochloride	Sigma
Lauria broth base	Invitrogen
LB agar	Invitrogen
Leptomycin B	Sigma, LC Laboratories
L-Leucine	Sigma
Malt extract	Difco
Methanol	Fisher
N,N,N',N',-tetramethylenediamine (TEMED)	Invitrogen
Nonidet P-40 (NP40)/IGEPAL CA-630	Sigma
Paraformaldehyde	Fisher
Phenol, buffer saturated	Invitrogen
Piperazine-N.N'-bis[2-ethanesulfonic acid] (PIPES)	Sigma
Polyethylene glycol (PEG) 3350	Baker
Protein-A sepharose	Amersham Biosciences
Restore^{TM} Western Blot Stripping Buffer	Pierce
Sodium azide	Sigma
Sodium chloride	Sigma
Sodium dodecyl sulphate (SDS)	Bio-Rad
Sodium hydroxide	Sigma
Sodium salicytate	EM Science
Sorbitol	Sigma
Sucrose	BDH
Sytox Green	Molecular Probes

Table 2.1 (continued)

Terrific Broth (TB)	GibcoBRL
Thiabendazole	Sigma
Tris base	Roche
Triton X-100	BDH
Tween 20 (polyoxyethylenesorbitan monolaureate)	Caledon
Uracil	Sigma
Vectashield mounting medium	Vector Laboratories
Yeast extract	Difco
Yeast nitrogen base without amino acids and ammonium sulfate	Difco
Zymicase I enzyme	InterSpex Products, Inc.

Table 2.2 Multi-component systems

System	Source
Expand High Fidelity PCR system	Roche
QIAEXII Gel Extraction kit	Qiagen
QIAquick PCR Purification kit	Qiagen
QIAGEN Plasmid Midi kit	Qiagen
Superscript II	Invitrogen
TnT Coupled Transcription/Translation kit	Promega
Wizard Plus Minipreps DNA purification system	Promega

Table 2.3 DNA modifying enzymes

Enzymes	Source
Calf intestinal alkaline phosphatase	NEB, Roche
DNA polymerase I, large fragment (Klenow)	Invitrogen
Micrococcal nuclease	Dr. M. Schultz (Dept. Biochemistry, University of Alberta)
Restriction Endonucleases	NEB, Promega, Invitrogen
Shrimp alkaline phosphatase	Invitrogen
T4 DNA ligase	NEB, Invitrogen

Table 2.4 Radiochemicals

Radiochemicals	Source
^{32}P-dCTP	Amersham Biosciences
^{35}S methionine (in vitro translation grade)(1000 Ci/mmol)	Amersham Biosciences
Pro-mix ^{35}S methionine-cysteine (1000 Ci/mmol)	Amersham Biosciences

Table 2.5 Detection systems

System	Source
Immobilon-P polyvinylidene fluoride (PVDF) membrane	Millipore
Rx film (Western Blot)	Fuji
Supersignal Westpico Chemiluminescent Substrate	Pierce
Trans-Blot Transfer Medium-nitrocellulose membrane	Bio-Rad
X-Omat AR film (Fluorography)	Kodak

Table 2.6 Molecular size standards

Marker	Source
1 kb DNA ladder	Invitrogen
10 kDa prestained protein Ladder	NEB
^{14}C-labelled protein standards	Amersham Biosciences
PageRule pre-stained ladder	Fermentas
Pre-stained protein ladder (10-180 kDa)	Fermentas

2-2 Commonly used buffers, media and drugs

Table 2.7 Commonly used buffers and solutions

Buffer	Ingredients
2 x protein sample buffer	200 mM DTT, 4% SDS, 0.2% bromophenol blue, 20% glycerol, 100 mM Tris-HCl, pH 6.8
2XYT	Bacto-tryptone (16 g/L), bacto-yeast extract (10 g/L), NaCl (5 g/L), pH 7.5
5 x First strand buffer	250 mM Tris-Cl, pH 8.3, 375 mM KCl, 15 mM $MgCl_2$
6 x DNA gel loading buffer	40% sucrose, 0.25% bromophenol blue, 0.25% xylene cyanol FF
20 x SSC	175.3 g/L NaCl, 88.2 g/L citric acid
AE buffer	50 mM sodioum acetate, pH 5.3, 10 mM EDTA
Column Wash Solution (Merlin V)	200 mM NaCl, 20 mM Tris-HCl, pH 7.5, 5 mM EDTA, 50% isopropanol
Denaturing Buffer (Southern Blot)	0.5 M NaOH, 1.5 M NaCl
Fractionation Buffer 1	20 mM sodium citrate, 20 mM sodium phosphate, pH 5.6
Fractionation Buffer 2	50 mM citric acid, 50 mM sodium phosphate, 1.2 M sorbitol
Fractionation Buffer 3	0.1 M sorbitol, 20 mM potassium acetate, 20 mM HEPES
FSB	10 mM KAc, pH 7.5, 45 mM $MnCl_2$, 10 mM $CaCl_2$, 10 mM KCl_3, 3 mM hexaminecobalt chloride, 10% glycerol
Neutralizing Buffer (Southern Blot)	0.5 M Tris-Hcl, pH 7.0, 1.5 M NaCl
Phosphate buffered saline (PBS)	137 mM NaCl, 2.7 mM KCl, 8mM Na_2HPO_4, pH 7.4
PEM	100 mM PIPES, pH 6.9, 1 mM EGTA, 1 mM $MgSO_4$
PEMS	PEM, 1 M sorbitol
PEMBAL	PEM, 1% bovine serum albumin, 0.1% sodium azide, 0.1 M L-lysine
Quick Hybridizing Solution (Southern Blot)	6 x SSC, 7% SDS, 100 µg/ml ssDNA
Radioimmunoprecipitation buffer (RIPA)	150 mM NaCl, 0.5% sodioum deoxycholate, 0.1% SDS, 1% NP40, 50mM Tris-HCl, pH 8.0
SDS-PAGE running buffer	250 mM glycine, 0.1% SDS, 100 mM Tris Base
SDS-PAGE resolving gel buffer	0.1% SDS, 374 mM Tris-Hcl, pH 8.8
SDS-PAGE stacking gel buffer	0.1% SDS, 250 mM Tris-HCl, pH 6.8
Solution I	50 mM glucose, 10 mM EDTA, 25 mM Tris-Cl, pH 8.0, 100 µg/ml RNaseA
Solution II	0.2 M NaOH, 1% SDS
Solution III (Merlin III)	5.0 M potassium acetate (60 ml), glacial acetic acid (11.5 ml), sterile water (28.5 ml)/100 ml
SP1	1.2 M sorbitol, 50 mM sodium citrate, 50 mM sodium phosphate, 40 mM EDTA, pH 5.6
SP2	1.2 M sorbitol, 50 mM sodium citrate, 50 mM sodium phosphate, pH 5.6
TAE	40 mM Tris acetate, 1 mM EDTA, pH 8.0
TBS	137 mM NaCl, 2.7 mM KCl, 24 mM Tris-HCl, pH 7.4
TBS-T	TBS, 0.05% Tween 20
Protein transfer buffer	200 mM glycine, 25 mM Tris Base, 20% methanol
TE	1 mM EDTA, 10 mM Tris-HCl, pH 7.5
TEN	20 mM Tris, pH 7.5, 50 mM EDTA, 100 mM NaCl

Table 2.8 Yeast media

Media	Ingredients
Edinburg minimal media (EMM)	As per Stratagene or Bio 101 Systems + 225 mg/L adenine, histidine, leucine, uracil and lysine hydrochloride
Malt extract (ME)	3% (w/v) Bacto-malt extract (pH 5.5)
Yeast Extract (YE)	0.5% (w/v) Oxoid yeast extract, 3% (w/v) glucose
Yeast extract + supplements (YES)	YE + 225 mg/L adenine, histidine, leucine, uracil and lysine hydrochloride
For solid media add 20 g/L agar	

Table 2.9 Drugs and antibiotics

Drug	Source	Stock	Working Concentration	Usage
Camptothecin (CPT)	Sigma	100 mM in $dH_2$0	1 µM	Topoisomerase inhibitor, DNA strand breaks
G418	Sigma	N/A	200 mg/L	Integration selection
Hydroxyurea (HU)	Sigma	1.5 M in $dH_2$0	5-10 mM	Ribonucleotide reductase inhibitor (S-M arrest)
Leptomycin B (LMB)	Sigma	5.53 µg/ml	100 ng/ml	Nuclear export inhibitor
Thiabendazole (TBZ)	Sigma	20 mg/ml in DMSO	10 µg/ml	Microtubule destabilizing (G_2-M arrest)

2-3 Antibodies

Table 2.10 Primary antibodies

Primary antibody	Dilution (WB)	Source
Mouse anti-Cdc2 (PSTAIRE)	1:1000	Sigma
Mouse anti-C-myc (9E10)	1:1000	ATCC
Rabbit anti-Ago1 (GST-fusion) (amino acid residues 320-627)	1:600	This study
Rabbit anti-Ago1 (amino terminal peptide)	1:600	This study
Rabbit anti-BiP (JARM13)	1:10000	Dr. John Armstrong, University of Sussex
Rabbit anti-Cdc2-P Tyr-15	1:1000	Cell Signaling Technology
Rabbit anti-Cnx1	1:5000	Dr. Luis Rokeach, University of Montreal
Rabbit anti-GAPDH	1:1000	Abcam
Rabbit anti-G6PDH	1:1000	Abcam
Rabbit anti-GFP	1:3000	Dr. Luc Berthiaume, University of Alberta
Rabbit anti-SKL	1:1000	Dr. Richard Rachubiniski, University of Alberta
Rat anti-HA (3F10)	1:1000	Roche

Table 2.11 Secondary antibodies

Secondary antibody	Source
Goat anti-Rabbit-HRP	Jackson Immuno Research
Goat anti-Rabbit-FITC	Biomedia
Goat anti-Rat-HRP	Serotec
Goat anti-Mouse-HRP	Jackson Immuno Research

2-4 Oligonucleotides

Table 2.12 Primers used in this study

Primer Title	Primer Sequence	Engineered Sites	Production Usage
1fEgfp	5'-agctctgcagggatccttagcggccgcttggtaccatggtgagcaagggcgag-3'	*Pst*1, *BamH*1, *Not*1, *Kpn*1	C-terminal EGFP cassette
1rEgfp	5'-tcgagagctcggccggtcacttgtacagctcgtccatg-3'	*Sac*1	C-terminal EGFP cassette
2fEgfp	5'-acgtctgcagggccggaccatggtgagcaagggcgag-3'	*Pst*1	N-terminal EGFP cassette
2rEgfp	5'-tgacgagctcgtcatggatcctcttaagtggtacccttgtacagctcgtccatg-3'	*Sac*1, *BamH*1, *Afl*II, *Kpn*1	N-terminal EGFP cassette
fRDPn	5'-attgggtaccatggcagtttcgttaaatgactttataag-3'	*KpnI*	Egfp:rdp1
r2RDPn	5'-attaggatccgcaaaattattagcagtaagcatggcttttc-3'	*BamH*1	Egfp:rdp1
GFPf(Pst1)	5'-ggcctgcaggttatgagtaaaggagaagaa-3'	*Pst*1	GFP-megaprimer forward
GFPr:Ago1f	5'-gctatttctgagcttggtttatacgatttgtatagttcatccatg-3'		GFP-magaprimer reverse
Ago1r(Sac1)	5'-gggagctcttacatataccacatctttg3'	*Sac*1	GFP:ago1
AgoF(Sal1)	5'-ggggtcgacgatgtcgtat-3'	*Sal*1	N-terminal HA:ago1 (pSLF273)

Table 2.12 (continued)

AgoR(Sal1)	5'-gggtcgacttacataccac-3'	*Sal*1	N-terminal HA:ago1 (pSLF273)
Frdcr1	5'-ctgcaggtcgacaccatggatatttcaagttttc-3'	*Pst*1	Recombination into pAAUN-C-terminal Egfp. dcr1:EGFP
Rrdcr1	5'-cgagctcggtactcacttgtacagctcgtc-3'	*Sac*1	Recombination into pAAUN-C-terminal Egfp. dcr1:EGFP
RdpF(Not1)	5'-tttgcggccgcgcagtttcgttaaatgac-3'	*Not*1	N-terminal HA:rdp1 (pSLF273)
RdpR(BglII)	5'-tttagatctttaaaaattattagctgtaagc-3'	*Bgl*II	N-terminal HA:rdp1 (pSLF273)
5'ago1utrF	5'-agcagtgttcaaaaaaacaagcgg-3'		One-step ago1 replacement
5'ago1utrR/pFA6aF	5'cctaatctagggtttggtatatataagcttccaaccgccaaagcgaattbtcttcagccaactcgtcctttatgattcagaattcgagctcgtttaaac-3'		One-step ago1 replacement
5'ago1utrFprobe	5'-ggagtcaagttcaccttt-3'		Probe production
5'ago1utr-Rprobe	5'-cgtgtcgttaatatactacta-3'		Probe production
3'ago1utrF/pFA6aR	5'-ataaggaagtaaaagttgtgggcaatccagtagtcaatcgtatatctatttcattacttattgcatgcaatccatcaaagaattcgagctcgtttaaac-3'		One-step ago1 replacement
3'ago1utrR	5'-cattattgacttgtttttgc-3'		One-step ago1 replacement

2-5 Plasmids

Table 2.13 Plasmids used in this study

Vector	Source	Institution
pGEM-T	Promega	
pREP3X	Dr. S. Forsburg	University of Southern California
pSLF273	Dr. S. Forsburg	University of Southern California
pDS473a	Dr. S. Forsburg	University of Southern California
pREP41X-HA	Dr. P. Provost	Centre de Recherche du CHUL
PREP41X-dcr1-HA	Dr. P. Provost	Centre de Recherche du CHUL
pREP41X-GFP	Dr. P. Young	Queens University
pAAUN	Dr. D. Beach	Cold Spring Harbor Laboratory
pAALN	Dr. D. Beach	Cold Spring Harbor Laboratory
pGBK-T7	Clontech	
pGAD-T7	Clontech	

2-6 *Schizosaccaromyces pombe* strains used in this study

Table 2.14 Strains

Strain	Genotype	Source	Institution
FY254	*can1-1 leu1-32 ade6-M210 ura4-D18* h$^-$	Dr. S. Forsburg	University of Southern California
FY261	*can1-1 leu1-32 ade6-M216 ura4-D18* h$^+$	Dr. S. Forsburg	University of Southern California
JC254K	*ago1*$^+$*::G418*^{R} *can1-1 leu1-32 ade6-M210 ura4-D18* h$^-$	Lab Stock	
JC261K	*ago1*$^+$*::G418*^{R} *can1-1 leu1-32 ade6-M216 ura4-D18* h$^+$	Lab Stock	
TV292	*ago1*$^+$*::kanMX6 ura4-D18* DS/E h$^-$	Dr. T. Volpe	Cold Spring Harbor Laboratory
TV293	*dcr1*$^+$*::kanMX6 ura4-D18 DS/E* h$^-$	Dr. T. Volpe	Cold Spring Harbor Laboratory
TV294	*ura4-D18 DS/E* h$^-$	Dr. T. Volpe	Cold Spring Harbor Laboratory
TV296	*rdp1*$^+$*::kanMX6 ura4-D18 DS/E* h$^-$	Dr. T. Volpe	Cold Spring Harbor Laboratory
Q2016	*cdc25-GFPint cdc25:ura4*$^+$ *ura4-D18 leu1-32* h$^-$	Dr. P. Young	Queens University
Q2017	*cdc25-GFPint cdc25:ura4*$^+$ *ura4-D18 leu1-32* h$^+$	Dr. P. Young	Queens University
Hu906	*dcr1-HA:kanMX leu1-32 ade6-DN/N ura4-DS/E*	Dr. P Provost	Centre de Recherche du CHUL

2-7 DNA analyses and modification

2-7-1 *Isolation of plasmid DNA from E. coli*

Plasmid DNA was prepared using commercially available preparation kits [WizardPlus (miniprep) or Qiagen (midiprep)] according to the manufacturers' specifications. Alternatively, a diatomaceous earth protocol was employed as follows. Bacterial pellets were resuspended in 100 μl of Solution I (Table 2.7). Freshly prepared Solution II (200 μl) (Table 2.7) was added and the tube was inverted 4 times followed by a 5 minute incubation at room temperature to allow for lysis of the bacteria. Proteins were precipitated upon addition of Solution III (150 μl) (Table 2.7) followed by centrifugation at 14 000 x g for 10 minutes to pellet proteins and chromosomal DNA. The supernatant fractions were transferred to new tubes containing 600 μl of diatomaceous earth slurry. The slurry/supernatant mixture was rocked for 10 minutes and transferred to a column comprised of a 1 ml stuffed micropipette tip under vacuum. The DNA-bound diatomaceous earth trapped on top of the filter after the application of the vacuum was washed 2 times with 1 ml column wash (Table 2.7) and subsequently centrifuged at 5000 x g for 1 minute to remove any residual column wash. MilliQ H_2O preheated to 70°C was then applied to the column which was then centrifuged at 5000 x g for 1 minute to facilitate the elution of the DNA from the diatomaceous earth.

Diatomaceous earth was prepared as follows: 3 grams of diatomaceous earth was washed on filter paper using 300 ml de-ionized water, dried in a desiccator for 24 hours and mixed with 300 ml of guanidine-HCl and Merlin III (Table 2.7) using gentle heating.

2-7-2 *Isolation of yeast genomic DNA*

Yeast strains were grown to an OD_{595}= 1.0 at 30°C. Cells were pelleted by centrifugation at 3000 x g for 5 minutes and washed with 5 ml of SP1 (Table 2.7). The cells were pelleted, resuspended in 5 ml of SP2 (Table 2.7) containing 20 mg/ml Zymicase I enzyme and incubated for one hour at 37°C to allow for digestion of the cell walls and production of spheroplasts. The spheroplasts were pelleted by spinning at 3000 x g for 5 minutes and resuspended in 3 ml of TE (Table 2.7) containing 1% SDS. Lysis was verified by phase contrast microscopy. In some cases the mixture was heated to 65°C to increase the amount of cell lysis. One ml of 5 M potassium acetate was added and the mixture was incubated for 30 minutes on ice. Unlysed cells and debris were pelleted by centrifugation at 5000 rpm for 15 minutes and an equal volume of ice-cold isopropanol was added to the supernatant followed by incubation for 5 minutes on ice. Nucleic acids were pelleted by a 5000 x g spin for 15 minutes. The pellet was washed with 70% ethanol and dried at room temperature for approximately 15 minutes. The pellet was then resuspended in 200 μl of TE containing 0.05 mg/ml RNaseA and incubated for one hour at 37°C followed by a 30 minute incubation at 50°C upon addition of proteinase K (0.02 mg/ml). The DNA-containing solution was then phenol-chloroform extracted. To precipitate DNA from the aqueous fraction, 0.1 volumes of 3 M sodium acetate and 2 volumes of 95% ethanol were added, incubated for 15 minutes on ice and centrifuged at 14000 x g for 15 minutes at 4°C. The pellet was then washed in 70% ethanol, dried for 15 minutes at room temperature and resuspended in 100 µl of TE (Table 2.7).

2-7-3 *Isolation of Plasmid DNA from Yeast*

Cultures (10 ml) were grown to an OD_{595}=1.0 and pelleted at 3000 x g for 5 minutes. The cells were resuspended in 1.5 ml of 50 mM citrate/phosphate buffer (0.2 M sorbitol, 20 mg/ml Zymicase, pH 5.6) and incubated for 1 hour at 37°C. The resulting spheroplasts were harvested by centrifugation at 1000 x g for 5 minutes. Spheroplasts were resuspended in 300 µl TE (Table 2.7) containing 1% SDS (v/v) and subsequently incubated for 5 minutes at 65°C. Potassium acetate (5 M) was added (0.1 volumes) to the mixture and a 30 minute incubation on ice ensued. The slurry was then centrifuged for 10 minutes at 14000 x g at 4°C and the supernatant was subjected to phenol-chloroform extraction and ethanol/sodium acetate precipitation as detailed in Section 2.7.2.

2-7-4 *Polymerase chain reaction*

DNA sequences were amplified using indicated primers (Table 2.12) in conjunction with Expand High Fidelity Polymerase (Roche) according to the manufacturer's specifications. The reactions normally contained approximately 100 ng of cDNA or 1µg of genomic DNA templates, 10µM dNTPs, 2 units of polymerase and 1 x reaction buffer. Thirty cycles for all reactions were performed using either a

DeltaCycler II™ (Ericomp) or Robocycler Gradient 40 (Stratagene) Hot Top system. dNTPs and proteins were removed from the PCR products using a QIAquick PCR purification kit (QIAGEN) before they were subjected to restriction endonuclease digestion and/or gel electrophoresis.

2-7-5 *Restriction endonuclease digestion*

Reaction volumes of 20 µl were typically used for complete digestion of 0.5 to 3 µg of DNA as per the manufacturer's specifications.

2-7-6 *Dephosphorylation of 5', 3' or blunt ended linearized vectors*

To enrich the proportion of positive clones and minimize the occurrence of vector self-ligation when using blunt-ended or single cut vectors, calf intestinal alkaline phophatase or shrimp alkaline phosphatase was used to dephosphorylate the ends of linearized vectors. The dephosphorylation proceeded according to the manufacturer's recommendations. Termination of the reaction was mediated by heat inactivation of the reaction mixture at 65°C for 15 minutes.

2-7-7 *Filling-in of 5' overhangs*

To generate blunt-ends for ligation, 5' DNA overhangs were filled in using the Klenow fragment of DNA polymerase I. Five units of enzyme and 25 µM of dNTPs were used in reactions containing 1-2 µg of DNA and incubated for 30 minutes at 30°C. Reactions were terminated by heat inactivation at 75°C for 10 minutes.

2-7-8 *Ligation of DNA*

T4 DNA ligase was used to ligate DNA fragments. Reactions were carried out according to the manufacturer's specifications. Typically a 20 µl reaction contained

10 fmol of vector and 30 fmol of insert for sticky-end ligations. Blunt-end reactions required approximately 30 fmol of vector and 90 fmol of insert. Reactions were carried out for 1 hour at room temperature (sticky-end) or 16 hours at room temperature (blunt-end).

2-8 Transformation with plasmid DNA

2-8-1 *Transformation of* E. coli

2-8-1-1 Transformation of chemical competent *E. coli*

Chemically competent *E. coli* DH5αwere prepared as follows: Bacterial cultures were grown at 37°C to an OD_{600}= 0.3-0.5 in 30 ml 2XYT (Table 2.7). Cells were collected by centrifugation (4000 x g, 15 minutes) at 4°C and then washed in 5 ml of ice-cold FSB (Table 2.7). After centrifugation, cells were resuspended in 3 ml FSB containing 105 µl DMSO, incubated on ice for 15 minutes, washed twice with ice-cold FSB, aliquoted into 200 µl volumes and frozen in a dry ice-ethanol bath and then stored at –80°C.

To transform chemical competent bacteria, DNA was added to ice-thawed transformation competent *E. coli* DH5α cells. The mixture was incubated on ice for 30 minutes, subjected to a 42°C heat shock for 45 seconds followed by incubation on ice for a 2 minute recovery period. The cells were then incubated in 2XYT (Table 2.7) for one hour at 37°C and spread onto LB agar plates containing the appropriate antibiotics.

2-8-1-2 Transformation of electrocompetent *E. coli*

Electrocompetent *E. coli* DH5α were prepared as follows: Bacterial cultures (100 ml) were grown in LB at 37°C with shaking to an OD_{600}= 0.5-0.8. Cells were collected by centrifugation (4000 x g, 15 minutes, 4°C) and washed 2 times with 500 ml ice-cold water. This was followed by a wash in ice-cold 10% glycerol (v/v). Samples were subsequently resuspended in 1 ml of ice-cold 10% glycerol and then divided into 50 μl aliquots that were frozen in a dry ice-ethanol bath and stored at –80°C.

Cells were thawed on ice prior to transformation with 0.5% of a ligation mixture. Briefly, cells and DNA were incubated together on ice for 5 minutes and transferred to an ice-cold 0.1 cm gap electroporation cuvette (Bio-Rad). The cuvette and contents were subjected to the manufacturers' pre-set electrical pulse using a Bio-Rad Micropulser. Directly after the electrical pulse, 1 ml of TB (Table 2.7) was added to the cuvette and the contents were then transferred to a microfuge tube, which was incubated for 1 hour at 37°C. Cells were plated onto LB agar containing the appropriate antibiotic.

2-8-2 *Transformation of S. pombe strains*

2-8-2-1 Large-scale transformation

Typically, 50 ml cultures of *S. pombe* strains were grown to OD_{595}= 1.0 (1 X10^7 cells/ml) in YE (Table 2.7). Cells were pelleted (3000 x g, 10 minutes), washed in 50 ml sterile water and then resuspended in 1 ml of sterile water prior to transfer to a microfuge tube. The cells were then washed with 1 ml of 0.1 M lithium acetate-TE and subsequently resuspended at 2 x 10^9 cells/ml in 1.0 M lithium acetate-

TE. Salmon sperm DNA (2 µl of a 10mg/ml stock) and 1 µg of transforming DNA were added to 100 µl of cells and incubated at room temperature for 10 minutes. Forty percent PEG-lithium acetate-TE (260 µl) (Table 2.7) was added and cells were incubated for 30 minutes at 30°C. Following incubation, 43µl of pre-warmed DMSO was added and the mixture was subjected to heat shock at 42°C for 5 minutes. The cells were pelleted by centrifugation (3000 x g, 5 minutes), washed in sterile water, resuspended in 150 µl water and spread on plates lacking specific nutrients to allow for selection of transformants.

2-8-2-2 Small-scale transformation

Approximately 25 µl of yeast colonies obtained from solid media cultures less than 1 week old were suspended in sterile water, pelleted at 14000 x g (5 seconds), resuspended in 1 ml of 0.1 M lithium acetate and incubated for 5 minutes at 30°C. The cells were then pelleted and the following were added in order; 240 µl PEG (50% w/v), 36 µl 1.0 M lithium acetate, 50 µl ssDNA (2 mg/ml stock), 1 µg plasmid DNA and 20 µl sterile water. The mixture was vortexed at top speed for one minute followed by heat shock at 42°C for 20 minutes. Cells were pelleted, resuspended in 100 µl of sterile water and plated according to auxotrophic requirements for selection.

2-9 Isolation of *S. pombe* RNA

Cultures (10 ml) were grown to OD_{595}= 1.5 at 30°C, harvested at 3000 x g and resuspended in 300 µl AE buffer (Table 2.7). The mixture was transferred to a microfuge tube and 40 µl of 10% SDS was added and mixed by vortexing for 1 minute. An equal volume of phenol, pre-equilibrated with AE buffer, was added, vortexed briefly and incubated for 4 minutes at 65°C. The mixture was chilled on dry ice-ethanol until crystals appeared in the microfuge tube, at which time the tube was centrifuged for 2 minutes at 14000 x g. The upper aqueous phase was added to an equal volume of phenol-chloroform, vortexed 10 seconds and then centrifuged at room temperature (14000 x g) for 5 minutes. To the aqueous phase was added 0.3 M (pH 5.3) sodium acetate and 2.5 volumes of ethanol. The RNA was pelleted by centrifugation (14000 x g, 5 minutes), washed in 80% ethanol, dried and resuspended in 20 µl of nuclease-free water. Long-term storage of the RNA was at –80°C.

2-10 Reverse transcriptase-polymerase chain reaction (RT-PCR)

The cDNA encoding Ago1 was generated using first strand synthesis followed by PCR. Briefly, a 12 µl reaction containing 200 ng of random primers (Invitrogen), 3 µg of total RNA and sterile water were heated to 70°C for 10 minutes and chilled on ice. Four µl of first strand buffer (Table 2.2), 2 µl of 0.1 M DTT and 1 µl of a 10 mM dNTP mixture were added to the contents of the tube, mixed by pipetting and incubated for 2 minutes at 42°C. Two hundred units of Superscript II were added followed by incubation at 25°C for 10 minutes. The tube was then transferred to 42°C for a further 50 minutes before heat inactivation of the enzyme (70°C incubation for 15 minutes). Complementary RNA was removed by incubation of the mixture in the presence of RNaseH (37°C, 20 minutes). Using the manufacturers' specifications, Expand high fidelity polymerase (Roche) was used to amplify the cDNA using primers AgoF(SalI) and AgoR(SalI) (Table 2.12) in addition to 2 µl of the cDNA template.

2-11 Agarose gel electrophoresis

2-11-1 *DNA agarose gel electrophoresis*

Electrophoresis grade agarose (0.8-1.5% (w/v)) was dissolved by heating in TAE (Table 2.7). Prior to congealing of the gel, 0.3 µg/ml ethidium bromide was added. DNA samples mixed with 6 x gel loading dye (Table 2.7) were resolved while immersed in TAE (Table 2.7). The fragments were visualized and images captured using a Fluorochem imaging system (Alpha Innotech Corporation).

2-11-2 *RNA agarose gel electrophoresis*

The quality of the RNA used for RT-PCR was assessed by the method indicated in DNA agarose gel electrophoresis (Section 2.11.1). The appearance of distinct, non-smeared ribosomal RNA bands at approximately 1.8 and 3.5 kb, indicated a successful extraction of quality RNA.

2-12 Southern Blot analyses

2-12-1 *Transfer of DNA fragments to nitrocellulose membranes*

Genomic DNA was subjected to restriction endonuclease digestion (Section 2.7.5) and the resulting fragments separated on 1% agarose gels (Section 2.11.1). DNA was denatured in Denaturing Buffer (Table 2.7) for 30 minutes at room temperature, rinsed with MilliQ water and incubated for a further 30 minutes in Neutralizing Buffer (Table 2.7). The gels were then incubated in 20 x SSC for 30 minutes prior to transfer of DNA to nitrocellulose membranes using a Turboblotter™ Rapid downward transfer system (Schleicher & Schuell) as per manufacturer's specifications. DNA fragments were covalently bound to the wet membranes by UV cross-linking (120 J/m^2) (Hoeffer UVC500) prior to hybridization (Section 2.17.1.2.3).

2-12-2 *^{32}P-labelled probe production*

Genomic DNA was used as a template for the amplification of an *ago1* 5'UTR region to be used as a probe for detection of *ago1* gene replacement. The fragment was amplified by PCR using the primers 5'ago1utrFprobe and 5'ago1utrRprobe (Table 2.12) and radiolabelled follows: The purified fragment (25 ng) was mixed with 200 ng of random label primers (Invitrogen) and water was added to a volume of 29.5 µl. The mixture was boiled for 5 minutes followed by incubation on ice for 5 minutes. To the cooled mixture was added 10 x dNTP-C mix (Invitrogen), 5 x random label buffer (Invitrogen), 2 U of large fragment polymerase I (Invitrogen) and 5 µl ^{32}P-dCTP (10mCi/ml). The resulting volume was 50 µl. This mixture was incubated at 37°C for 2 hours after which time 50 µl of TEN (Section 2.2, Table 2.7) was added. The mixture was filtered through a Sephadex/glass wool filter by centrifugation at 500 x g for 3 minutes to remove unincorporated isotopes. Incorporation of the radiolabelled nucleotide into the probe was assayed using a Beckman Coulter LS6500 Multi-Purpose Scintillation Counter.

2-12-3 *Southern blot hybridization*

Nitrocellulose membranes containing UV cross-linked fragments were pre-hybridized for 2 hours at 62°C in Quick Hybridizing Solution (Table 2.7). Following the pre-hybridization, boiled radiolabelled probe (Section 2.17.1.2.2) was added to pre-heated (62°C) Quick Hybridization Solution (10^6 cpm/ml). The membranes were hybridized overnight in a HYBAID micro-4 rotator. Membranes were rinsed once in

1 x SSC containing 0.1% SDS and then washed for 15 minutes at room temperature in a fresh aliquot of the same solution. Membranes were then washed twice in 1 x SSC/0.1% SDS at 45°C for 15 minutes, wrapped in Saran Wrap™ and exposed to X-Omat AR film over night at –80°C. For re-probing, membranes were stripped by incubation in freshly boiled (5 minutes) 0.1% SDS and rotated for 30 minutes at room temperature. Membranes were then washed 2 times in 2 x SSC at room temperature and pre-hybridized as described above.

2-13 Construction of cDNAs encoding tagged RNAi effector proteins

All primers and cDNAs used for the production of epitope tagged cDNAs are documented in Table 2.12 and Table 2.13 respectively. The production of GFP tagged fusion proteins was as follows.

2-13-1 *GFP-Agol construction*

GFP cDNA containing 16 bases of complementary *ago1* sequence was amplified from pREP41-GFP by PCR using primers GFPf(*Pst*1) and GFPr:ago1f. The resulting cDNA was purified and used as a mega-primer together with primer Ago1r(*Sac*1) to amplify *ago1*-specific cDNA from an *ago1* cDNA template resulting in a cDNA encoding GFP-Ago1. Fragments were directionally ligated into pAALN using *Pst*1 and *Sac*1 sites resulting in pAALN-GFP-*ago1*.

2-13-2 *EGFP-Rdpl construction*

rdp1 (SPAC6F12.09) was amplified from genomic DNA using primers Rdpf(Not1) and Rdp1r(BglII). The resulting product was ligated to pGEM-T vector to be used as a template. Primers fRDPn and r2RDPn were used to amplify *rdp1* cDNA containing engineered sites *Kpn*1 and *Bam*H1. The PCR product was digested with *Kpn*1 and *Sac*1 and ligated-in frame with the EGFP amino-terminal tagging cassette cloned into pAAUN resulting pAAUN-EGFP-*rdp1*.

2-13-3 *Dcr1-EGFP construction*

A *dcr1* cDNA was amplified from pREP41X-dcr1:HA (Table 2.13) using primers Frdcr1 and Rrdcr1, and then inserted into pAAUN by recombination. Briefly, 0.4 pmol of PCR product and 0.1 pmol of linearized vector were incubated in a reaction mixture totaling 20 μl containing vector, insert, 1x recombination buffer (30 mM Tris, pH 7.9, 5 mM $MgCl_2$, 70 mM NaCl, 1.8 mM DTT and 80 μg/ml acetylated bovine serum albumin), single strand binding protein (500 ng) and Vaccinia virus recombination enzyme (12 ng/μl) (a kind gift from Dr. David Evans) diluted in dilution buffer (25 mM potassium phosphate buffer, pH 7.4, 5 mM β-mercaptoethanol, 1 mM EDTA, 50% glycerol and 100 μg/ml bovine serum albumin). The reaction mixture was incubated at 37°C for 20 minutes. Stop buffer (3.2 μl) (0.4 M EDTA, 4 mg/ml proteinase K and 0.6% SDS) was added followed by an incubation at 37°C for 20 minutes. One microlitre of recombination mixture was used for transformation of *E. coli*.

2-13-4 *HA-Ago1 and HA-Rdp1 construction*

The production of HA-tagged Ago1 and Rdp1 was as follows. *ago1*$^+$ cDNA was amplified using primers AgoF(Sal1) and AgoR(Sal1). *rdp1*$^+$ cDNA was amplified using primers RdpF(Not1) and RdpR(BglII). The resulting products were ligated into pSLFS273 at *Sal*1 or *Not*1/*Bgl*II sites respectively, resulting in amino terminal fusions with the influenza HA epitope.

2-14 Automated DNA sequencing

All DNA fragments amplified by PCR were sequenced using the core facilities within the departments of Biological Sciences, Biochemistry and Cell Biology at the University of Alberta to verify the sequence of the products. The sequencing facilities use a protocol based on the incorporation of fluorescently labeled dideoxy terminators during the elongation stage.

2-15 Protein gel electrophoresis and detection

2-15-1 *Sodium dodecyl-sulphate polyacrylamide gel electrophoresis (SDS-PAGE)*

SDS-PAGE was used to resolve proteins as described by Sambrook *et al.* (1989). Sample buffer (5x) was added to protein samples to a final volume of 1 x which were then denatured at 95°C for 5 minutes and separated by discontinuous gel electrophoresis. To prepare the stacking gel, 4% acrylamide/Bis-acrylamide was added to the SDS-PAGE stacking buffer (Table 2.7). The resolving gel was comprised of 5, 8, 10 or 12% acrylamide/Bis-acrylamide added to the SDS-PAGE resolving buffer (Table 2.7). Prior to gel casting, 0.1% TEMED (v/v) and 0.1% ammonium persulphate (w/v) were added. Electrophoresis was conducted in SDS-PAGE running buffer (Table 2.7) using a Bio-Rad mini Protean II or Protean III vertical gel system.

2-15-2 *Western blot analyses*

2-15-2-1 Protein transfer

In preparation to transfer of proteins to PVDF membranes, SDS-PAGE gels were equilibrated for 5 minutes in protein transfer buffer (Table 2.7). PVDF membranes were wet in methanol for 1 minute, rinsed in deionized water and equilibrated in protein transfer buffer for 5 minutes. Transfer of the proteins to the membrane was achieved using a Bio-Rad Mini Trans-Blot™ Electrophoretic Transfer Cell at 280 mAmp for 1 hour. During the transfer, the apparatus was chilled in an ice water bath.

2-15-2-2 Immunoblotting

Following transfer of proteins, membranes were washed in TBS-T (Table 2.7) for 10 minutes and then blocked in TBS-T containing 5% skim milk for 1 hour at room temperature or overnight at 4°C. Primary antibodies were diluted in TBS-T/5% skim milk as described (Table 2.10). Typically, membranes were incubated with antibodies for 1 hour at room temperature. The exceptions were rat anti-HA and rabbit anti-Cdc2-P, which required overnight incubations at 4°C. Following incubation with primary antibodies, membranes were washed in TBS-T for 1 hour. During this wash period the TBS-T solution was changed a minimum of 5 times. Secondary antibodies were used according to the manufacturer's specifications (Table 2.11). Typically, a secondary antibody was incubated with the membrane for 1 hour after which the membrane was washed 3 times in TBS-T over 30 minutes. Membranes were incubated for 60 seconds with Supersignal Westpico Chemiluminescent Substrate (Pierce) and exposed to Fuji R_X film.

2-15-3 *Protein preparations*

2-15-3-1 Whole cell extracts

Lysates were prepared by mechanically breaking cells in RIPA buffer (Table 2.7) with glass beads using a Beadbeater 8 device (Bio Spec Products). Cells were subjected to three cycles of bead beating on the maximum setting (30 seconds beating followed by one minute on ice per cycle). SDS was added to a final concentration of 1% and the resulting mixtures were boiled for 3 minutes. Lysates were subsequently cleared by centrifugation (1000 x g) for 15 minutes at 4°C and the supernatants stored at –80°C.

2-15-3-2 Subcellular Fractionation

Lysates were prepared from mid-log cultures (OD_{595}= 0.8). Two milliliters of pelleted cells were washed twice with Fractionation buffer 1 (Table 2.7) followed by 1 wash in Fractionation buffer 2 (Table 2.7). Cells were resuspended in 5 ml of Fractionation buffer 2 containing 20 mg/ml Zymicase and incubated for 1 hour at 37°C. The resulting spheroplasts were harvested by centrifugation (500 x g, 4°C) and resuspended in 2 ml Fractionation buffer 3 (Table 2.7) containing Complete™ EDTA-free protease inhibitors (Roche). Spheroplasts were subjected to 4 rounds of 15 second homogenization at 4°C using a Cole Palmer dounce homogenizer set at speed 3. The mixtures were chilled on ice for 1 minute between each homogenization cycle. Unbroken cells and nuclei were removed by centrifugation (1000 x g) for 10 minutes at 4°C. The resulting post-nuclear supernatants were fractionated by centrifugation (20000 x g, 20 minutes, 4°C). Equivalent proportions of 20000 x g supernatant and pellet fractions were resolved by SDS-PAGE prior to transfer to PVDF membranes.

2-15-4 *Immunoprecipitation assay*

All immunoprecipitations performed in this study were done using antibodies against GFP and blotting for HA-tagged protein association with the GFP-tagged proteins. Lysates were prepared from *S. pombe* strains expressing GFP- and HA-tagged proteins. Lysate preparation was as follows: Pelleted cells (500 µl) were resuspended in 1 x PBS + 0.1% TX-100 containing Complete™ EDTA-free protease inhibitors (Roche). Samples were subjected to 4 cycles of homogenization at 4°C by bead beating (Mini Beadbeater8, Bio Spec Products) and the resulting slurries were clarified by centrifugation (1000 x g, 10 minutes). The supernatants were pre-cleared by incubation with Protein A Sepharose beads (Amersham Biosciences) for 2 hours. The GFP- and HA-chimera containing lysates were mixed together in the presence of anti-GFP bound Protein A Sepharose at 4°C for 12 hours on a rotator. The mixtures were then washed 3 times in 1 x PBS + 0.1% Triton-X 100 and Complete EDTA-free inhibitors, resuspended in sample buffer and boiled. Protein complexes were resolved by SDS-PAGE. In some instances, micrococcal nuclease was added to the bound complexes after the first wash step and incubated on ice for one hour. One unit of micrococcal nuclease degraded 1 µg of DNA in 30 minutes on ice.

2-16 Microscopy

2-16-1 *Fluorescence microscopy*

2-16-1-1 Live cell imaging

Liquid cultures of yeast expressing GFP-tagged chimeras were grown in EMM to an OD_{595} = 0.8–1.0. Where indicated, cultures were treated with leptomycin B (LMB) (100ng/ml), camptothecin (CPT) (1 µM) or thiabendazole (TBZ) (10 µg/ml) for 2 hours prior to microscopy. In some instances, cells were grown overnight in low glucose/low nitrogen media to induce a G_1 block. Samples were prepared for microscopy by washing in water and resuspending the cells in 4',6-

diamidino-2-phenylindole (DAPI) (1mg/ml) (Sigma). Cells were immobilized on slides coated with poly-L lysine (2mg/ml) (Sigma) or on slides containing 0.8 % agarose. Cells were analyzed using a Zeiss LSM510 confocal microscope.

2-16-1-2 Immunofluorescence microscopy

Mid-log cultures were prepared for immunofluorescence (Dunaway et al., 2005) as follows. Briefly, cells were fixed 1:10 in 37% paraformaldehyde for 30 minutes, washed three times in PEM and once in PEMS. Spheroplasts were produced by digesting cells in PEMS containing 20mg/ml Zymicase 1 (InterSpex Products Inc.) for 20 minutes followed by 2 washes in PEMS. The spheroplasts were incubated with 1% Triton-X 100 (Sigma) for 1 minute, washed once in PEMS and twice with PEM. Cells (1.5×10^7) were resuspended in PEMBAL and incubated at room temperature with rotation for 2 hours. Cells were then pelleted (3000 x g, 5 minutes), resuspended in 100 μl PEMBAL and incubated with rat anti-HA (3F10) (Roche) (1:100) at room temperature overnight with rotation. Cells were washed 3 times in PEMBAL (30 minutes per wash) and incubated in PEMBAL containing goat anti-Rat fluorescein isothiocyanate (FITC) (Jackson ImmunoResearch) (1:100) for 8 hours. Cells were then washed once in PEMBL (30 minute rotation), twice in PEM, resuspended in DAPI (1 mg/ml) and heat fixed on slides containing 2 mg/ml poly-L lysine. Samples were overlayed with Vectashield-DAPI solution (1mg/ml DAPI) and viewed using a Zeiss LSM510 confocal microscope.

2-16-2 *Differential interference contrast microscopy*

Cells were adhered to slides using poly-L-lysine (2 mg/ml) and viewed using a Zeiss Axioskop2. Digital images were captured using a Spot™ Camera.

2-16-3 *Immunoelectron microscopy*

Cells from exponential phase cultures were fixed in suspension for 15 minutes by adding an equal volume of freshly prepared 8% formaldehyde in PBS (pH 7.4). The cells were pelleted, resuspended in PBS containing 4% formaldehyde and re-fixed for 18-24 hours at 4°C. The cells were then washed briefly in PBS, and resuspended in 1% low temperature gelling agarose. After cooling, agarose blocks were trimmed into 1 mm^3 pieces, cryoprotected by infiltration with a mixture of 2.3M sucrose/20% polyvinyl pyrrolidone (10K), pH 7.4, for 2 hours and mounted onto cryo-pins. The cryo-pins were then rapidly frozen in liquid nitrogen. Ultrathin cryosections were cut on a Leica UCT ultramicrotome equipped with an FC-S cryo-attachment and collected onto formvar/carbon coated nickel grids. The nickel grids were washed through several drops of PBS containing 5% fetal bovine serum, and 10 mM glycine (pH 7.4), blocked in 10% fetal bovine serum for 30 minutes and incubated overnight in 20 µg/ml polyclonal anti-HA antibody. After washing, the grids were incubated for two hours in 5 nm donkey anti-mouse gold conjugate (Jackson ImmunoResearch). The grids were then washed with several changes of PBS followed by several washes in water and subsequently embedded in an aqueous solution containing 3.2% polyvinyl alcohol (10K), 0.2% methyl cellulose (400 centiposes) and 0.1% uranyl acetate. The grids were observed on a Philips 420 TEM at 80 kV. Images were recorded with a Soft Imaging System Megaview III digital camera.

2-17 Flow Cytometry

Aliquots of 10^6 cells were collected from mid-log liquid cultures, pelleted and fixed by resuspension in 1 ml of 70% ethanol. Cells were washed in 3 ml of 50 mM sodium citrate, resuspended in 0.5 ml of 50 mM sodium citrate containing 0.1 mg/ml RNaseA and incubated at 37°C for 2 hours. Cells were stained by adding 0.5 ml sodium citrate solution containing the DNA stain Sytox Green (2 mM)(Molecular Probes) and stored at 4°C until processing. Cells were vortexed for 45 seconds prior to analyses on a Becton Dickson FACScan. Twenty thousand counts were collected per run.

2-18 Yeast techniques

2-18-1 *One-step gene replacement*

The entire *ago1* open reading frame was replaced with a G418^R cassette. Primers 5'ago1utrF and 5'ago1utrR/pFA6aF (Table 2.12) were used to amplify 1000 bp of the *ago1* 5' UTR. Primers 3'ago1utrR and 3'ago1F/pFA6aR (Table 2.12) were used to amplify 502 bp of the *ago1* 3' UTR using genomic DNA as a template. The resulting two fragments were used as mega-primers for the amplification of a G418^R cassette flanked by the *ago1* 5' and 3' UTRs. The resulting fragment was transformed into FY254 using the large-scale transformation protocol (Section 2.8.2.1) and individual colonies were selected by growth on G418 (200 mg/L). Transformants were subjected to Southern blot analyses (Section 2.17.1.2) for verification of the *ago1* deletion.

2-18-2 *Mating assays*

Heterothallic strains were grown to mid-log phase in YE broth. Equivalent numbers of opposite mating type cells were mixed together and spotted onto malt extract plates. Homothallic (h^{90}) strains were cultured in YE until mid-log phase, washed and resuspended in media lacking nitrogen or low glucose/low nitrogen media. Mating assays were conducted over a range of 18-30 hours. Mating frequencies were determined by dividing the number of zygotes formed by the total number of cells. Three independent mating assays were performed for each data point with at least 300 cells scored per assay.

2-18-3 *Tetrad analysis*

Yeast strains of opposite mating types were mixed on ME plates and incubated for 24 hours at 30°C to allow for the formation of zygotes. The zygotes were then spread onto EMM lacking specific nutrients to allow for growth of diploid yeast. Diploid yeast were then sporulated by incubation on ME for 24 hours at 30°C. Asci were placed on YE plates and each of 4 spores in the ascus were separated using a Zeiss tetrad dissecting scope.

2-18-4 *Determination of growth rates*

Overnight cultures were diluted in fresh media to an approximate OD_{595}=0.05. The samples were cultured at 30°C in a shaking incubator and the optical density for each strain was measured every 12 hours for 72 hours using a Pharmacia Biotech Ultrospec 3000.

2-18-5 *Functionality assay*

To assess the ability of the GFP- and HA-tagged chimeras to rescue the growth defects associated with their cognate deletant strain, vector or plasmid encoding epitope tagged Ago1, Dcr1 or Rdp1 were transformed into deletion mutants, grown under selection to mid-log phase and dot serial dilutions were applied to EMM plates containing either TBZ or HU. The ability to rescue growth on selective media was taken as evidence of function.

2-18-6 *Septation analyses*

Yeast strains were cultured at 30°C in YE to mid-log phase (OD_{595} =0.6-0.9), stained with DAPI and placed onto microscope slides coated with poly L-lysine. Samples were examined by fluorescence and differential interference contrast microscopy. Representative fields were photographed and scored for nuclei and the presence of septa. For each sample, at least 500 cells were scored.

2-18-7 *UV irradiation survival assay*

Yeast were grown to OD_{595}= 0.8 in YE, counted and spread on YE plates at a density of 100 to 300 cells per plate. The plates were irradiated (0, 75, 150, 225, or 300 J/M^2) using a Hoefer UVC 500 apparatus, wrapped in aluminum foil and incubated for 24 hours at 30°C. The foil was removed and incubation was continued at 30°C for an additional 72 hours. Surviving colonies were counted and plotted as a percentage of the surviving non-irradiated cells.

2-19 Drug-induced cell cycle arrest

2-19-1 *Survival assay*

Serial dilutions of yeast strains were cultured for the indicated time periods at 30°C on YE or EMM plates in the presence of the S-phase arrest inducing drug, HU (3.5-10 mM), or the G2-M phase arresting drug, TBZ (10 μg/ml), and assayed for growth under these conditions.

2-19-2 *Cdc2 phophorylation analysis*

Strains were cultured in YE to $OD_{595} = 0.3$ at which time HU (10 mM) was added. Four hours post-HU treatment, cultures were washed, resuspended in YE and incubations continued at 30°C. Whole cell lysates for all Cdc2 phosphorylation assays were prepared by mechanically breaking cells in RIPA buffer (Section 2.14.3.1) and protein preparations were subjected to SDS-PAGE followed by immunoblotting. Total Cdc2 levels and Cdc2 (tyrosine-15) phosphorylation levels were detected using anti-PSTAIR (Sigma) and anti-Phospho-cdc2 (Y15) (Cell Signaling Technology), respectively. The relative levels of Cdc2-p:Total Cdc2 were determined by Spot densitometry using a FluorChem Imager (Alpha Innotech Corporation).

CHAPTER 3

Ago1 and Dcr1 RNAi-Independent Cell Cycle Regulation

A version of this chapter has been published in "Jon B. Carmichael, Patrick Provost, Karl Ekwall and Tom C. Hobman (2004) Ago1 and Dcr1, two core components of the RNA interference pathway, functionally diverge from Rdp1 in regulating cell cycle events in *Schizosaccharomyces pombe*. *Mol Biol Cell*, 15, 1425-1435".

3-1 Overview

In the fission yeast *S. pombe*, the three core genes that function in the classical RNA interference (RNAi) pathway, *ago1*$^+$, *dcr1*$^+$ and *rdp1*$^+$, have also been shown to be important for timely formation of heterochromatin and accurate chromosome segregation. We observed that null mutants for *ago1*$^+$ and *dcr1*$^+$, but not *rdp1*$^+$, exhibit abnormal cytokinesis, cell cycle arrest deficiencies and mating defects. In addition, biochemical analyses of these strains revealed that *ago1*$^+$ and *dcr1*$^+$, but not *rdp1*$^+$, are required for regulated Y15 phosphorylation of Cdc2 upon encountering genotoxic insults. Further, overexpression of Ago1 was found to complement the cytokinesis and S-phase cell cycle arrest defects arising from loss of Dcr1 function. However, overexpression Ago1 was not able to suppress the heterochromatic defects associated with loss of Dcr1 function. Since *rdp1*$^+$ and *dcr1*$^+$ are both required for accumulation of siRNAs in *S. pombe*, this suggests that the functions of *ago1*$^+$ and *dcr1*$^+$ in this cell cycle regulatory pathway are independent of their roles in siRNA-mediated heterochromatin formation and chromosome segregation. Finally, exogenous expression of human Ago2, a S. *pombe* Ago1 homologue sharing 33% identity and 52% similarity, compensated for the loss of *ago1*$^+$ function in *S. pombe*. This suggests that PPD proteins may also be important for regulation of cell cycle events in humans.

3-2 *ago1*$^+$ and *dcr1*$^+$ null mutants are delayed in cytokinesis

One-step targeted gene disruption was used to replace the entire *ago1*$^+$ open reading frame with a G418 resistance cassette in the haploid strain FY254 (Figure 3-

1A). Disruption of the *ago1⁺* locus in the resulting strains, Δ1 and Δ16, was confirmed by Southern blot analyses (Figure 3-1B). The Δ1 strain was chosen to be used for further study and was named JC254K. In agreement with a recent study (Volpe et al., 2002), we found that *ago1⁺* was not essential for viability but it was also clear that deletion of this gene resulted in morphological defects (Figure 3-2A) including uncondensed and/or mis-localized chromosomes, distended DNA and lagging DNA. As well, cut phenotypes, in which one daughter of a septated cell contains no genome, were observed (Figure 3-2A). The latter phenotype is indicative of cytokinesis being uncoupled from DNA segregation and is in agreement with a recent study (Hall et al., 2003). In addition, the deletion strain exhibited a slower growth rate (Figure 3-2B, left panel). Introduction of a plasmid encoding Ago1 resulted in growth rates similar to that of the parental strain (Figure 3-2B, right panel). Back-crossing of the Δ*ago1* strain with FY261 followed by sporulation of the diploid, tetrad dissection and Southern blot analyses showed that the morphological defects observed for the JC254K strain were not the result of second site mutations.

The loss of function of any one of Ago1, Dcr1 or Rdp1 results in disruption of RNAi-related pathways and an inability to efficiently form heterochromatin (Volpe et al., 2002). A hallmark of non-nucleated centromeric chromatin is the presence of lagging DNA and chromosome loss (Hall et al., 2003; Provost et al., 2002). We asked if the apparent cell cycle defects observed in our *ago1⁺* null strain were directly linked to ablation of the RNAi pathway.

To determine the requirement for RNAi pathways or core RNAi proteins independent of a functioning RNAi pathway in cell cycle regulation, we obtained a

Figure 3-1. Deletion of the *ago1*$^+$ open reading frame. A) Schematic of the integration of the G418^R cassette into the *ago1*$^+$ open reading frame (orf) complete with 5'untranslated region (UTR), 3' UTR and relative positions of the restriction sites of *Bgl*II (B), *Cla*I (C), *Sty*I (S) and *Nde*I (N) used in the diagnostic analyses for detection of recombination. The black bar represents the region of the 5'UTR used to probe for the integration of the G418^R cassette. B) Southern blot analyses of two putative *ago1*$^+$ deletion mutants (Δ1, Δ16). Five micrograms of genomic DNA was digested overnight with the indicated enzyme, separated by electrophoresis on a 0.8% agarose gel, transferred to nitrocellulose membrane and probed with ^{32}P-labelled *ago1*$^+$ 5'UTR. The expected DNA fragment sizes for the parental type (PT) and integrants digested with *Bgl*II, *Cla*I, *Nde*I and *Sty*I are listed below the blot.

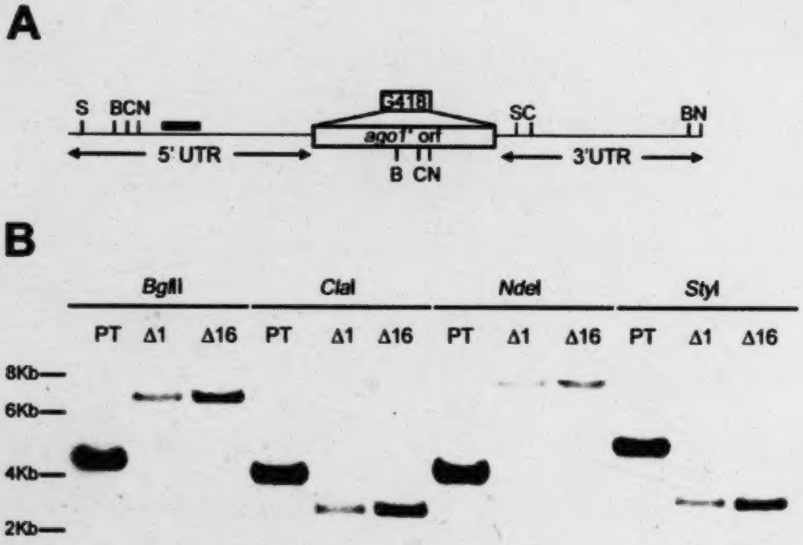

Enzyme	Expected Size (kb)	
	WT	Integrant
BglII	4.4	7.3
ClaI	4.1	3.7
NdeI	4.2	7.6
StyI	5.8	3.7

parental strain (TV294) and isogenic null mutations for *ago1*$^+$ (TV292), *dcr1*$^+$ (TV293), *rdp1*$^+$ (TV296) (kind gifts from Dr. T. Volpe). We determined that the proportions of bi-nucleated cells were significantly higher in the Δ*dcr1* and Δ*ago1* strains compared to the parental strain whereas the proportion of bi-nucleated cells in the Δ*rdp1* strain was similar to that of the wild type (Figure 3-3A). Bi-nucleated cells represented approximately 3% of the parental and Δ*rdp1* populations whereas the proportion of bi-nucleated cells in the Δ*ago1* and Δ*dcr1* strains under the same culture conditions was increased three-fold to approximately 9% (Figure 3-3A).

Since cytokinesis is preceded by septum formation in fission yeast, we also used the septation index as an indicator of cell division (Alfa et al., 1993). As shown in Figure 3-3B, the proportions of septated cells were significantly reduced in comparison to the parental strain when *ago1*$^+$ or *dcr1*$^+$ gene function was ablated. Notably, deletion of *rdp1*$^+$ had no effect on this process. Plasmid-driven over-expression of Ago1 or the human PPD protein hAgo2 corrected the cytokinesis defect in *ago1*$^+$ mutants (Figure 3-3C). Although it cannot be ruled out that loss of *ago1*$^+$ or *dcr1*$^+$ results in accelerated mitosis, these results suggest that Ago1 and Dcr1 may function together to regulate septum formation and subsequent cytokinesis in *S. pombe*. Moreover, since human Ago2 was able to rescue the *ago1*$^+$ mutant septation defect, it is likely that PPD proteins regulate this process in mammals.

Figure 3-2. Morphology and growth of Δ*ago1* cells. A) Strains were grown in YE to mid-log phase (OD_{595} =0.6-0.9), stained with DAPI (1 μg/ml), placed onto microscope slides coated with poly L-lysine (5 mg/ml) and examined by fluorescence microscopy. Ago1 mutants exhibit uncondensed nuclei (*), lagging DNA (**), distended nuclei (single arrowhead), mis-localized nuclei (double arrowheads) and cut phenotypes (arrow). Inset shows the parental type cells. (Scale bar = 10 μm). B) Heterothallic strains were grown in YE (left panel) or strains encoding vector alone or encoding Ago1were grown in EMM lacking leucine (right panel) overnight at 30°C to an OD_{595}=1.0. Cultures were then inoculated at an OD_{595}=0.05 and readings were obtained every 12 hours.

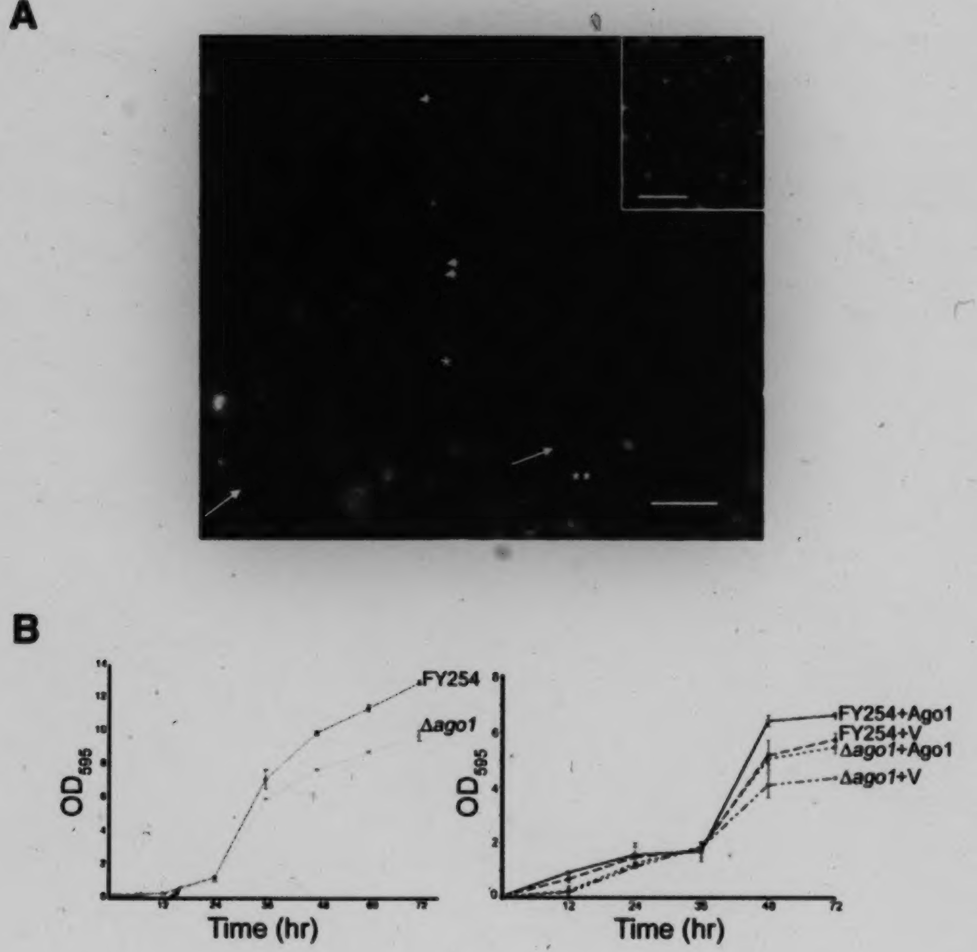
A
B
14
12
10
8
6
4
2
0
12
24
36
48
60
72
OD$_{595}$
Time (hr)
FY254
Δago1
8
6
4
2
0
12
24
36
48
72
OD$_{595}$
Time (hr)
FY254+Ago1
FY254+V
Δago1+Ago1
Δago1+V

3-3 *ago1*$^+$ and *dcr1*$^+$, but not *rdp1*$^+$ are required for G_1-arrest and mating in response to nitrogen starvation

To enable survival when starved of nitrogen, *S. pombe* cells normally arrest in G_1 and if a partner of opposite mating type is in close proximity such that pheromones are sensed, commit to sexual differentiation and subsequent meiosis (Breeding et al., 1998; Crandall et al., 1977; Egel and Egel-Mitani, 1974). Alternatively, cells enter a quiescent state (G_0) when mating partners are absent. In addition, upon arresting due to nitrogen starvation cells adopt a characteristic short round morphology (Alfa et al., 1993; Breeding et al., 1998; Su et al., 1996). We observed that when depleted of nitrogen the parental strain (TV294) and the Δ*rdp1* strain (TV296) both arrested in G_1 as indicated by a 1N DNA content (Figure 3-4A). Morphological changes in cell shape and size (Figure 3-4D, -Nitrogen) were also observed in these strains when cultured in nitrogen-limiting conditions. In contrast, under the same conditions, the Δ*ago1* and Δ*dcr1* strains were unable to arrest in G_1, instead exhibiting a 2N DNA content (Figure 3-4A). These strains also did not undergo the typical morphological changes characteristic of G_1-arrested cells (Figure 3-4D, -Nitrogen). Since G_1 block is required for mating, we predicted that the Δ*ago1* and Δ*dcr1* strains would be compromised in their abilities to undergo sexual differentiation. Indeed, heterothallic Δ*ago1* (TV292) and Δ*dcr1* (TV293) strains were unable to mate efficiently with a Δ*ago1* (JC261K) strain of the opposite mating type (Figure 3-4B). In contrast, crossing null *ago1*$^+$ and *dcr1*$^+$ strains with FY261 resulted in formation of zygotes at the same level as TV294/FY261 crosses or as crosses with the *rdp1*$^+$ null strain (Figure 3-4B).

Figure 3-3. *ago1*$^+$ and *dcr1*$^+$ are both required for normal cytokinesis. All strains were cultured at 30°C in YE to mid-log phase (OD_{595} =0.6-0.9), stained with DAPI (1 μg/ml) and placed onto microscope slides coated with poly L-lysine (5 μg/ml). Samples were examined by fluorescence and differential interference contrast microscopy. Representative fields were photographed and scored for number of nuclei per cell or septation. For each sample, at least 500 cells were counted (n=3). A) Quantitation of binucleated cells in parental strain TV294, Δ*ago1* (TV292), Δ*dcr1* (TV293) and Δ*rdp1* (TV296) strains. B) Determination of septation indices (number of cells with a septum/total number of cells) for TV294, Δ*ago1*, Δ*dcr1* and Δ*rdp1*. C) Septation indices in FY254 and Δ*ago1* (JC254K) strains transformed with vector (pREP3X), pREP3X+*ago1*$^+$ (+ Ago1) or pREP3X+hAgo2 (+ hAgo2).

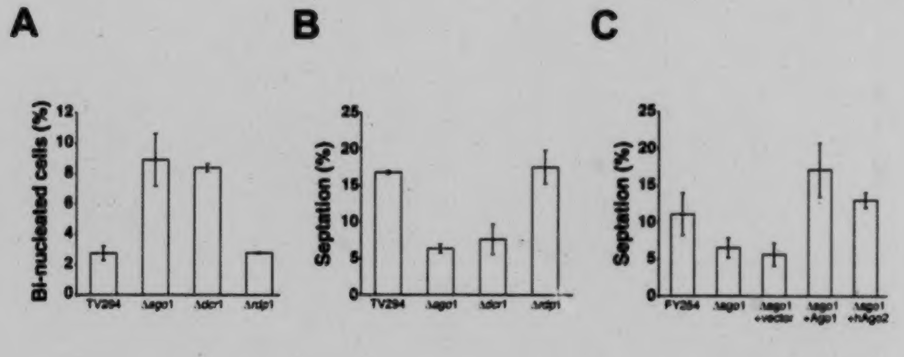
A
Bi-nucleated cells (%)
0
2
4
6
8
10
12
TV294
Δago1
Δdcr1
Δrdp1
B
Septation (%)
0
5
10
15
20
25
TV294
Δago1
Δdcr1
Δrdp1
C
Septation (%)
0
5
10
15
20
25
FY254
Δago1
Δago1 +vector
Δago1 +Ago1
Δago1 +hAgo2

Since mating is dependent upon sexual partners being in close proximity to each other, any mating defect associated with the *ago1*$^+$ null phenotype would be exaggerated by using two different mating strains. To circumvent this problem, we constructed an h^{90} strain capable of mating type switching and tested the ability of this strain to form zygotes. The advantage of using this strain is that approximately 50% of the population around any given cell will be of opposite mating type and therefore the proximity issue inherent with using strains of opposite mating types is eliminated. The h^{90} *ago1*$^+$ null strain (h^{90}Δ*ago1*) mated at a greatly reduced frequency compared to the parental strain (h^{90}) under nitrogen deficient conditions (Figure 3-4C). It has been shown that some mating defective mutants unable to arrest in G$_1$ in nitrogen limiting conditions can be induced to mate when incubation occurs in a low glucose/low nitrogen environment (Okazaki et al., 1998; Tsukahara et al., 1998). In agreement we found that the h^{90}Δ*ago1* strain mated with the same efficiency as the parental h^{90} strain during nitrogen and glucose limiting conditions (Figure 3-4C, lowG lowN). These data indicate that *ago1*$^+$ and *dcr1*$^+$, but not *rdp1*$^+$, are required for mating through the facilitation of a nitrogen-specific block in G$_1$.

3-4 *ago1*$^+$ and *dcr1*$^+$ null mutants fail to enact and/or maintain the S-M checkpoint

Cyclin-dependent kinase 2 (Cdc2) is the central regulator of the cell cycle controlling passage through S-phase and into mitosis in *S. pombe* (Fisher and Nurse, 1996; Nurse, 1990). It has been shown that regulated phosphorylation of Cdc2 on Y15 is required for cytokinesis and mating to occur. As well, in response to the

Figure 3-4. *ago1⁺* and *dcr1⁺* mutants are defective for G_1-arrest and mating following nitrogen limitation. A) FACS analyses of log phase (Unstarved) and nitrogen starved (-Nitrogen) Parental type TV294 (PT), Δ*ago1* (TV292), Δ*dcr1* (TV293) and Δ*rdp1* (TV296) cultures. B and C) Mating mixtures were incubated at 30°C for 18-30 hours on malt extract plates and scored for zygote production microscopically. B) Mating frequencies of TV294 (PT), Δ*ago1* (TV292), Δ*dcr1* (TV293) and Δ*rdp1* (TV296) crossed with FY261 (parental type) or JC261K (Δ*ago1*) of opposite mating type. The mating type is indicated by h^- or h^+. The low level of self-mating in strains FY261 and JC261K presumably occurs due to mating type switching. C) Mating frequencies for homothallic wild type (h^{90}) or homothallic *ago1⁺* null (h^{90}Δ*ago1*) strains under nitrogen deficient (-Nitrogen) or low glucose/low nitrogen condition (lowG lowN). D) DAPI stained cells (1 µg/ml) and corresponding DIC images of TV294, Δ*ago1*, Δ*dcr1* and Δ*rdp1* strains cultured under normal growth (Unstarved), nitrogen starvation (-Nitrogen) and low glucose/low nitrogen (lowG lowN) conditions. Average cell lengths for each strain (unstarved condition) are shown at the bottom of the DIC panels.

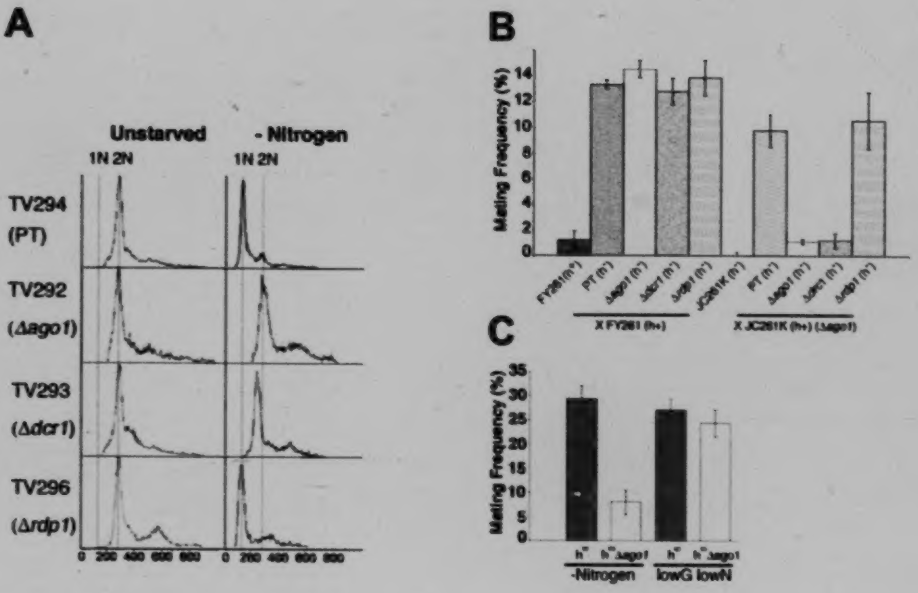
A
Unstarved
- Nitrogen
1N 2N
1N 2N
TV294
(PT)
TV292
(Δago1)
TV293
(Δdcr1)
TV296
(Δrdp1)
0 200 400 600 800
0 200 400 600 800
B
Mating Frequency (%)
0
2
4
6
8
10
12
14
FY261(h+)
PT (h-)
Δago1 (h-)
Δdcr1 (h-)
Δrdp1 (h-)
JC261K (h-)
PT (h-)
Δago1 (h-)
Δdcr1 (h-)
Δrdp1 (h-)
X FY261 (h+)
X JC261K (h+) (Δago1)
C
Mating Frequency (%)
0
5
10
15
20
25
30
35
h90
h90 Δago1
h90
h90 Δago1
-Nitrogen
lowG lowN

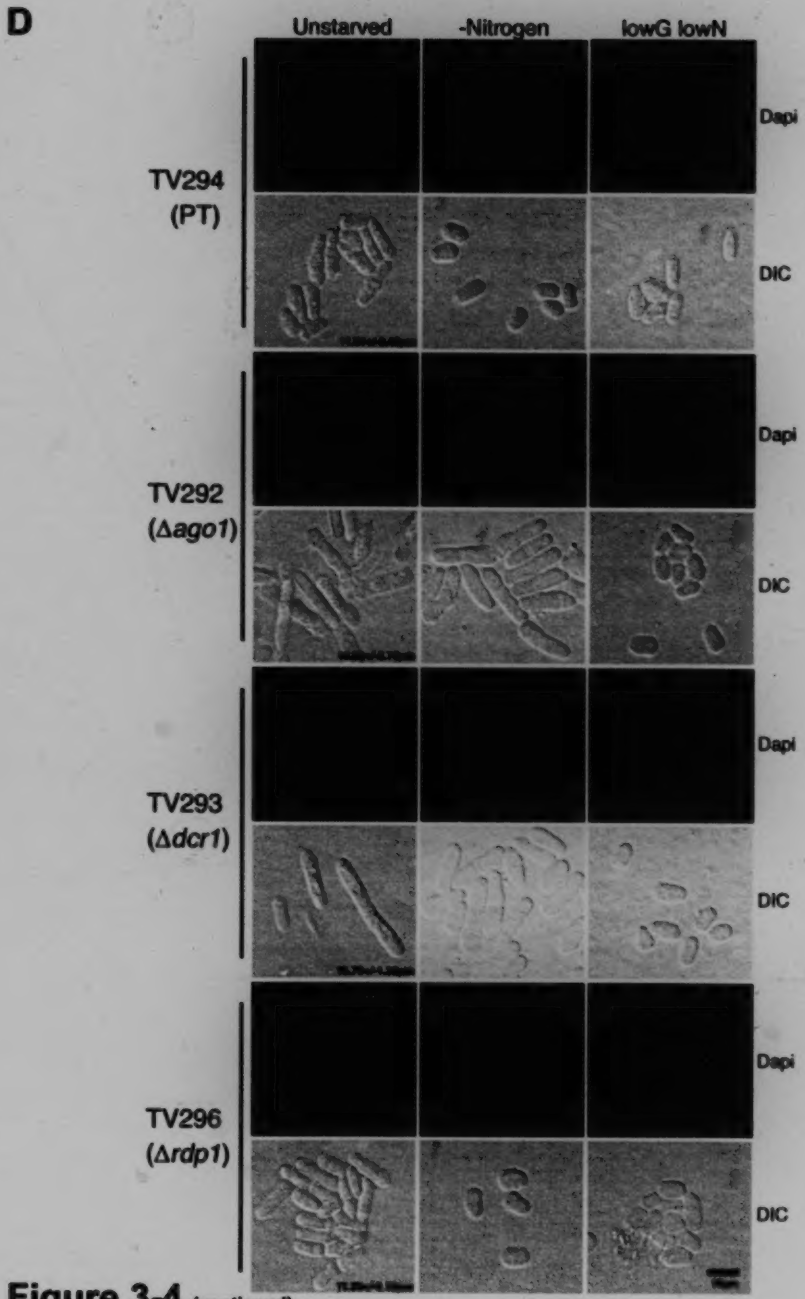

Figure 3-4 (continued)

ribonucleotide reductase inhibitor hydroxyurea (HU), checkpoint kinases ultimately mediate enactment of the S-M checkpoint through inhibitory phosphorylation of Y15 on Cdc2 (al-Khodairy and Carr, 1992; Enoch et al., 1992; Furnari et al., 1997; Rhind and Russell, 1998). To gain further insight as to where the defect in cell cycle regulation caused by loss of Ago1 and Dcr1 function was occurring, we examined the level of Cdc2 Y15 phosphorylation in response to HU treatment. The results shown in Figure 3-5A offered the first clue that *ago1*$^+$ may be important for enactment of the S-M checkpoint. JC254K *(*Δ*ago1)* and the parental strain FY254 transformed with vector pREP3X, pREP3X+*ago1*$^+$ or pREP3X+hAgo2 were streaked onto plates containing 10 mM HU to test their abilities to activate the DNA replication checkpoint. After three days, Δ*ago1* cells transformed with vector alone were not able to grow under these conditions indicating that they were unable to activate, maintain or recover from activation of this checkpoint (Figure 3-4A). In comparison, the Δ*ago1* strain ectopically expressing Ago1 or hAgo2 grew well on HU-containing media indicating there is a conserved function for this family of proteins in enacting or recovering from S-phase cell cycle arrest (Figure 3-5A).

Since tyrosine-15 phosphorylation of Cdc2 is required for initiation of the S-M checkpoint, we predicted that phosphorylation of this kinase would be decreased in the Δ*ago1* strain. As expected, in response to HU treatment, the levels of phosphorylated Cdc2 in the parent strain FY254 increased after addition of HU (Figure 3-5B). The increase in Cdc2 phosphorylation in response to HU coincided with a decrease in the septation index (Figure 3-5C). Upon removal of HU, the levels of phosphorylated Cdc2 decreased and were accompanied by a concomitant increase

Figure 3-5. *ago1*$^+$ null mutants fail to activate the S-M DNA replication checkpoint. A) Parental strain, FY254, and Δ*ago1* strains transformed with vector (pREP3X), pREP3X+*ago1*$^+$, or pREP3X+hAgo2 were streaked onto leucine-deficient EMM plates containing 10 mM hydroxyurea (HU) and incubated for three days at 30°C. B) Immunoblot analyses of total and tyrosine-15 phosphorylated (Cdc2-P) Cdc2 from FY254 and Δ*ago1* strains in unsynchronized cultures (US), during HU treatment (+10 mM HU) and after removal of HU (Wash Out). C) Mean septation indices determined from four independent experiments are shown for each time point.

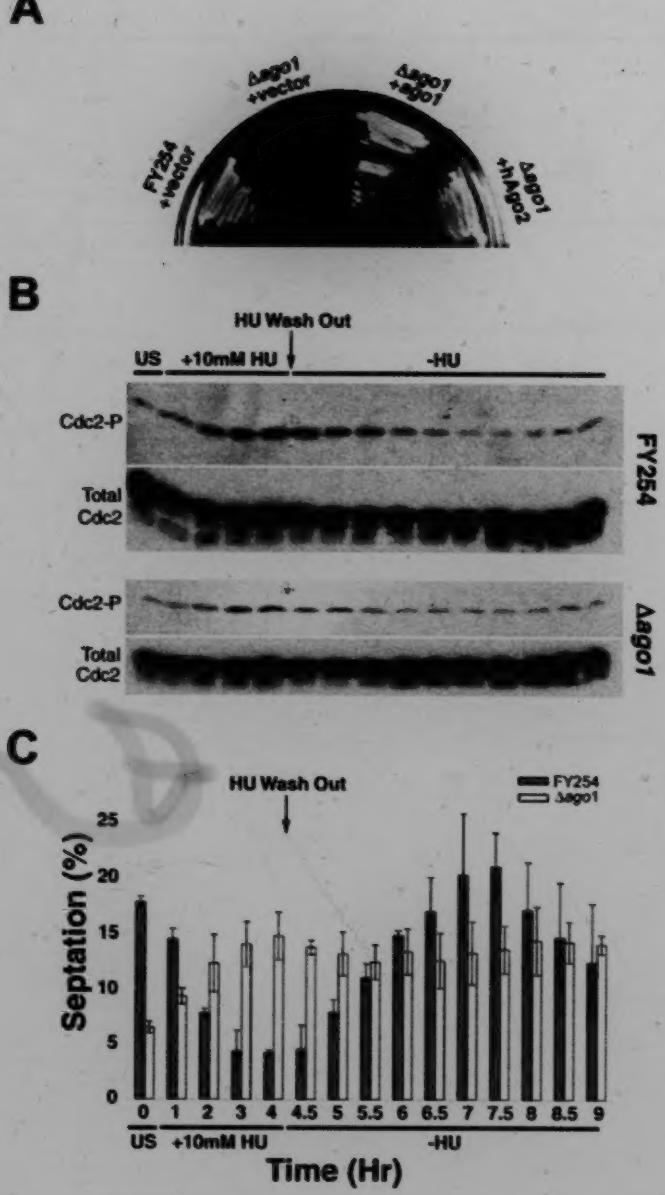
A
Δago1 +vector
Δago1 +ago1
FY254 +vector
Δago1 +hAgo2
B
HU Wash Out
US
+10mM HU
-HU
Cdc2-P
Total Cdc2
FY254
Cdc2-P
Total Cdc2
Δago1
C
HU Wash Out
FY254
Δago1
Septation (%)
25
20
15
10
5
0
0
1
2
3
4
4.5
5
5.5
6
6.5
7
7.5
8
8.5
9
US
+10mM HU
-HU
Time (Hr)

in the number of septated cells (Figure 3-5B and C). In contrast, Cdc2 Y15 phosphorylation was delayed in Δ*ago1* cultures and peak phosphorylation levels were substantially lower than those seen in FY254 (Figure 3-5B). Consequently, the septation index of Δ*ago1* cultures continued to increase rather than decrease in the presence of HU (Figure 3-5C).

We also tested the Δ*dcr1* and Δ*rdp1* mutants for sensitivity to HU and found that loss of Dcr1 function, similar to the deletion of *ago1*$^+$, resulted in hypersensitivity to HU (Figure 3-6A). In contrast, the Δ*rdp1* mutant was significantly less sensitive to this drug (Figure 3-6A). Acting on the premise that the HU-sensitivity of the Δ*dcr1* strain, like that of the *ago1*$^+$ mutant, was a result of an inability to activate/maintain the S-M checkpoint, we assayed the ability of this mutant to undergo phosphorylation of Cdc2 under S-M arrest conditions. Indeed, like *ago1*$^+$ mutants, the *dcr1*$^+$ null strain did not enact tyrosine-15 phosphorylation of Cdc2 in response to HU treatment (Figure 3-6B). In contrast, HU-induced phosphorylation of Cdc2 was not affected by loss of Rdp1 function (Figure 3-6B). Overexpression of Ago1 and Dcr1 in *ago1*$^+$ and *dcr1*$^+$ null mutants respectively, restored the ability of these mutants to phosphorylate Cdc2 on Y15 in response to HU treatment (Figure 3-6C). The above results suggest that Ago1 and Dcr1 are involved in enactment of cell cycle checkpoints through the regulated phosphorylation of Cdc2 on Y15 and that this process is independent of Rdp1. Moreover, this suggests that the cell cycle regulated functions exhibited by Ago1 and Dcr1 are siRNA-independent.

Figure 3-6. *ago1*$^+$ and *dcr1*$^+$ are both required for hyper-phosphorylation of Cdc2 and enactment of the replication checkpoint. A) Serial dilutions of parental strain (PT) and isogenic Δ*ago1*, Δ*dcr1* and Δ*rdp1* strains were spotted on YE (-HU) and YE containing 3.5mM HU (+HU). Samples were cultured for three and five days at 30°C respectively. B) Liquid cultures were grown at 30°C to an OD_{595}=0.5 and aliquots were removed before (-) or after (+) a four hour HU treatment. Whole cell lysates were prepared and separated by SDS-PAGE before immunoblot analyses of total and phosphorylated Cdc2. The normalized ratios of HU-induced Cdc2 phosphorylation are indicated below the immunoblots in panels B and C. The ratios were derived using the equation: $(\text{Cdc2-P/Cdc2-Total})_{HU+}/(\text{Cdc2-P/Cdc2-Total})_{HU-}$ and are representative of the change in Cdc2 phosphorylation from untreated (-HU) to treated (+HU) for each strain. C) Levels of total and phosphorylated Cdc2 were analyzed in the parental type (PT), Δ*ago1* and Δ*dcr1* strains transformed with vector alone or plasmid encoding Ago1 or Dcr1.

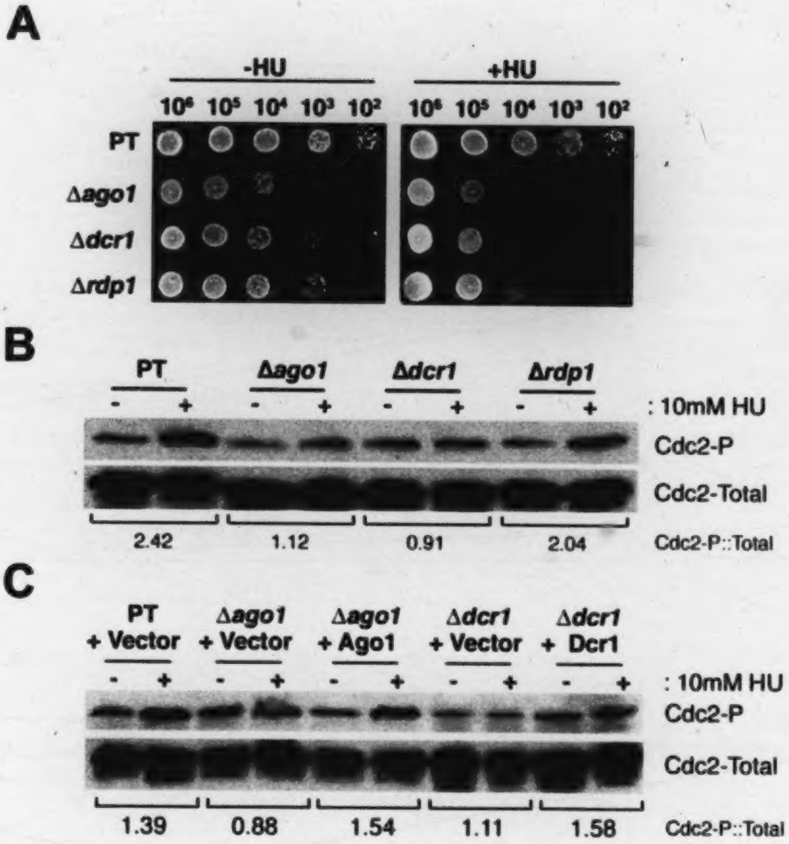
A
-HU
+HU
10⁶ 10⁵ 10⁴ 10³ 10²
10⁶ 10⁵ 10⁴ 10³ 10²
PT
Δago1
Δdcr1
Δrdp1
B
PT
Δago1
Δdcr1
Δrdp1
- + - + - + - +
: 10mM HU
Cdc2-P
Cdc2-Total
2.42
1.12
0.91
2.04
Cdc2-P::Total
C
PT + Vector
Δago1 + Vector
Δago1 + Ago1
Δdcr1 + Vector
Δdcr1 + Dcr1
- + - + - + - + - +
: 10mM HU
Cdc2-P
Cdc2-Total
1.39
0.88
1.54
1.11
1.58
Cdc2-P::Total

3-5 *ago1*$^+$ and *dcr1*$^+$ null mutants are defective for the DNA damage checkpoint

The degree of overlap between components of the DNA replication and DNA damage checkpoints is considerable (al-Khodairy and Carr, 1992; Furnari et al., 1997; Raleigh and O'Connell, 2000; Rhind et al., 1997; Rhind and Russell, 1998; Rowley et al., 1992). In both cases, activation of the checkpoints following exposure to genotoxic insults requires Cdc2 Y15 phosphorylation. Accordingly, we predicted that Δ*ago*1 and Δ*dcr*1 strains would be hyper-sensitive to ultraviolet irradiation, a commonly used inducer of the DNA damage checkpoint. Indeed, the ability to survive post-irradiation was compromised in Δ*ago1* and Δ*dcr1* strains (Figure 3-7A). Moreover, this sensitivity manifested itself at relatively low dosages of UV light. Rad3 is a major component of the protein complex required for sensing and responding to DNA damage (Jimenez et al., 1992). As deletion of *rad3*$^+$ results in hyper-sensitivity to UV irradiation, the Δ*rad3* strain was used as a control for survival at various dosages of UV irradiation (Figure 3-7A).

To confirm that the sensitivity of *ago1*$^+$ and *dcr1*$^+$ null mutants to UV light was the result of a failure to activate the DNA damage checkpoint rather than an inability to release the arrest, strains were irradiated and the septation indices were determined over a six hour time period (Figure 3-7B). As expected, the parental and Δ*rdp1* strains exhibited decreased septation after exposure to UV light, an indication that the DNA damage checkpoint was functioning (Francesconi et al., 2002). In contrast, *ago1*$^+$ and *dcr1*$^+$ null mutants did not exhibit decreased septation indices. Rather, septation indices increased followed by a plateau in these strains following UV exposure (Figure 3-7B). The *ago1*$^+$ and *dcr1*$^+$ null mutants' response to UV light

Figure 3-7. *ago1*$^{+}$ and *dcr1*$^{+}$ are both required for enactment of the DNA damage checkpoint. A) TV294 (PT), Δ*ago1*, Δ*dcr1* Δ*rdp1* and Δ*rad3* strains were grown at 30°C to an $OD_{595}=0.8$, spread at a density of 100-300 cells per plate and then exposed to ultraviolet irradiation (UV) (0, 75, 150, 225, or 300 J/M^2). Cell survival is shown as a percentage of the non-irradiated control cell survival three days post UV irradiation. B) TV294 (PT), Δ*ago1*, Δ*dcr1* and Δ*rdp1* were subjected to mock (0 J/m^2) treatment and UV irradiation (75 J/m^2) and the septation index for each strain was determined. At least 300 cells were counted per time point (n=3).

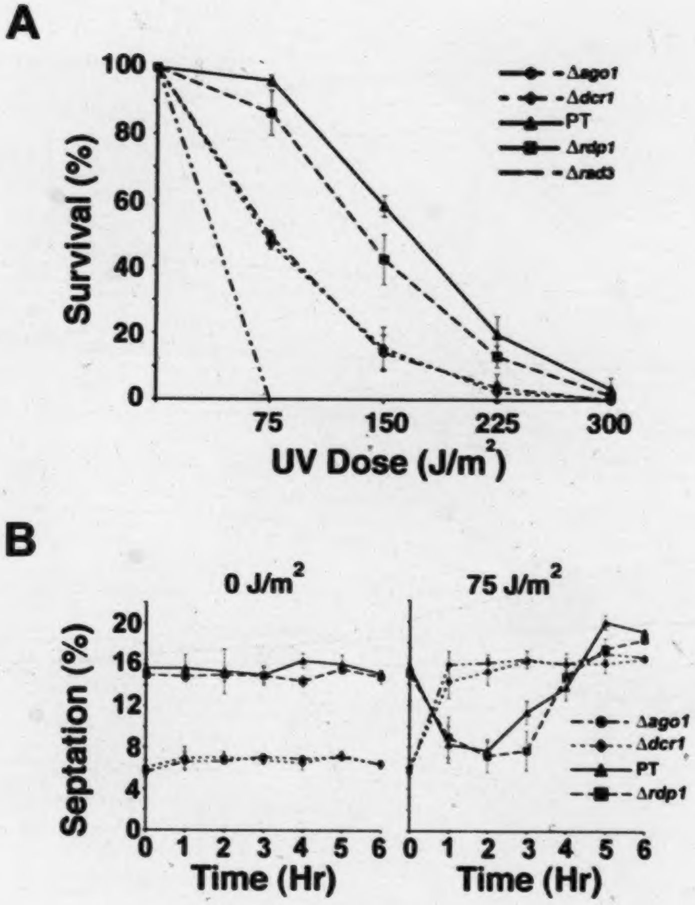
A
Survival (%)
100
80
60
40
20
0
75
150
225
300
UV Dose (J/m^2)
Δago1
Δdcr1
PT
Δrdp1
Δrad3
B
0 J/m^2
75 J/m^2
Septation (%)
20
16
12
8
4
0
0 1 2 3 4 5 6
Time (Hr)
0 1 2 3 4 5 6
Time (Hr)
Δago1
Δdcr1
PT
Δrdp1

is reminiscent of strains deleted for the DNA damage response complex protein, Rad1 (Kanter-Smoler et al., 1995), although there is no mechanism to explain why the rise followed by a plateau in septation occurs, it is plausible that cells die after septation but prior to cytokinesis of the following cell cycle. These results indicate that *ago1*$^{+}$ and *dcr1*$^{+}$ are both required for survival when encountering DNA damaging conditions, possibly through Cdc2-dependent activation of the DNA damage checkpoint.

3-6 Ago1 may function downstream of Dcr1 to regulate cell cycle events

To gain insight as to how Ago1 and Dcr1 interact genetically we asked whether over-expression of Ago1 could compensate for lack of Dcr1 function and vice versa. We first assayed whether Ago1 over-expression could correct the cytokinesis defect associated with loss of Dcr1 function. Figure 3-8A shows that Ago1 expression restores the septation index of Δ*dcr1* cells to normal levels. In contrast, over-expression of Dcr1 was unable to complement the cytokinesis defect of Δ*ago1* strains (Figure 3-8A). Moreover, ectopic expression of Ago1 complemented the S-M checkpoint deficiency of both Δ*ago1* and Δ*dcr1* strains (Figure 3-8B), whereas Dcr1 over-expression corrected the checkpoint deficiency in Δ*dcr1* strains only (Figure 3-8B). These results suggest that the requirement for Ago1 in the regulation of cytokinesis and in the enactment of cell cycle checkpoints is downstream of Dcr1. In addition, it seems that Dcr1-derived siRNAs are not required for checkpoint enactment. To further test the premise that the cell cycle functions of

Figure 3-8. *ago1*$^+$ functions downstream of *dcr1*$^+$ to regulate cell cycle events A) Yeast strains (TV294, Δ*ago1* and Δ*dcr1*) containing vector (V) pREP3X, or vector containing a cDNA encoding Ago1 or Dcr1, were grown in EMM-leu to log phase and the septation index for each sample was determined by phase contrast microscopy. At least 300 cells were counted for each condition (n=3). B) Yeast strains (TV294, Δ*ago1* and Δ*dcr1*) containing pREP3X (vector) or plasmid encoding Ago1 or Dcr1, were streaked onto EMM lacking leucine in the absence (EMM) or presence of 7.5 mM HU (+HU). Strains were incubated at 30°C for three and five days respectively. C) These same yeast strains were streaked onto EMM lacking leucine (EMM) with or without 10 µg/ml TBZ and incubated at 30°C for three (EMM) or five days (+TBZ).

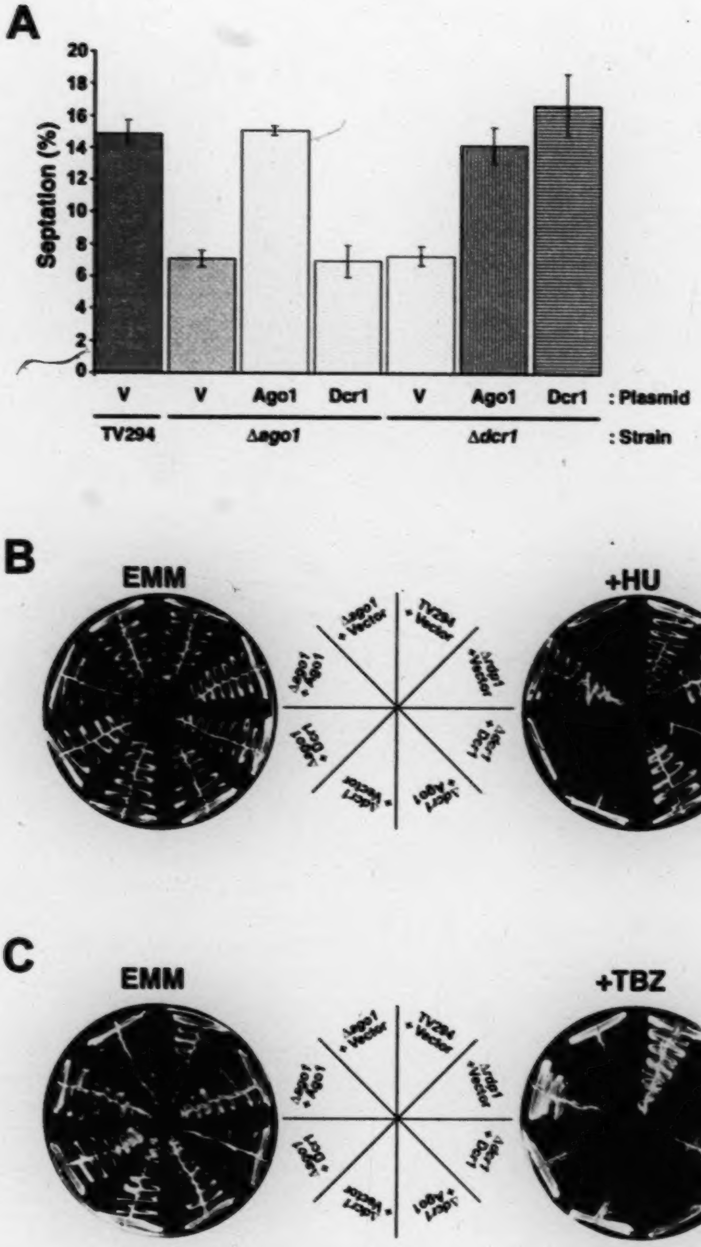
A
Septation (%)
20
18
16
14
12
10
8
6
4
2
0
V
V
Ago1
Dcr1
V
Ago1
Dcr1
: Plasmid
TV294
Δago1
Δdcr1
: Strain
B
EMM
+HU
Δago1 + Vector
TV294 + Vector
Δdcr1 + Vector
Δdcr1 + Dcr1
Δdcr1 + Ago1
Δdcr1 + Vector
Δago1 + Dcr1
Δago1 + Ago1
C
EMM
+TBZ
Δago1 + Vector
TV294 + Vector
Δdcr1 + Vector
Δdcr1 + Dcr1
Δdcr1 + Ago1
Δdcr1 + Vector
Δago1 + Dcr1
Δago1 + Ago1

Ago1 and Dcr1 were separate from their roles in RNAi, we asked whether over-expression of Ago1 and Dcr1 in *dcr1*$^+$ and *ago1*$^+$ null strains respectively, would correct the chromosomal segregation defect associated with the loss of Ago1, Dcr1 or Rdp1 function. Over-expression of Ago1 or Dcr1 in cognate null mutants resulted in decreased sensitivity to the microtubule destabilizing drug thiabendazole (TBZ) (Figure 3-8C). However, over-expression of Ago1 in Δ*dcr1* or Dcr1 in Δ*ago1* strains did not alleviate sensitivity to TBZ. This suggests that the segregation of chromosomes requires the generation and targeting of siRNAs. Any abrogation to this pathway through loss of the core RNAi proteins results in hyper-sensitivity to TBZ (Hall et al., 2003; Provost et al., 2002; Volpe et al., 2003).

3-7 Ago1 and Dcr1 functionally diverge from Rdp1 and RNAi to regulate cell cycle events

Our data are consistent with a functional divergence of Ago1 and Dcr1 from the siRNA-dependent pathway. Most recent research has focused on the role of these proteins in gene-silencing. By way of analogy to metazoans, the initiation stage of RNAi requires Dcr1 function for recognition and cleavage of long dsRNAs into siRNAs (Hamilton et al., 2002; Lagos-Quintana et al., 2001; Lau et al., 2001; Lee and Ambros, 2001). Although not encoded in mammalian or *D. melanogaster* genomes, Rdp1 has been shown to be required for RNAi in plants and fungi (Dalmay et al., 2000; Hall et al., 2002; Volpe et al., 2002). Recent evidence indicates that both Dcr1 and Rdp1 are required for accumulation of siRNAs in *S. pombe* (Sigova et al., 2004), suggesting that the role of Rdp1 in the initiation or persistence of RNAi is through its role in amplification of dsRNAs. At the core of the effector stage of RNAi is Ago1. Ago1 functions in the classic mRNA degradation pathway as a member of the RISC complex and in transcriptional silencing through its inclusion in the RITS complex (Sigova et al., 2004; Verdel et al., 2004). Although the function of *S. pombe* Ago1 within RISC has not been demonstrated, it is probable that as in metazoans, Ago1 is required for both the incorporation of siRNAs into RISC (Okamura et al., 2004) and the endonuclease activity required for cleavage of targeted mRNAs (Meister et al., 2004). As well, it is probable that the association of Ago1 with the RITS complex is similar to that of its role in RISC, notably to bind short heterochromatic RNAs derived from repetitive sequences and to guide chromatin-silencing machinery to those sites of heterochromatin formation (Reinhart and Bartel, 2002; Volpe et al., 2002).

In so much as the defects in cytokinesis and mating observed in *ago1*$^{+}$ and *dcr1*$^{+}$ null strains were not present in the *rdp1*$^{+}$ null strain, it is conceivable that these defects were pleotropic rather than specific. The inability to phosphorylate Cdc2 on Y15 in response to genotoxic insult was key to elucidating a role other than RNAi for these proteins. The lack of Cdc2 Y15 regulatory phosphorylation in *ago1*$^{+}$ and *dcr1*$^{+}$ null mutants, coupled with the ability of Ago1 to compensate for loss of Dcr1 function, suggests that siRNA generation by Dcr1 is not required for regulated Cdc2 phosphorylation. In addition, loss of Rdp1 function also results in a loss of siRNA accumulation in *S. pombe* (Sigova et al., 2004). The fact that Rdp1 function was not necessary for Cdc2 regulated phosphorylation again suggests that the generation of siRNAs is not required for the cell cycle checkpoints assayed. Together, these results indicate that the roles of Ago1 and Dcr1 in centromere function and chromosome segregation are distinct from their functions in cytokinesis and cell cycle checkpoints (Figure 3-9).

Figure 3-9. Model for RNAi and RNAi-independent functions of Ago1 and Dcr1. The right side of the model depicts the classical RNAi pathway in which Rdp1, as well Hrr1 and Cid12 function as part of the RNA-directed RNA polymerase complex (RDRC). The function of this complex is purported to be two fold, production/amplification of dsRNAs for cleavage by Dcr1 and possibly as a scaffold for RNA-induced transcriptional silencing complex dependent (RITS) localization of the histone methyltransferase, Clr4. Dcr1, a type III RNase detects and cleaves the dsRNAs into siRNAs that are then incorporated into Ago1-containing RISCs which facilitate mRNA degradation or RITS complexes, which facilitate heterochromatin formation, an event that is required for attachment of mitotic spindles to kinetochores and subsequent orderly chromosome segregation. The left side of the model depicts a pathway in which Dcr1 and Ago1, in response to genotoxic insults such as UV induced DNA damage or HU induced replication inhibition, mediate down-stream events that feed into the cell cycle regulatory machinery (box), ultimately rendering Cdc2 inactive through inhibitory phosphorylation. This process is proposed to be independent of siRNAs and Rdp1.

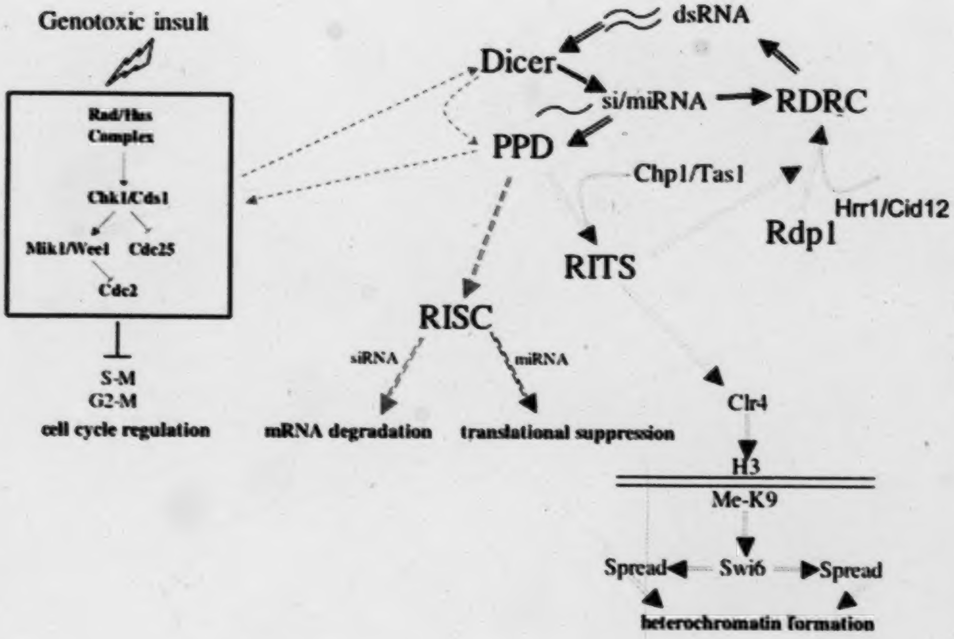
Genotoxic insult
Rad/Hus Complex
Chk1/Cds1
Mik1/Wee1
Cdc25
Cdc2
S-M
G2-M
cell cycle regulation
dsRNA
Dicer
si/miRNA
RDRC
PPD
Chp1/Tas1
Hrr1/Cid12
Rdp1
RITS
RISC
siRNA
miRNA
mRNA degradation
translational suppression
Clr4
H3
Me-K9
Spread
Swi6
Spread
heterochromatin formation

CHAPTER 4

Localizations and Interactions of Core RNAi Proteins

4-1 Overview

A number of recent studies suggest that Ago1 and Rdp1 reside primarily in the nucleus (Motamedi et al., 2004; Noma et al., 2004; Verdel et al., 2004). Moreover, Ago1 is reportedly associated with heterochromatic loci (Noma et al., 2004). These results are consistent with Ago1 functioning as part of the RITS complex that facilitates the formation of heterochromatin (Hall et al., 2002; Volpe et al., 2002) through sequence-specific targeting of this complex to non-coding centromeric repeats (Verdel et al., 2004). The association between RITS and RDRC in the nucleus is thought to be required for amplification of centromeric derived dsRNA and heterochromatin formation (Motamedi et al., 2004). This suggests that these complexes, despite performing very different roles within the RNAi pathway, must function cooperatively to fulfill their roles. In addition to their roles in chromatin modification, the *S. pombe* RNAi machinery is also known to function in siRNA-dependent targeting of the RISC complex to facilitate the degradation of mRNA in a sequence-specific manner (Sigova et al., 2004). By analogy with RNAi effector proteins in other eukaryotes, the study by Sigova *et al.* (2004) is consistent with a scenario in which pools of Ago1, and presumably Dcr1, exist in the cytoplasm where they function as components of ribonucleoprotein complexes that mediate mRNA degradation (Hannon, 2002). In addition, we have shown that Ago1 and Dcr1 functionally diverge from Rdp1 and siRNA-related mechanisms and function in the regulation of Cdc2 Y15 upon genotoxic insult (Carmichael et al., 2004). Presumably, functioning of the RNAi apparatus in these divergent pathways would require differential localizations of Ago1, Dcr1 and Rdp1 to allow for different protein-protein interactions in distinct complexes.

As a first step toward understanding the intracellular trafficking patterns of RNAi components, we constructed functional GFP- and HA-tagged Ago1, Dcr1 and Rdp1 chimeras. Immunoprecipitation assays discussed below revealed that Ago1 and Dcr1 interact in a nucleic acid-independent manner, whereas the Ago1-Rdp1 interaction was dependent on oligonucleic acid. No interaction was detected between Dcr1 and Rdp1. These results further highlight the necessity to understand the dynamics of Ago1, Dcr1 and Rdp1 localization. Chimera localizations were studied by fluorescence and immunoelectron microscopy. Our results indicate that Rdp1 is predominantly localized to the nucleus where it is thought to function in siRNA generation. In contrast, Ago1 and Dcr1 are predominantly associated with large cytoplasmic complexes. Blocking Crm1-dependent nuclear export did not result in nuclear accumulation of either Ago1 or Dcr1 chimeras. However, in the absence of Ago1 or exposure to insults that activate S- or M-phase checkpoints, a small pool of Dcr1 was observed in the nucleus. In addition, conditions that blocked cell cycle progression in G_1-phase resulted in nuclear localization of pools of both Ago1 and Dcr1.

4-2 Ago1 and Dcr1 associate with large cytoplasmic complexes

To determine if Ago1 and Dcr1 were present in cytoplasmic fractions, yeast homogenates were subjected to differential centrifugation and samples were separated

Figure 4-1. Ago1 and Dcr1 co-purify with large cytoplasmic structures. A and B) Exponentially growing yeast cultures were subjected to homogenization and differential centrifugation. A) Post-nuclear supernatants (PNS) were further separated into 20,000 x g supernatants (S) and pellets (P). Equivalent proportions of each fraction, relative to the original PNS volume, were resolved by SDS-PAGE, transferred to PVDF membranes and subjected to immunoblot analysis. The supernatant and pellet fractions are enriched in the soluble enzyme A) Glyceraldehyde-3-phosphate dehydrogenase (GAPDH) or B) Glucose-6-phosphate dehydrogenase (G6PDH) and peroxisomal matrix proteins that contain the SKL sequence respectively B) Samples were prepared as in A except that prior to the 20,000 x g centrifugation step, the PNS was divided into two equal volumes and either left untreated (-) or treated with 0.5 U/μl micrococcal nuclease (+) for one hour on ice. Fractions were resolved by SDS-PAGE, transferred to PVDF membranes and subjected to immunoblot analysis.

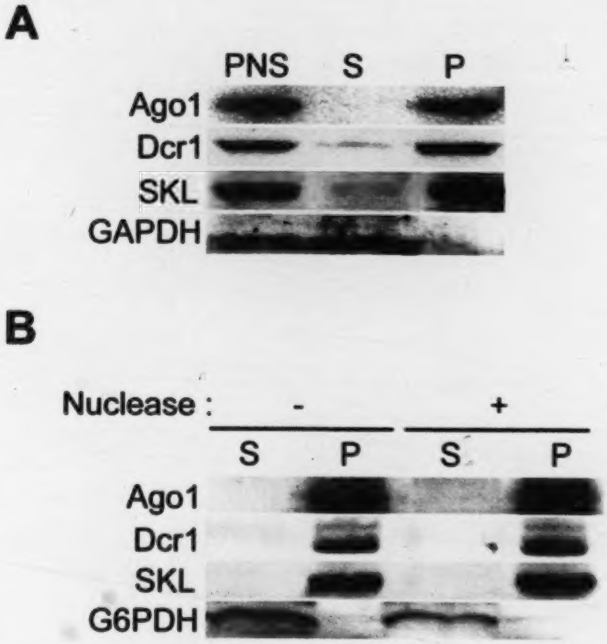
A
PNS
S
P
Ago1
Dcr1
SKL
GAPDH
B
Nuclease :
-
+
S
P
S
P
Ago1
Dcr1
SKL
G6PDH

into soluble fractions, enriched in the cytosolic enzymes glyceraldehydes-3-phosphate dehydrogenase (GAPDH) or glucose-6-phosphate dehydrogenase (G6PDH), and large organelle fractions, enriched in membrane-associated proteins including the SKL-bearing peroxisomal matrix proteins (Figure 4-1A). Ago1 was detected by immunoblotting using polyclonal antibodies generated in our laboratory. Since anti-Dcr1 reagents are not available, we used anti-HA and a genomically tagged yeast strain that encodes HA-tagged Dcr1 (Provost et al., 2002). Data in Figure 4-1 show that significant quantities of both Ago1 and Dcr1 were present in post-nuclear supernatant fractions. The bulk of cytoplasmic Ago1 and Dcr1 were recovered in the 20,000 x g pellet fractions, suggesting that both proteins are associated with large structures. In addition, treatment of the post-nuclear supernatant (PNS) with micrococcal nuclease prior to differential centrifugation did not alter the distribution of Ago1 and Dcr1 (Figure 4-1B). This suggests that, in addition to being associated with large structures, either membranous or otherwise, their interaction is probably not dependent upon the presence of intact RNA or DNA.

4-3 Interactions among RNAi effector proteins

It is likely that direct and/or indirect interactions between Rdp1, Dcr1 and Ago1 are required to fulfill their roles in transcriptional and post-transcriptional gene-silencing. Whereas the interaction between PPD proteins and Dicer enzymes appears to be direct (Tahbaz et al., 2004), it is not clear if, how or where interactions between Ago1 and Rdp1, or Dcr1 and Rdp1 take place. To address these questions, we

Figure 4-2. Construction of functional epitope-tagged RNAi effector proteins. GFP or influenza HA tags were fused in frame with the amino or carboxyl termini of Ago1, Dcr1 or Rdp1 as indicated. The domains and proposed function of each domain based on homology and experimentation are as follows. PAZ domain: binding of 2-base 3' overhangs of siRNAs. PIWI domain: putative RNAseH domain required for cleavage of RNA and Dicer binding site. RdRP domain: required for amplification of si/miRNA. ResIII domain: catalysis of endonucleolytic cleavage of DNA. DUF283: unknown. Helicase C domain: ATP binding, nucleic acid unwinding. RNaseIII domain: endonucleolytic cleavage of dsRNA.

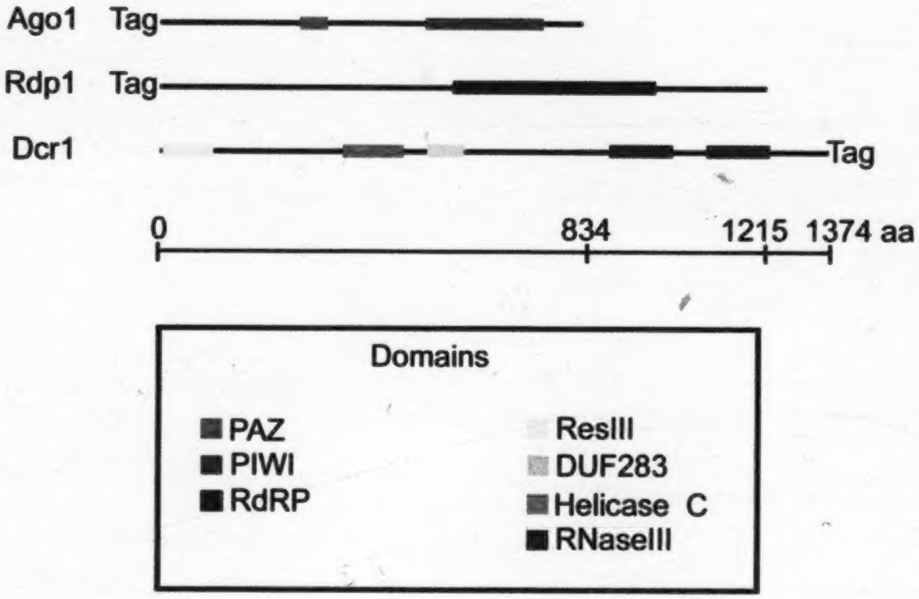
Ago1
Tag
Rdp1
Tag
Dcr1
Tag
0
834
1215
1374 aa
Domains
■ PAZ
■ PIWI
■ RdRP
■ ResIII
■ DUF283
■ Helicase C
■ RNaseIII

constructed cDNAs encoding GFP- and HA-tagged Ago1, Dcr1, and Rdp1 (Figure 4-2) to be used in both binding and intracellular localization studies.

To ensure that the chimeric proteins were functional, we tested the abilities of the GFP- and HA-tagged Ago1, Dcr1 and Rdp1 to complement the growth of cognate null strains under conditions that were previously shown to inhibit growth of RNAi mutants (Carmichael et al., 2004; Volpe et al., 2002). Yeast that lack Ago1, Dcr1 or Rdp1 activity exhibit chromosome segregation defects and as a result, are hyper-sensitive to the microtubule destabilizing drug TBZ (Provost et al., 2002; Volpe et al., 2003). In addition, we demonstrated that Ago1 and Dcr1 are required for enactment of the replication checkpoint and as such, null strains are hyper-sensitive to HU (Carmichael et al., 2004). The GFP- and HA-tagged chimeras were shown to be functional as evidenced by their abilities to compliment the growth defects of cognate null strains on HU and TBZ (Figure 4-3A and B).

To investigate the interactions between the core RNAi proteins in *S. pombe*, co-immunoprecipitation studies using the GFP- and HA-tagged chimeras were employed. HA-tagged Dcr1 and Rdp1 were both seen to co-immunoprecipitate with GFP-Ago1 (Figure 4-4A). Importantly, HA-Ago1 also co-immunoprecipiated with both Dcr1-GFP and GFP-Rdp1 (Figure4-4B). The interaction between Ago1 and Dcr1 was expected given that in *D. melanogaster* and humans, PPD proteins and Dicer are known to directly interact (Doi et al., 2003; Hammond et al., 2001; Tahbaz et al., 2004). Prior to this study, interactions between Ago1 and Rdp1 in *S. pombe* had not been documented although it was proposed by Motamedi *et al.* (2004) that an interaction between Ago1 and Rdp1 containing complexes, mediated by RNA, is

Figure 4-3. Assays to address the functionality of GFP- and HA-fusion proteins. A) GFP alone or GFP-tagged core RNAi proteins were over-expressed in cognate null strains, grown to an OD_{595}-0.6-1.0 and serially diluted at the indicated cell number onto EMM plates lacking leucine or uracil, EMM plates containing 10 µg/ml TBZ or 10mM HU. Plates were incubated at 30°C for 3 days (EMM) or 5 days (TBZ and HU). B) HA alone or HA-tagged core RNAi proteins were over-expressed in cognate null strains, grown to an OD_{595}-0.6-1.0 and serially diluted onto EMM plates lacking leucine or uracil, EMM plates containing 10 µg/ml TBZ or 10 mM HU. Plates were incubated at 30°C for 3 days (EMM) or 5 days (TBZ and HU). GFP-Rdp1 and Dcr1-GFP chimeras were constructed by Dr. H. Parker, Department of Cell Biology, University of Alberta.

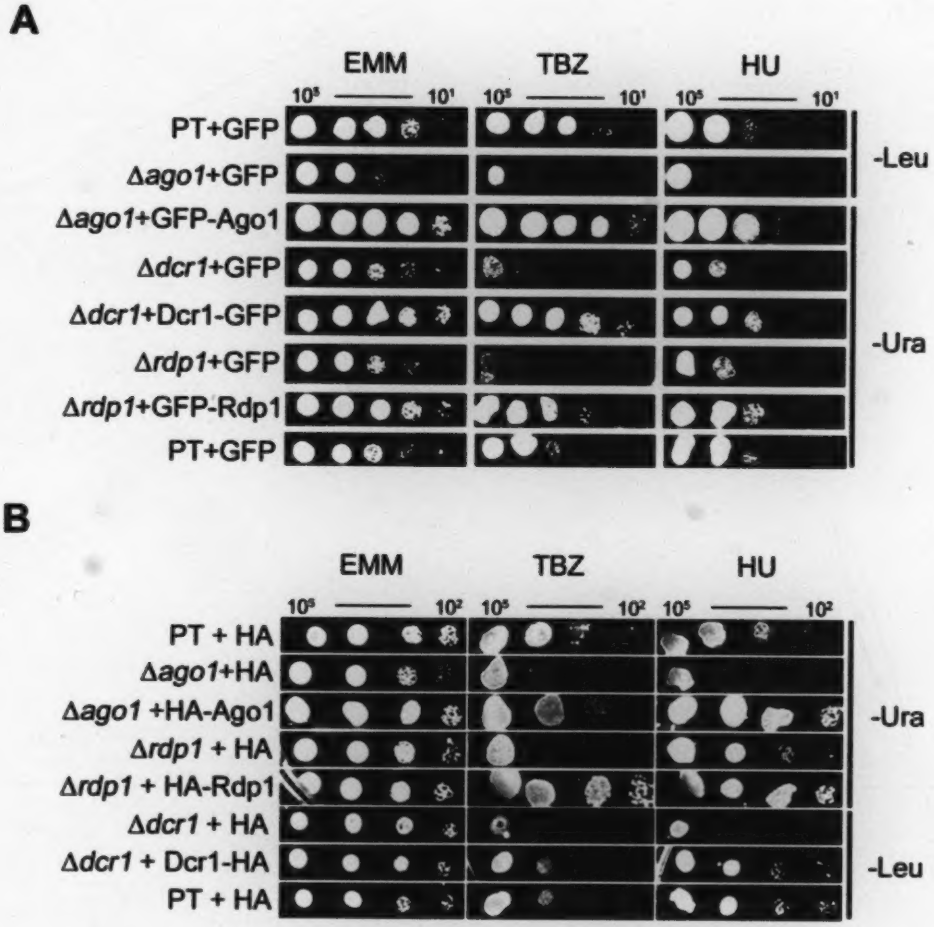
A
EMM
TBZ
HU
10⁵
10¹
PT+GFP
Δago1+GFP
Δago1+GFP-Ago1
Δdcr1+GFP
Δdcr1+Dcr1-GFP
Δrdp1+GFP
Δrdp1+GFP-Rdp1
PT+GFP
-Leu
-Ura
B
EMM
TBZ
HU
10⁵
10²
PT + HA
Δago1+HA
Δago1 +HA-Ago1
Δrdp1 + HA
Δrdp1 + HA-Rdp1
Δdcr1 + HA
Δdcr1 + Dcr1-HA
PT + HA
-Ura
-Leu

required for heterochromatin nucleation. Indeed, the Ago1-Rdp1 complexes were sensitive to treatment with micrococcal nuclease (Figure 4-4B), suggesting that interaction between these two proteins is probably mediated by intact RNA or DNA. In contrast, interactions between Dicer and PPD proteins do not require intact nucleic acids (Tahbaz et al., 2004) and, similarly, the stability of the Ago1-Dcr1 complex was not affected by treatment with nuclease (Figure 4-4B). We were unable to detect stable Rdp1-Dcr1 complexes using co-immunoprecipiation assays (Figure 4-4B) indicating that these proteins do not form functional complexes through direct interactions or RNA intermediates. These results also suggest that Ago1 and Rdp1 interact indirectly. In addition, Rdp1 is primarily a nuclear protein (Motamedi et al., 2004) and as such, these result underscore the necessity of determining the compartmental distribution of core RNAi proteins and their ability to affect both cytoplasmic and the nuclear events.

4-4 Analyses of RNAi effector proteins by fluorescence microscopy

To gain further insight as to where interactions between RNAi effector proteins take place, the subcellular localizations of Ago1, Dcr1 and Rdp1 were determined by fluorescence microscopy. First, we examined the distributions of GFP-tagged proteins in living cells. GFP-tagged Ago1, Dcr1 and Rdp1 were over-expressed in their cognate null strains and localizations were investigated by confocal microscopy. Similarly to findings in two recent reports (Motamedi et al., 2004; Verdel et al., 2004), we observed that Rdp1 was largely confined to nuclei (Figure 4-5). In conflict with a report that Ago1 is primarily associated with heterochromatic

Figure 4-4. Binding interactions among RNAi proteins. Lysates were prepared from yeast overexpressing GFP- or HA-tagged Ago1, Dcr1 and Rdp1 constructs (approximately 10-100 fold above endogenous levels). A) Samples were mixed together for 16 hours at 4°C and immunoprecipitated with rabbit anti-GFP, separated by SDS-PAGE and then subjected to immunoblot analysis. Membranes were probed with anti-HA or anti-GFP and then developed by ECL. B) Immunoprecipitated complexes bound to protein A Sepharose beads prepared as in A were divided into two equal parts and either left untreated (-) or treated with 0.5 U/μl micrococcal nuclease (+) for one hour on ice prior to separation by SDS-PAGE.

A

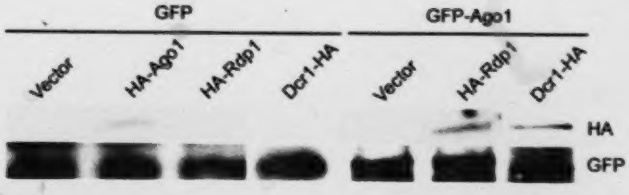

IP: αGFP
IB: αHA, αGFP

B

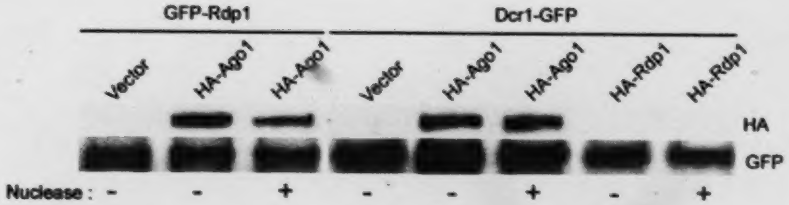

IP: αGFP
IB: αHA, αGFP

foci in the nucleus (Noma et al., 2004), we found that the vast majority of Ago1 was present in the cytoplasm (Figure 4-5). We also observed that the bulk of Dcr1, in keeping with the direct association of Ago1 and Dcr1 and their roles in RNAi-dependent mRNA degradation, was found in the cytoplasm (Figure 4-5).

To address the possibility that Ago1 and Dcr1 cycle in and out of the nucleus, cells were treated with leptomycin B (LMB) prior to examination. LMB inhibits nuclear export of substrates by binding to and blocking the function of the export factor Crm1 (Nishi et al., 1994). As a positive control for these experiments, a yeast strain with a GFP cassette genomically-integrated at the *cdc25* locus was employed (Chua et al., 2002). Cdc25 is a phosphatase that cycles in an out of the nucleus in a cell cycle-dependent manner (Lopez-Girona et al., 1999). At steady state, Cdc25-GFP was distributed throughout the cytoplasm and nuclei (Figure 4-5). However, LMB treatment resulted in an accumulation of Cdc25-GFP in the nuclei of all cells (Figure 4-5). In contrast, LMB treatment did not result in nuclear accumulation of GFP-Ago1 or Dcr1-GFP, nor did it affect the nuclear localization of GFP-Rdp1 (Figure 4-5).

The predominantly cytoplasmic distribution of GFP-Ago1 that we observed is in direct conflict with previous localization results indicating that Ago1 was primarily associated with centromeric heterochromatin (Noma et al., 2004). To address the possibility that the bulky GFP-tag (239 amino acids with an expected mass of 26.9 kDA) was causing a cytoplasmic distribution of Ago1 by inhibiting nuclear import, we examined the localization of these proteins tagged with a small epitope, influenza HA (10 amino acid residues). In agreement with the experiments using GFP-tagged

Figure 4-5. Localization of GFP-tagged core RNAi proteins. Cultures expressing Cdc25-GFP, GFP-Ago1, Dcr1-GFP or GFP-Rdp1 were grown in EMM lacking appropriate nutrients to mid-log phase (OD_{595} =0.6-0.9), stained with DAPI (1 µg/ml), placed onto microscope slides coated with poly L-lysine (5 mg/ml) and examined by fluorescence microscopy using a Zeiss LSM510 confocal microscope. Where indicated, cultures were treated for 2 hours with leptomycin B (LMB) prior to examination. Genomically integrated Cdc25-GFP was used as a positive control for the effect of LMB on nuclear export.

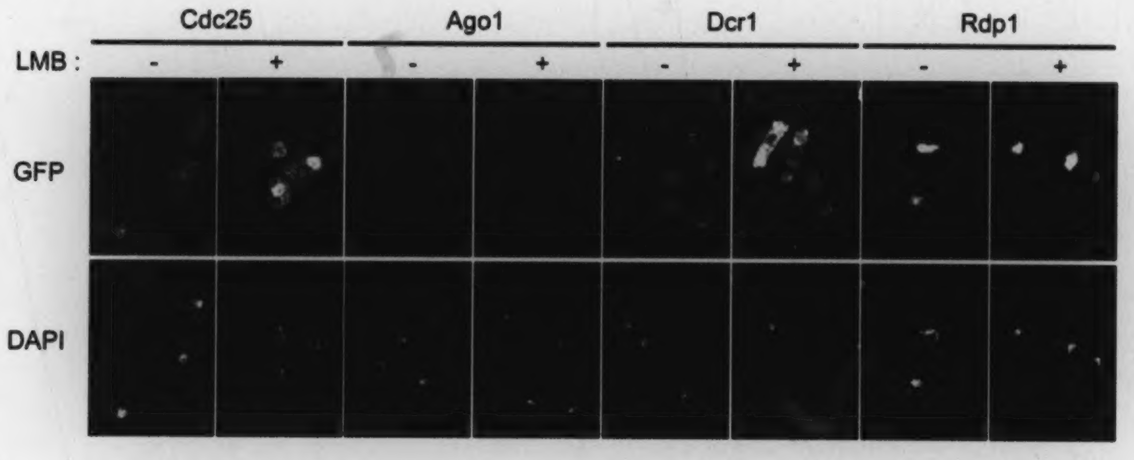
Cdc25
Ago1
Dcr1
Rdp1
LMB :
-
+
-
+
-
+
-
+
GFP
DAPI

chimeras, we did not observe detectable levels of Ago1 or Dcr1 in the nucleus (Figure 4-6). Moreover, LMB treatment did not result in significant nuclear accumulation of HA-Ago1 or Dcr1-HA (Figure 4-6). The results in Figure 4-6 support the earlier data indicating that Ago1 and Dcr1 reside primarily in the cytoplasm, whereas Rdp1 is primarily a nuclear protein.

4-5 Localization of HA-tagged Ago1 and Dcr1 chimeras by immunoelectron microscopy

The data from the subcellular fractionation experiments (Figure 4-1) and fluorescence microscopy (Figure 4-5 and 4-6) indicate that significant pools of Ago1 and Dcr1 localize to the cytoplasm in association with large structures. We used immunoelectron microscopy to determine if Ago1 and Dcr1 were associated with discrete cytoplasmic elements. Ultrathin cryosections were prepared from Δ*ago1* and Δ*dcr1* yeast strains expressing HA-Ago1 and Dcr1-HA respectively, and protein localization was visualized by immunogold labeling with anti-HA (Figure 4-7). Both HA-Ago1 (Figure 4-7B) and Dcr1-HA (Figure 4-7C) exhibited clustered distributions in association with amorphous electron dense regions in the cytoplasm. The regions of Ago1 and Dcr1 localization were not membrane-bound nor were they consistently associated with cytoskeletal structures. Together, these data are consistent with fractionation and fluorescence results showing that Ago1 and Dcr1 are associated with large complexes in the cytoplasm.

Figure 4-6. Localization of HA-tagged core RNAi proteins. Cultures expressing HA-Ago1, Dcr1-HA or HA-Rdp1 were grown in EMM lacking appropriate nutrients to mid-log phase (OD_{595} =0.6-0.9), fixed in paraformaldehyde and processed for indirect immunofluorescence. Rat anti-HA (Roche) was used to detect the HA epitope followed by incubation with goat anti-Rat fluorescein isothiocyanate (FITC). Samples were stained with DAPI (1 μg/ml), heat fixed on slides coated with 2 mg/ml poly-L lysine, overlayed with Vectashield-DAPI solution and viewed using a Zeiss LSM510 confocal microscope. Where indicated, samples were treated for 2 hours with LMB (+LMB) prior to fixation. Genomically integrated Cdc25-GFP was used as a positive control for the effect of LMB on nuclear export (Lower panel).

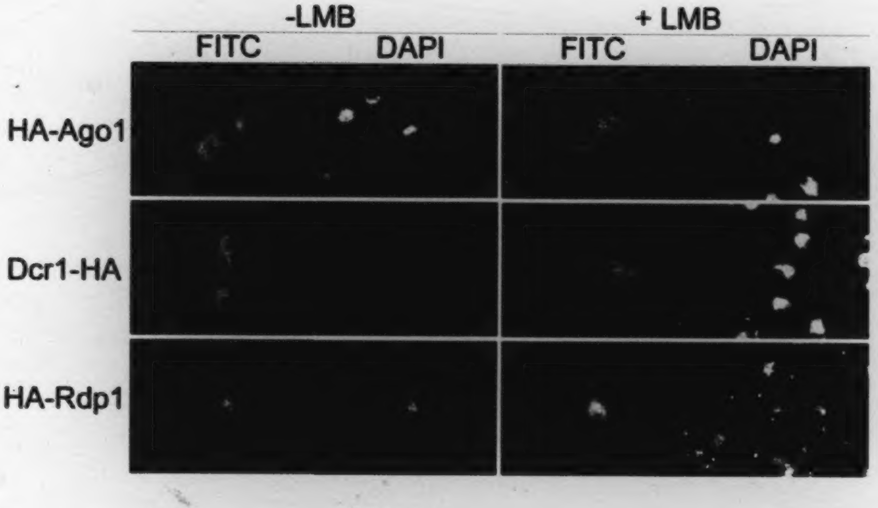
-LMB
+ LMB
FITC
DAPI
FITC
DAPI
HA-Ago1
Dcr1-HA
HA-Rdp1

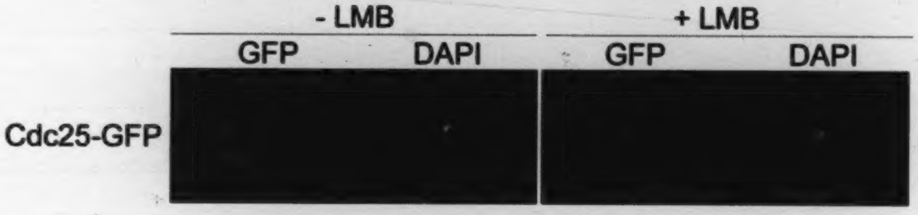
- LMB
+ LMB
GFP
DAPI
GFP
DAPI
Cdc25-GFP

4-6 Ago1 and Dcr1 are not excluded from the nucleus in G_1-arrested cells

The activities of Ago1 and Dcr1 are important for a number of cell cycle related processes including enactment of checkpoints (Carmichael et al., 2004). Under conditions commonly used to induce mating, conjugation is severely compromised in *ago1* and *dcr1* null mutants [Figure 3-4 and (Carmichael et al., 2004)]. For example, when deprived of nitrogen, these mutants fail to block the cell cycle at the G1-phase and as a consequence are unable to mate efficiently. However, *ago1* and *dcr1* mutants can be blocked in G_1 and induced to mate by limiting both nitrogen and glucose. Given the importance of Ago1 and Dcr1 in blocking the cell cycle in response to environmental cues and genotoxic stress, we elected to monitor the localization of these proteins under conditions that result in different cell cycle blocks.

Yeast strains expressing GFP-tagged Ago1 and Dcr1 were grown to mid-log phase and then treated with agents that disrupt the cell cycle at well-defined points. Live cell cultures were then subjected to analyses by confocal microscopy. Cells harvested from asynchronous cultures exhibited the characteristic localizations expected of these proteins. Specifically, Ago1 and Dcr1 were detected predominantly in the cytoplasm (Figure 4-8A). Under nitrogen-limiting conditions, the cells adopted a short, rounded morphology (Figure 4-8B). This morphological change is characteristic of cells under G_1-arrest (Breeding et al., 1998). Although Ago1 and Dcr1 did not concentrate in nuclei, neither protein was excluded from the nuclei of G_1-arrested cells (Figure 4-8B). These results indicate that the localizations of Ago1 and Dcr1 are dynamic and appear to be partially dependent on the cell cycle.

Figure 4-7. Ago1 and Dcr1 are associated with large cytoplasmic complexes. Ultrathin cryosections prepared from parental, Δ*ago1* and Δ*dcr1* cells expressing vector (A), HA-Ago1 (B) or Dcr1-HA (C) respectively, were labeled with anti-HA and colloidal gold and viewed by electron microscopy. Arrows denote association of Ago1 and Dcr1 with amorphous electron dense structures. (Scale Bars=0.05 μm). (Data provided by JM McCaffery, Johns Hopkins University, Integrated Imaging Center)

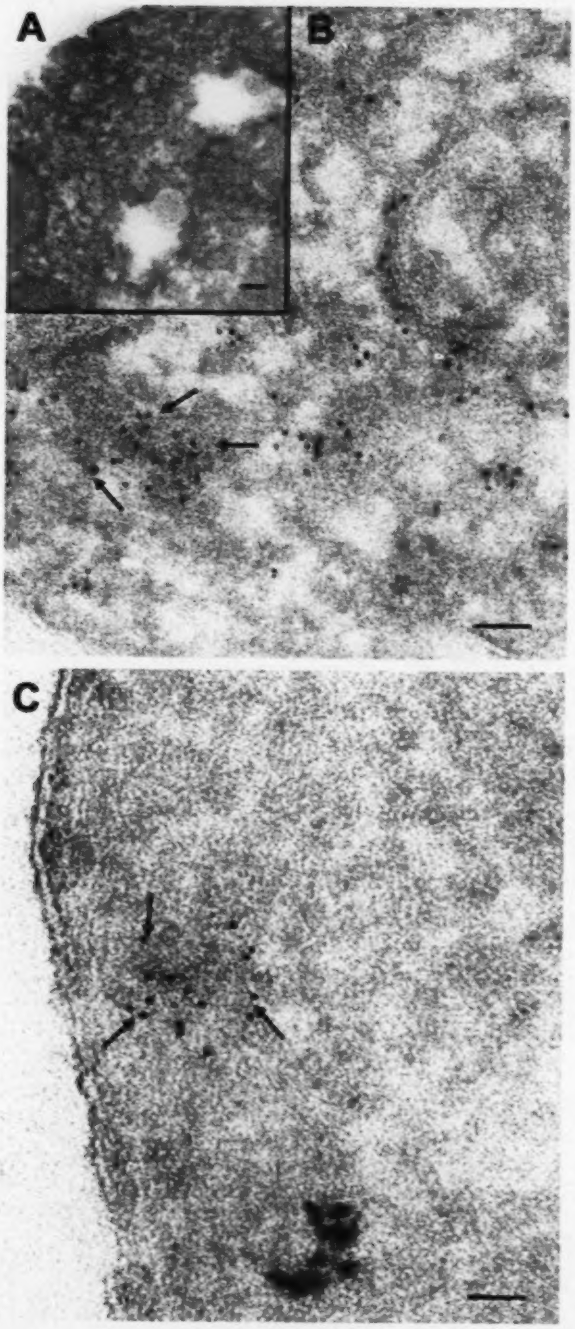
A
B
C

4-7 Localization of Ago1 and Dcr1 in S- and M-phase arrested cells

Previously, we reported that regulated phosphorylation of Cdc2 tyrosine-15 in response to genotoxic insults required Ago1 and Dcr1, but not Rdp1 [Figure 3-6 and (Carmichael et al., 2004)]. This led to the model where Ago1 and Dcr1 have RNAi-dependent gene-silencing functions and siRNA-independent cell cycle functions (Figure 3-9). We compared the localizations of the three core RNAi pathway proteins following camptothecin (CPT) and TBZ treatments which induce S-phase and M-phase blocks, respectively. Neither CPT nor TBZ treatment altered the cytoplasmic localization of GFP-Ago1 (Figure 4-9). Similarly, the nuclear distribution of GFP-Rdp1 was not altered during drug-induced S- and M-phase arrest (Figure 4-9). In contrast, Dcr1-GFP was not excluded from the nucleus when exposed to either CPT (Figure 4-9B) or TBZ (Figure 4-9C). Neither CPT nor TBZ treatment induced concentration of Dcr1 in the nucleus but these drugs did result in the appearance of Dcr1-GFP signal surrounding the nucleus (Figure 4-9B, C and D). These results suggest that a small pool of Dcr1 is able to gain access to the nucleus of cells exposed to genotoxic insults. It is also probable that nuclearly localized Dcr1 is required in S-phase in preparation for RNAi-dependent heterochromatin formation. The fact we do not detect a nuclear pool of Ago1 during S-phase suggests that only a limited amount of Ago1, below our detection level, is required for siRNA-targeted heterochromatin formation.

Figure 4-8. Localization of GFP-Ago1 and Dcr1-GFP following nitrogen-starvation. A and B) PT, Δ*ago1* and Δ*dcr1* cultures expressing GFP, GFP-Ago1 or Dcr1-GFP, respectively, were grown to an OD_{595} =0.6-0.9 in EMM lacking appropriate leucine or uracil (A) or EMM lacking leucine or uracil and nitrogen (B), stained with DAPI (1 μg/ml), placed onto microscope slides coated with poly L-lysine (5 mg/ml) and examined using a Zeiss LSM510 confocal microscope. The white lines indicate the paths drawn to determine the overlap profiles.

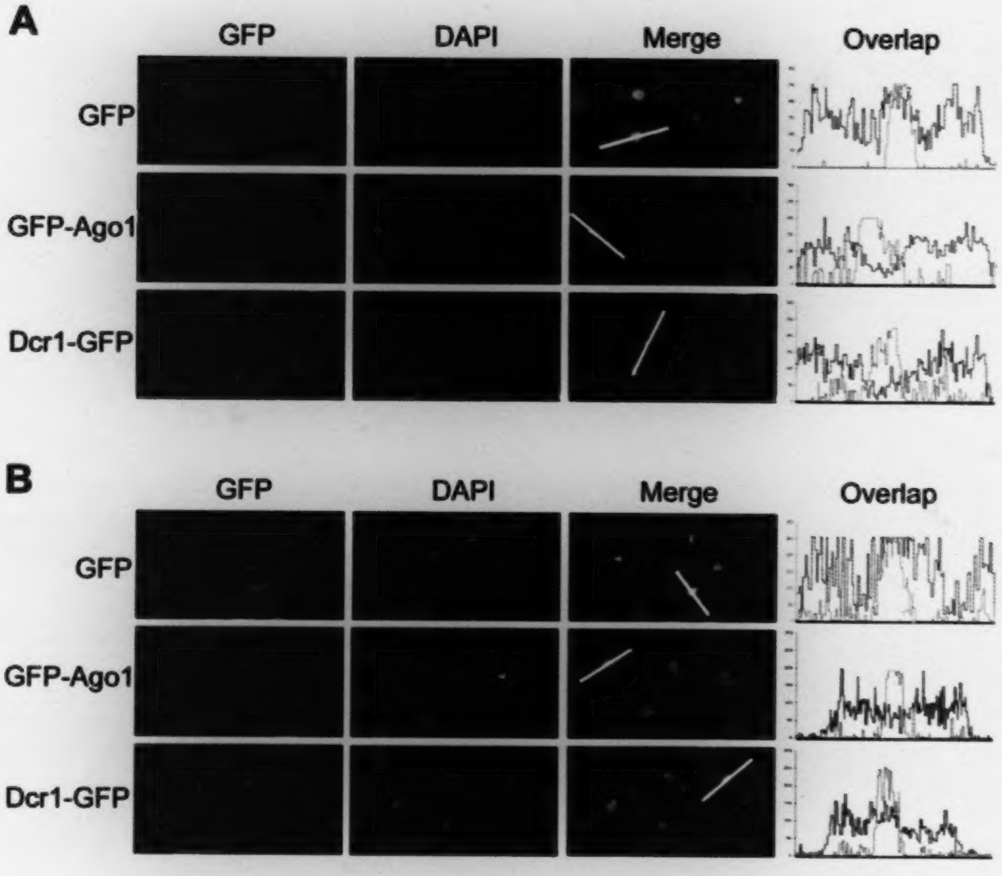
A
GFP
DAPI
Merge
Overlap
GFP
GFP-Ago1
Dcr1-GFP
B
GFP
DAPI
Merge
Overlap
GFP
GFP-Ago1
Dcr1-GFP

4-8 Ago1 is required for cytoplasmic retention of Dcr1

We next investigated whether the localization of RNAi effector proteins are dependent on one another. In addition to directly assessing the requirement of Ago1 for Dcr1 and Rdp1 localizations and visa versa, these experiments were expected to address the potential role of siRNAs in localization of RNAi effector proteins. For example, both Dcr1 and Rdp1 are required for accumulation of siRNAs in *S. pombe* (Sigova et al., 2004). Accordingly, *dcr1* and *rdp1* null mutants are not expected to contain siRNAs. The localization of HA-Rdp1 was not affected by the presence or absence of Ago1 and Dcr1 (Figure 4-10), exhibiting a primarily nuclear localization. Similarly, the cytoplasmic distributions of HA-Ago1 were unchanged in *ago1*, *dcr1* and *rdp1* null strains (Figure 4-10). In contrast, loss of Ago1 expression resulted in a pool of Dcr1-HA entering nuclei (Figure 4-10), reminiscent of Dcr1 localization during cell cycle arrest. These results suggest that the presence or absence of siRNAs does not affect the distribution of Ago1, Dcr1 or Rdp1, but that Ago1 is required for the cytoplasmic retention of Dcr1.

4-9 Conclusion

From the data generated here I am proposing a model whereby a cytoplasmic pool of Ago1 and Dcr1 are directly associated in a siRNA-independent manner (Figure 4-12). This suggests that for RNAi-related mechanisms, Ago1 and Dcr1 may both be required for the effector stage of mRNA degradation as has been suggested in other systems (Lee et al., 2004). Our localization results are in conflict with others regarding the nuclear localization of Ago1 (Noma et al., 2004). Although we were

Figure 4-9. Distribution of core RNAi proteins subjected to S- and M-phase arrest. A) PT, Δ*ago1*, Δ*dcr1* and Δ*rdp1* cultures expressing ectopic GFP, GFP-Ago1, Dcr1-GFP or GFP-Rdp1, respectively, were grown in EMM lacking appropriate nutrients to mid-log phase (OD_{595} =0.6-0.9), stained with DAPI (1 μg/ml), placed onto microscope slides coated with 0.8% agarose and using a Zeiss LSM510 confocal microscope. The arrows indicate the cells used for generation of the overlap profiles. B and C). Cells were grown as described in part A except that 2 hours prior to examination, cells were induced to arrest in S-phase by addition of camptothecin (CPT) (1.0 μM) (B), or M-phase, by thiabendazole (TBZ) (10 μg/ml) treatment (C). Arrows indicate the cells used to generate the overlap data. The arrowheads indicate the perinuclear region in Dcr1-GFP expressing cells (B and C). D) Enlargement of GFP-Ago1 and Dcr1-GFP expressing cells for clearer visualization of the perinuclear region (arrowheads) of Dcr1-GFP expressing cells upon encountering CPT and TBZ. Asterisks are used to denote the position of the nuclei.

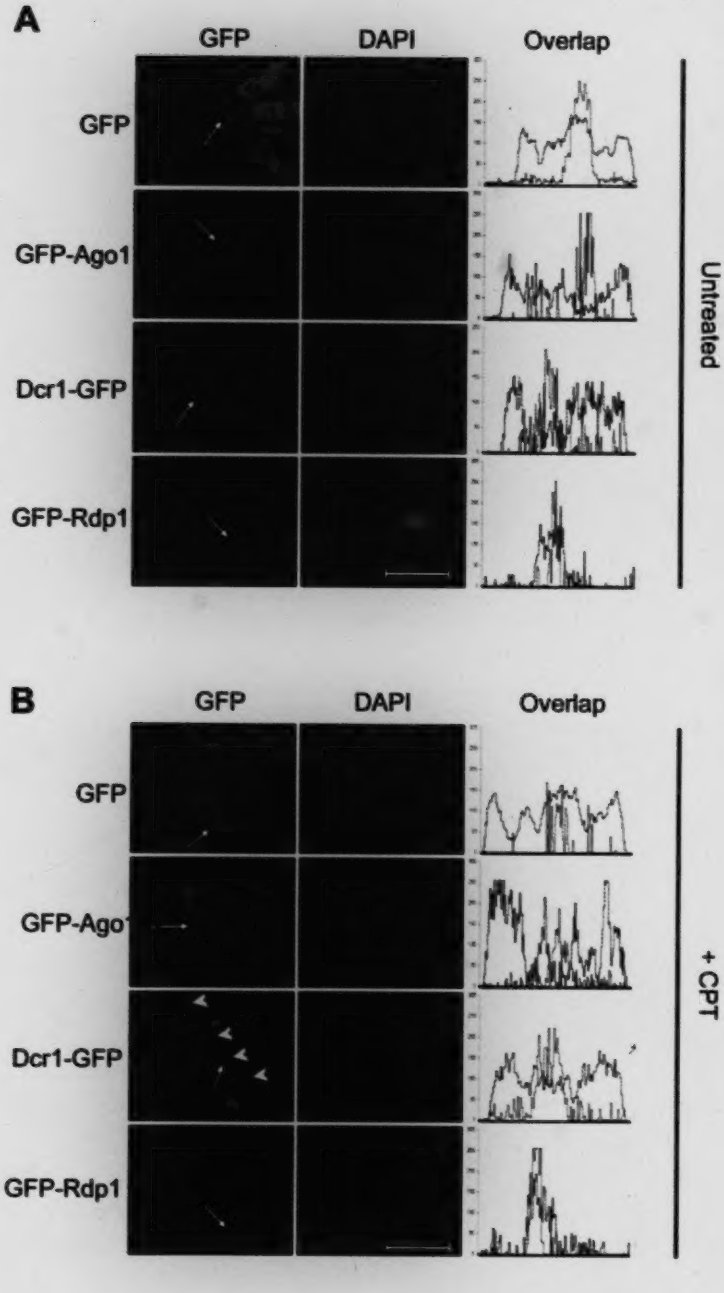
A
GFP
DAPI
Overlap
GFP
GFP-Ago1
Dcr1-GFP
GFP-Rdp1
Untreated
B
GFP
DAPI
Overlap
GFP
GFP-Ago1
Dcr1-GFP
GFP-Rdp1
+ CPT

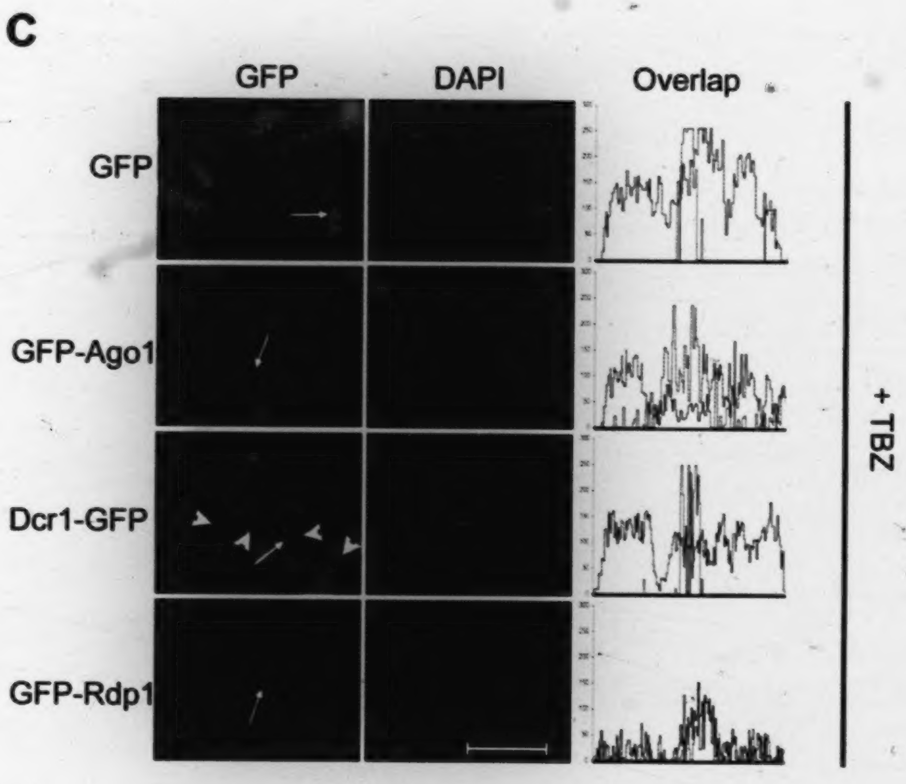
C
GFP
DAPI
Overlap
GFP
GFP-Ago1
Dcr1-GFP
GFP-Rdp1
+ TBZ

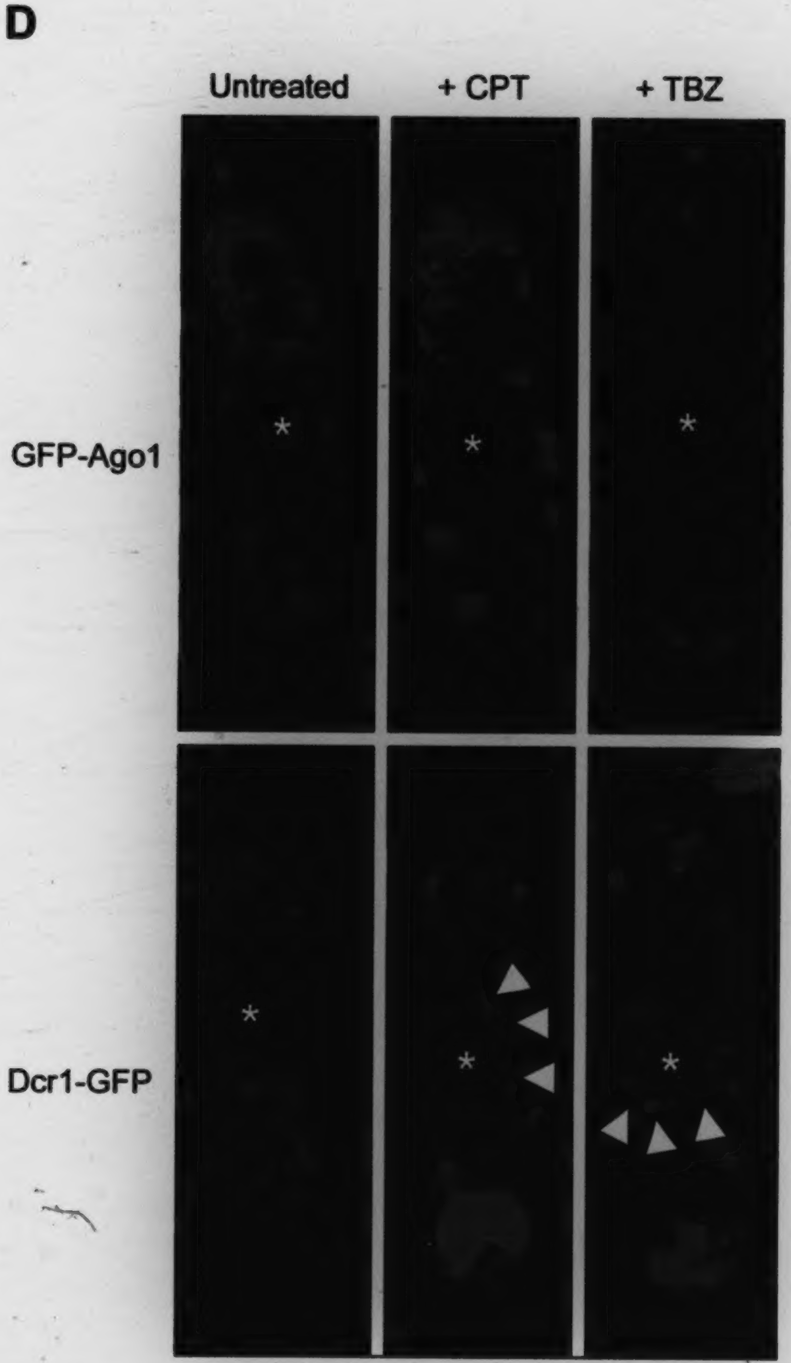
D
Untreated
+ CPT
+ TBZ
GFP-Ago1
Dcr1-GFP
*

unable to detect nuclear Ago1 under normal growth conditions, it is reasonable to expect that there is a pool of nuclear Ago1 required for siRNA-dependent heterochromatin formation (Motamedi et al., 2004; Noma et al., 2004).

Upon S- and M-phase arrest, we observed a redistribution of a pool of Dcr1 from the cytoplasm to the nucleus. It is suspected that the presence of Dcr1 in the nucleus during these insults is required for RNAi-mediated gene silencing in response to genotoxic insults. Further, heterochromatin formation occurs during S-phase (Bailis and Forsburg, 2004) and it is likely that nuclear Dcr1 is required to process Rdp1-amplified centromeric dsRNAs at this stage. With respect to DNA damaging agents, it is likely that during DNA damage, the RNAi pathway intersects with DNA repair pathways. Indeed, the identified interaction of the DNA repair protein Ku70 with HP1α (Song et al., 2001) coupled with the RNAi-dependent heterochromatin association of HP1, suggests that the RNAi pathway is involved in responses to DNA damage (Pal-Bhadra et al., 2004; Song et al., 2001). In addition, we found that loss of Ago1 results in the delocalization of a pool of Dcr1 to the nucleus, suggesting that Ago1 tethers Dcr1 in the cytoplasm. In so much as Ago1 did not show a dynamic localization, I can still make the assumption that Ago1 is present in two pools based on a previous report (Noma et al., 2004). I suggest that the cytoplasmic pool is primed for RNAi-dependent mRNA degradation as Ago1 and Dcr1 are bound to one another in an RNA-independent manner. In the presence of cell cycle-inhibiting agents, I believe that a factor(s) binds Ago1 causing the observed release and nuclear localization of Dcr1. This nuclear pool of Dcr1 then processes Rdp1-amplified dsRNAs that are then loaded onto Ago1 for siRNA-mediated heterochromatin

Figure 4-10. Ago1-dependent localization of Dcr1. Ectoplically introduced HA-tagged Ago1, Dcr1 and Rdp1 were expressed in *ago1*, *dcr1* and *rdp1* null strains that were grown in EMM lacking appropriate nutrients to mid-log phase (OD_{595} =0.6-0.9). Cells were paraformaldehyde-fixed and processed for indirect immunofluorescence. Rat anti-HA (Roche) was used to detect the HA epitope followed by incubation with goat anti-Rat FITC. Cells containing DAPI (1 µg/ml) were applied to microscope slides coated with 0.8% agarose and viewed using a Zeiss LSM510 confocal microscope. The lines indicate the paths used to generate the overlap profiles and arrows indicate nuclei. In panel 2 (Dcr1-HA) arrows point to nuclei void of Dcr1 staining, asterisk (*) indicates nuclear staining and arrowheads indicate the perinuclear increase in Dcr1-HA.

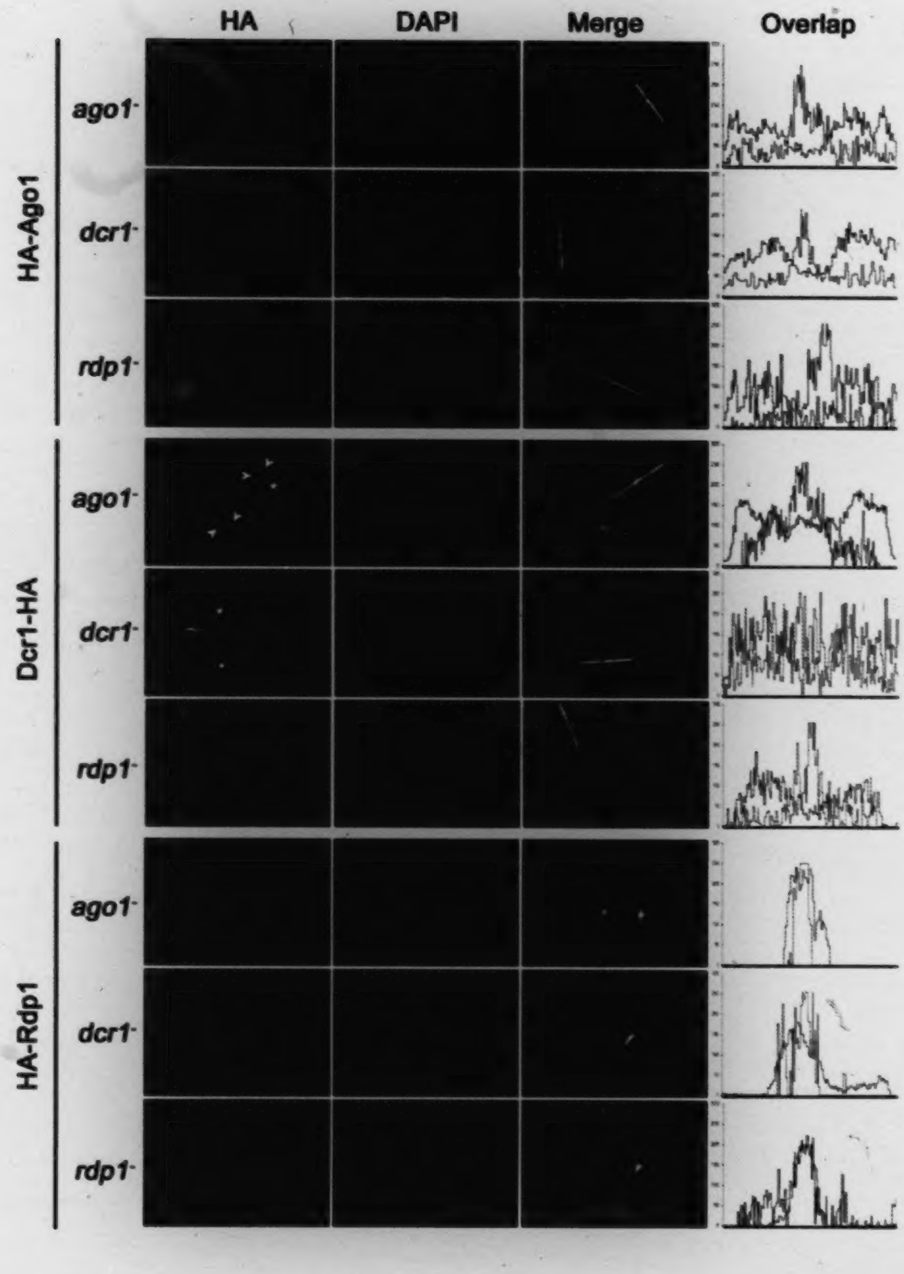
HA
DAPI
Merge
Overlap
HA-Ago1
Dcr1-HA
HA-Rdp1
$ago1^{-}$
$dcr1^{-}$
$rdp1^{-}$
$ago1^{-}$
$dcr1^{-}$
$rdp1^{-}$
$ago1^{-}$
$dcr1^{-}$
$rdp1^{-}$

ormation and DNA repair protein targeting. The fact that Ago1 overexpression complements Δ*dcr1* cell cycle defects indicates that Dcr1 is not necessarily required for cell cycle regulation, rather the requirement for Dcr1 in checkpoint enactment may be to stabilize Ago1 for binding to a cell cycle regulating factor(s).

CHAPTER 5

DISCUSSION

5-1 Overview

Since the discovery that dsRNA could invoke a specific and persistent down-regulation of protein expression through interference with mRNA (Fire et al., 1998), many labs have combined to give us an understanding of the phenomenon we now call RNAi. In yeast, the genes encoding the core components of the RNAi pathway have well documented roles in gene-silencing at both the transcriptional and post-transcriptional levels (Catalanotto et al., 2002; Chicas et al., 2004; Cogoni and Macino, 1999; Hall et al., 2002; Motamedi et al., 2004; Sigova et al., 2004; Sugiyama et al., 2005; Volpe et al., 2003; Volpe et al., 2002). Gene silencing is initiated by the detection and cleavage of dsRNA by Dcr1 into siRNAs. These cleavage products are incorporated into effector complexes such as RITS and RISC which are targeted to DNA and mRNA respectively in a homology-dependent manner. Targeting of the RITS complex to homologous DNA loci by siRNAs derived from centromeric repeats results in formation of heterochromatin (Hall et al., 2002; Provost et al., 2002; Verdel et al., 2004; Volpe et al., 2002).

In mammals, the endonuclease activity of Argonaute proteins associated with the RISC complex is required for the degradation of mRNAs in a siRNA-dependent manner (Liu et al., 2004a; Meister et al., 2004a; Meister et al., 2004b; Song et al., 2004). Loss of Ago1 function in *S. pombe* results in an inability to perform siRNA-directed mRNA degradation, suggesting that Ago1 also is required for the endonuclease activity of RISC (Sigova et al., 2004). Moreover, it has been reported that Argonaute proteins function in translational repression through the binding of miRNAs to 3' untranslated regions of mRNAs (Mourelatos et al., 2002; Okamura et al., 2004; Pillai et al., 2004; Schwarz et al., 2003; Vaucheret et al., 2004). In *S. pombe* there is no evidence for the occurrence of translational repression.

In addition to the Argonaute and Dicer families a third family of proteins, RNA dependent RNA polymerases, have been shown to be required for RNAi in *N. crassa*, *S. pombe*, *A. thaliana* and *C. elegans* (Cogoni and Macino, 1999; Dalmay et al., 2000; Mourrain et al., 2000; Smardon et al., 2000; Volpe et al., 2002). Surprisingly these proteins are not encoded by either *D. melanogaster* or mammalian genomes. In the absence of Rdp1 expression in *S. pombe*, there is no accumulation of siRNAs for RISC-dependent mRNA degradation (Sigova et al., 2004) nor is there RITS-dependent centromeric silencing (Sugiyama et al., 2005). Importantly, it has been shown that loss of either Ago1 or Dcr1 in *S. pombe* also results in loss of both mRNA degradation and chromatin silencing (Hall et al., 2002; Sigova et al., 2004; Volpe et al., 2002). Therefore, it is probable that Ago1, Dcr1 and Rdp1 each reside in nuclear and cytoplasmic pools or that their localizations are dynamic, dictated by the requirement for RISC and RITS complexes.

The cellular localizations of PPD family members, particularly those of the Argonaute sub-family, were largely assumed to be cytoplasmic due to their roles in RISC-mediated mRNA degradation and translational inhibition (Billy et al., 2001; Zeng and Cullen, 2002). The finding that this family is also involved in chromatin modification through a related mechanism suggests that at least some PPD proteins have nuclear localizations (Cox et al., 2000; Noma et al., 2004; Zilberman et al., 2004). In metazoans, there are multiple PPD family members and it is evident that these proteins perform very specific functions. For instance, in mammalian cells the endonuclease activity of RISC is dependent on Ago2, whereas Ago1, Ago3 and Ago4 do not exhibit this activity (Liu et al., 2004a; Meister et al., 2004b). In addition, *D. melanogaster* Ago1 is required for miRNA biogenesis but is dispensable for siRNA-directed mRNA degradation, a process that requires Ago2 (Okamura et al., 2004).

In so much as PPD proteins exhibit different cellular locations, so do members of the Dicer family. *A. thaliana* and *D. melanogaster* both encode for multiple Dicer proteins, some of which appear to localize to the nucleus (Han et al., 2004; Lee et al., 2003; Lee et al., 2004; Park et al., 2002; Pham et al., 2004; Schauer et al., 2002; Xie et al., 2003). DCR2 is required for both siRNA formation and RISC assembly in *D. melanogaster,* whereas another type III RNase, Drosha, is required for processing of pri-miRNAs which occurs in the nucleus (Lee et al., 2003; Lee et al., 2004).

Our findings also suggest that in *S. pombe*, Ago1 and Dcr1 function in an RNAi-independent cell cycle regulatory pathway. In this discussion I will address the requirement of Ago1 and Dcr1 for cell cycle regulation and the potential importance of their cellular localizations in both RNAi-dependent and independent mechanisms.

5-2 Ago1 and Dcr1 function to regulate cell cycle events

5-2-1 *Ago1 and Dcr1 are required to couple completion of mitosis to cytokinesis*

Deletion of *ago1*$^+$ or *dcr1*$^+$ results in an array of defects such as cut phenotypes, fragmented DNA, decreased septation indices and increased numbers of bi-nucleated cells within a population. These initial observations suggested that Ago1 and Dcr1 are required for coupling mitosis to septum formation and cytokinesis. Septum formation and cytokinesis in *S. pombe* are regulated by the septation initiation network, a signaling pathway that ensures that there is establishment of a septum in the medial portion of a dividing cell after the segregation of DNA (Balasubramanian et al., 2000; Le Goff et al., 1999; McCollum and Gould, 2001). Mutations that uncouple septum formation and cytokenisis from mitosis result in elongated, multi-nucleated cells (Marks et al., 1992). Since the defects observed for *ago1*$^+$ and *dcr1*$^+$ deletions were not evident in *rdp1*$^+$ deletion mutants, it is probable that they do not result from loss of RITS and RISC-dependent functions, both of which are dependent on *rdp1*$^+$ expression for activity (Hall et al., 2003; Hall et al., 2002; Motamedi et al., 2004; Sigova et al., 2004; Sugiyama et al., 2005; Volpe et al., 2003).

5-2-2 *Ago1 and Dcr1 function independently of Rdp1 and the RNAi pathway for conjugation in a nitrogen-dependent manner*

A hallmark phenotype for PPD and Dicer mutations in metazoans is infertility (Cox et al., 2000; Grishok et al., 2001; Knight and Bass, 2001; Parrish and Fire, 2001; Smardon et al., 2000). We also found that Δ*ago1* and Δ*dcr1* mutants in *S. pombe* were mating defective. In *S. pombe,* silencing of the *mat2/mat3* mating type region is required for conjugation and an inability to silence this region results in expression of both mating type loci and subsequent abortive meiosis (Thon et al., 1994). Although the role RNAi plays in heterochromatin formation at centomeres is becoming well established (Bernard et al., 2001; Ekwall, 2004; Fukagawa et al., 2004; Hall et al., 2002; Motamedi et al., 2004; Pal-Bhadra et al., 2004; Verdel et al., 2004; Volpe et al., 2002), its function in silencing of the mating type region is more ambiguous. At least one study indicates that silencing of the *mat* locus occurs in RNAi-defective mutants suggesting that either the establishment or maintenance of the nucleated chromatin state can be accomplished in the absence of Ago1, Dcr1 or Rdp1 (Hall et al., 2002). Furthermore, two members of the RITS complex Tas3 and Chp1, can associate with the *mat* locus in the absence of Ago1 (Noma et al., 2004; Petrie et al., 2005). Establishment of heterochromatin at the *mat* locus appears to be a cooperative venture between the siRNA-directed RITS and the stress-activated MAPK pathway. Heterochromatin formation at this location is abolished only when both pathways are lost (Jia et al., 2004). It is not clear how RNAi-dependent and independent pathways converge at this locus to ensure silencing nor what role RITS proteins Chp1 and Tas3 play in the absence of siRNAs to enact chromatin modification. Yet, there does appear to be a functional redundancy between RNAi-dependent and independent pathways. Specifically, heterochromatin formation at the *mat* locus is only abolished when collectively, siRNA-mediated RITS targeting has failed, Chp1 function outside of the context of the RITS complex is abolished, and failure of the MAP kinase pathway to activate Atf1 occurs (Jia et al., 2004; Noma et al., 2004; Petrie et al., 2005).

Initial observations in *S. pombe* suggested that strains deleted for core RNAi proteins were mating-competent (Volpe et al., 2002). This is somewhat surprising given the apparent linkage between RNAi and fertility in metazoans, specifically, loss of RNAi results in infertility. However, evidence does exist that these mechanisms can be uncoupled. For example, mutants of *A. thaliana* AGO1 have been isolated that are fertile yet RNAi defective and vice versa (Morel et al., 2002).

Fission yeast when deprived of nitrogen will arrest in G_1 and either enter a dormant state or undergo conjugation if partners of opposite mating type are available (Nurse and Bissett, 1981). Our results indicate that the ability to enter or maintain a G_1-arrest when starved of nitrogen is dependent on both *ago1*$^+$ and *dcr1*$^+$ but not *rdp1*$^+$. In lieu of this finding it was not surprising to note that both Δ*ago1* and Δ*dcr1* strains are severely impaired for mating when cultured in nitrogen-limiting environments. Although in contrast to Volpe *et al.* (2002), this does not lend evidence that the ability to mate was a physical manifestation of an inability to silence the *mat2/3* locus, rather it suggested that the upstream stage of arresting when deprived of nitrogen was impaired. As such, we employed the use of conditions that limit both nitrogen and glucose. This treatment has been shown to induce mating, presumably through facilitating a G_1-arrest through a different pathway (Okazaki et al., 1998). When we performed mating assays with Δ*ago1* strains under these conditions, we found that the mutants mated with the same frequencies as parental strains. These data, in combination with the low nitrogen mating defects, suggest that the mating defects associated with the *ago1* and *dcr1* null mutants are not due to global defects stemming from a lack of a functioning RNAi pathway. Rather, the defect in mating associated with loss of Ago1 and Dcr1 function arises from a failure to initiate a cell cycle block in G_1 when nitrogen is absent.

5-2-3 *Ago1 and Dcr1 are required for enactment of replication and DNA damage checkpoints through regulated tyrosine-15 phosphorylation of Cdc2 in an sRNAi-independent manner*

The link between normal cell cycle progression and the commitment to undergo conjugation appears to be disparate, yet there is a tangible connection between these mechanisms. Cdc2 is the only cyclin-dependent kinase in *S. pombe* and, as such, it is central to coupling DNA replication to mitosis (Enoch et al., 1992; Enoch and Nurse, 1990; Fisher and Nurse, 1996) and cytokinesis (Fankhauser et al., 1993; Fankhauser and Simanis, 1993). Activation of the septation initiation network and subsequent septation requires a reduction in Cdc2 activity (Beltraminelli et al., 1999; Fankhauser et al., 1993; Fankhauser and Simanis, 1993; Guertin et al., 2000; He et al., 1997; Murone and Simanis, 1996). In addition, upon nitrogen starvation a decrease in Cdc2 activity occurs through degradation of cyclins coupled with a persistence of Cdc2 tyrosine 15 phosphorylation (Chang et al., 1994; Stern and Nurse, 1998; Wu and Russell, 1997). Our observations indicate that the cell cycle defects associated with loss of Ago1 or Dcr1 are probably related to a loss of Cdc2 regulation.

Genotoxins that uncouple replication from mitosis cause enactment of checkpoint arrest at defined points in the cell cycle through a common set of gene products (al-Khodairy and Carr, 1992; Furnari et al., 1997; Raleigh and O'Connell, 2000; Rhind et al., 1997; Rhind and Russell, 1998; Rowley et al., 1992). The collective function of these proteins is to regulate the activity of Cdc2 such that inhibitory phosphorylation of tyrosine 15 leads to a block in the cell cycle until replication inhibition or DNA damage is relieved or repaired, respectively (Fisher and Nurse, 1996; Gould and Nurse, 1989; Lee et al., 1994; Lundgren et al., 1991; Millar et al., 1991; Rhind et al., 1997; Rhind and Russell, 1998). Using Cdc2 tyrosine phosphorylation as a determinant of checkpoint activation, we found that *ago1*$^+$ and *dcr1*$^+$ function in the initiation and/or maintenance of DNA replication and damage checkpoints. Failure to enact these checkpoints in *ago1*$^+$ and *dcr1*$^+$ null mutants likely results from their inability to affect tyrosine-15 phosphorylation of Cdc2 when cells are exposed to hydroxyurea. The sensitivity of *ago1*$^+$ and *dcr1*$^+$ null mutants to UV light is likely a result of an inability to activate the DNA damage checkpoint through regulatory phosphorylation of Cdc2.

We discovered that hAgo2 was able to complement the cytokinesis defect and DNA replication checkpoint deficiencies of *ago1* mutants. This suggests that PPD proteins regulate cell cycle events in mammalian cells, a function not reported previously. These findings are significant as they point to alternative roles for core RNAi proteins in humans. For instance, the cross-talk between Piwi and hedgehog signaling pathways in *D. melanogaster* (King et al., 2001) further supports the observation of RNAi-independent roles for core RNAi proteins. Although we cannot discount the potential role of si/miRNAs in Piwi regulatory pathways, it is interesting that Piwi has not been shown to bind si/miRNAs (Liu et al., 2005). Further, the Hedgehog signaling pathway has not been shown to be dependent on the RNAi pathway. Intriguingly, binding of Sonic hedgehog to the human tumor suppressor protein Patched1 (Ptc1) facilitates CyclinB1 nuclear localization, increased Cdc2 activity and progression through mitosis (Barnes et al., 2001). In addition, ectopic expression of Piwi increases the division rate of germline stem cells, whereas mutations that compromise Piwi function(s) have the opposite effect (Cox et al., 2000). The observations by Cox *et al.* (2000) are consistent with our observations that Ago1 and Dcr1 perform roles in cell cycle regulation independent of the production of siRNAs.

5-2-4 Convergence of Ago1 and Dcr1 RNAi-independent functions with the stress-activated MAP kinase pathway

Considering the phenotypes of *ago1*$^+$ and *dcr1*$^+$ deletion mutants, there is a striking degree of similarity with those observed in stress-response MAP kinase mutants. Specifically, yeast with mutations in genes that encode the MAP kinase kinase Wis1, the MAP kinase Sty1, or their downstream target, the transcription factor Atf1, cannot arrest in G_1 upon nitrogen deprivation, exhibit mating defects and sensitivity to ultraviolet radiation (Millar et al., 1995; Shiozaki and Russell, 1995; Warbrick and Fantes, 1991). These findings suggest that response to environmental or genotoxic stress requires linking the cell cycle regulatory machinery to stress-response pathways (Shiozaki and Russell, 1995). Interestingly, the Sty1 activated kinase Srk1, has been shown to inhibit Cdc25 activity by promoting Cdc25 retention in the cytoplasm in a Rad24-dependent manner (Lopez-Aviles et al., 2005). It is also known that the Sty1-activated transcription factor Atf1 is required for nucleation of heterochromatin in the absence of the RNAi machinery (Jia et al., 2004). Furthermore, it appears that the RNAi pathway, in addition to Chp1 and Tas3 (Noma et al., 2004; Petrie et al., 2005) functions cooperatively with the stress-activated MAP kinase pathway for establishment of silencing of the *mat* locus (Jia et al., 2004). Thus, it is conceivable that just as proteins in the MAP kinase pathway can functionally intersect with both the cell cycle regulatory machinery and RNAi-dependent pathways, that Ago1 and Dcr1 crossover to function in pathways that ultimately affect Cdc2 regulation (Figure 5-1).

The possibility must be considered that the cell cycle defects associated with *ago1* and *dcr1* mutants are the result of an inability to enact transcriptional and/or post-transcriptional silencing of genes that modulate the cell cycle. However, if this is the case it is difficult to explain why no known cell cycle regulatory genes are regulated by siRNA-mediated silencing (Hansen et al., 2005; Provost et al., 2002).

Loss of Ago1, Dcr1 or Rdp1 activity results in significant MAP kinase or Atf1-dependent upregulation of *cta3* and *hsp16* (Hansen et al., 2005; Nishikawa et al., 1999; Taricani et al., 2001). The finding that loss of a functional RNAi pathway in *S. pombe* leads to upregulation of *hsp16* is relevant to this discussion in that nucleotide depletion or DNA damage also results in enhancement of *hsp16* expression (Taricani et al., 2001). This suggests that either the RNAi apparatus is required for the regulation of some stress-response factors that respond to DNA damage or that the MAPK pathway functions in a compensatory role as a consequence of defective RNAi. Given these observations, it is possible that the RNAi pathway and Ago1 and Dcr1 independent of siRNAs converge with the stress-activated MAPK pathway to ensure DNA lesions are corrected prior to mitosis.

Figure 5-1 Convergence of the RNAi, SAPK and cell cycle regulatory pathways in the maintenance of genome integrity. Briefly, RNAi-dependent histone H3-MeK9 and heterochromatin formation is connected with black lines, cell cycle regulation is outlined in red and the stress response cascade in indicated in blue. The core RNAi proteins diverge from RNAi-dependent heterochromatin formation and integrate into the cell cycle regulation of Cdc2 through some unknown interaction. The RNAi-dependent targeting of Swi6/HP1 to heterochromatin is followed by the Swi6/HP1-dependent recruitment of DNA repair proteins to sites of DNA damage. Independent of siRNAs, SIR-dependent chromatin nucleation results in targeting of DNA damage sensing proteins. The MAPK pathway intersects the RNAi pathway through its cooperative role in heterochromatin formation through histone H3-MeK9 and subsequent recruitment of DNA damage response proteins. In addition, the upregulation of Atf1 stimulated genes in response to loss of core RNAi proteins are indicated (dashed blue line). Activation of Srk1 by Spc1 MAPK results in an accumulation of Cdc25 in the cytoplasm and a decrease in Cdc2 activity. Cell cycle regulation of Cdc2 activity is controlled by the apposing actions of the kinases Mik1/Wee1 and the phosphatase Cdc25. Upon DNA damage or incomplete replication a signal is transduced by the chromatin bound Rad/Hus complex and activates Chk1. Chk1 activation results in decreased Cdc2 activity and arresting of the cell cycle.

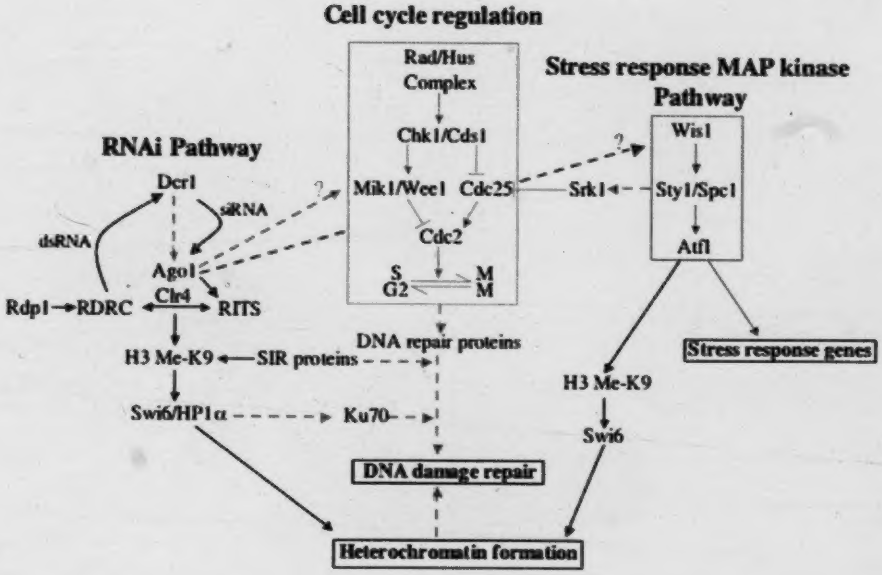
Cell cycle regulation
Rad/Hus Complex
Chk1/Cds1
Mik1/Wee1
Cdc25
Cdc2
S
G2
M
M
Stress response MAP kinase Pathway
Wis1
Sty1/Spc1
Atf1
Srk1
?
?
RNAi Pathway
Dcr1
siRNA
dsRNA
Ago1
Clr4
Rdp1
RDRC
RITS
H3 Me-K9
SIR proteins
DNA repair proteins
Swi6/HP1α
Ku70
DNA damage repair
Heterochromatin formation
H3 Me-K9
Swi6
Stress response genes

5-3 Interactions between Ago1, Dcr1 and Rdp1

In humans, the direct interaction between PPD and Dicer proteins occur between their PIWI and RNase III domains, respectively (Doi et al., 2003; Tahbaz et al., 2004). The stability of human Dicer and PPD proteins in soluble and membrane-associated fractions is dependent on the activity of the heat shock protein Hsp90 (Tahbaz et al., 2001; Tahbaz et al., 2004) suggesting that RISC assembly or function in humans occurs in different intracellular locations.

In *S. pombe*, the interaction between Ago1 and Dcr1 occurs in a nucleic acid-independent manner and it is likely that the interaction is direct in keeping with the situation in other organisms (Doi et al., 2003; Tahbaz et al., 2004). It is conceivable that a pool of Ago1 and Dcr1 exist in pre-assembled complexes prior to encountering dsRNA triggers and that this interaction is required for generation of siRNAs and/or RISC formation and function. The importance of this interaction is illustrated by the importance of PPD-Dicer interactions in *D. melanogaster*. The presence of both DCR2 and Ago2 in the holo-RISC complex is required for unwinding of the siRNA guide duplex (Tomari et al., 2004). In addition, a complex containing DCR1 and DCR2 is required for siRNA-directed mRNA cleavage (Lee et al., 2004), presumably facilitated by Ago2. Thus, it is likely that in *S. pombe* Ago1 and Dcr1 function together at the effector stage of RNAi in mRNA degradation.

Recently, it was suggested that Ago1-incorporated RITS complexes and the Rdp1-containing RDRCs interact at sites of centromeric silencing in a Dcr1/Clr4-dependent manner (Motamedi et al., 2004). Further, our observation that the Ago1-Rdp1 interaction decreases upon nuclease treatment, suggests that this interaction is mediated by nucleic acids. It is feasible to assume that the requirement for Dcr1 is not direct as we were unable to detect an interaction between Rdp1 and Dcr1. It is more likely that the requirement for Dcr1 in the RITS-RDRC interaction is associated with siRNA biogenesis. *D. melanogaster* requires that the dsRNA binding proteins Pasha, Loquacious and R2D2 associate with Drosha, DCR-1 and DCR-2 respectively for miRNA and siRNA biogenesis (Denli et al., 2004; Forstemann et al., 2005; Saito et al., 2005). This may indicate that in *S. pombe* Rdp1 products are transferred to Dcr1 by an as yet unidentified dsRNA biding protein.

The requirement for Clr4 in the RITS-RDRC interaction is perplexing unless one makes the assumption that the requirement for Clr4 in this process occurs downstream of Clr4 targeting. Methylation of histone 3 on lysine 9 requires targeting of Clr4 by RITS through Dcr1-derived siRNAs (Volpe et al., 2002). This methylation imprint is required for the recruitment of Swi6 followed by cohesins (Bernard et al., 2001; Hall et al., 2002; Volpe et al., 2002). It is likely that targeting of Clr4 and recruitment of cohesins stabilizes RITS-loaded siRNAs on the nascent RDRC transcript. The resulting duplex of RITS siRNAs and RDRC transcript may serve to clamp RDRC to the original transcript and enhance the efficiency of amplification of centromerically derived dsRNAs. This essentially links the two processes as suggested by Sugiyama *et al.* (2005), such that the amplification event is as dependent on RITS-targeting of Clr4 as RITS activity is on RDRC-derived dsRNAs.

5-4 Localizations of Ago1, Dcr1 and Rdp1

Our binding studies (Section 4-2) bring up some very important questions regarding the mechanisms that are brought to bear to enable the amplification, initiation and effector stages of RNAi. When we consider that Ago1 and Dcr1 also function independently of Rdp1 and siRNAs in cell cycle regulation, the picture becomes even more confounding. It is likely that the localization of the core RNAi proteins plays a significant role in determining their function. For example, in the budding yeast *S. cerevisiae*, it was recently discovered that type III RNases function in cell cycle regulation. Although this organism does not utilize RNAi, it does encode the Dcr1 homolog Rnt1, that is required for cell cycle progression and nuclear division (Catala et al., 2004). Importantly, the RNase activity of Rnt1 and presumably its small RNA products are not required for cell cycle regulation. Rather, the cellular localization of this RNase is critical for its regulation of cell cycle events. By analogy, it could be inferred that the role Dcr1 plays in cell cycle regulation is not dependent on its ability to cleave dsRNA but on its controlled access to downstream cell cycle regulating factors.

5-4-1 *Rdp1 is largely confined to nuclei in S. pombe*

In *S. pombe*, both the degradation of mRNA by RISC and the silencing of heterochromatin by RITS requires Ago1, Dcr1 and Rdp1 (Motamedi et al., 2004; Noma et al., 2004; Sigova et al., 2004). As these processes likely occur in different cellular locations, the question arises as to how these proteins are localized to fulfill their respective roles in gene-silencing.

The function of Rdp1 in mRNA degradation is potentially different than its role in heterochromatin formation. Similar to the role of RdRP family members in other systems, Rdp1 is thought to be an amplifier of dsRNAs derived from Dcr1 cleavage products during mRNA degradation (Makeyev and Bamford, 2002; Sijen et al., 2001; Vaistij et al., 2002). The implication is that Rdp1 functions downstream of Dcr1 in a cytoplasmic location.

In contrast, the production and subsequent amplification of dsRNA from centromeric repeats would seem to require a nuclear Rdp1 activity prior to Dcr1 processing of dsRNA. Our results, in accordance with a previously published report (Motamedi et al., 2004), indicate that Rdp1 is located primarily in the nucleus, although we were unable to discern if it was associated with specific heterochromatic loci. Although this result was expected given the role of Rdp1 in heterochromatin formation via the RDRC complex (Motamedi et al., 2004), it was not clear as to why we failed to detect significant levels of Rdp1 in the cytoplasm. One explanation for the low levels of observable cytoplasmic Rdp1 may be due to the differences between cytoplasmic and nuclear volumes. If we assume that the nucleus of a fission yeast occupies approximately 20% of a cell volume, then the relative signal strength observed for 1:1 nuclear:cytoplasmic Rdp1 stoichiometry would be 4:1. The low level of cytoplasmic Rdp1 may also be indicative of the importance of RDRC-dependent heterochromatin formation in comparison to mRNA-degradation in *S. pombe*. Indeed, evolutionarily the RNAi pathway may have been solely required for genome protection and epigenetic silencing. The roles in post-trascriptional gene silencing probably evolved as a secondary protective mechanism utilizing this conserved module of proteins.

In *Xenopus* and human systems, dsRNAs in the form of hairpins are exported from the nucleus for Dicer processing by Exportin-5 (Bohnsack et al., 2004; Yi et al., 2003). As there is no Exportin-5-like protein in *S. pombe*, although there is a low level of similarity to Crm1, it is probable that the core RNAi proteins are present in cytoplasmic and nuclear pools or that they can be dynamically localized depending on the requirement for mRNA degradation or heterochromatin nucleation. Indeed, the two other known members of the RDRC, Hrr1 and Cid12, in addition to existing in the nucleus, appear to localize albeit at low levels, to the cytoplasm (Motamedi et al., 2004). Thus it is probable that RDRC amplification of dsRNA likely occurs in the cytoplasm and the nucleus to enable RISC and RITS gene-silencing respectively.

5-4-2 *Ago1 is largely confined to the cytoplasm in S. pombe*

Ago1 is the only PPD protein in *S. pombe* so localization of this protein is expected to be important in regulating access to binding partners for its respective functions in RISC, RITS and cell cycle regulation. Our biochemical data coupled with live cell GFP imaging and immmunofluorescence data suggest that Ago1 is associated with cytoplasmic complexes. This was not surprising when one considers that mRNA degradation occurs in the cytoplasm and that Ago1 is required for this process (Sigova et al., 2004). Recently, hAgo2 was identified as associating with processing bodies (P-bodies), known centers containing decapping enzymes required for mRNA degradation (Bashkirov et al., 1997; Cougot et al., 2004; Liu et al., 2005; Sen and Blau, 2005). It seems fitting that hAgo2 would be identified in association with P-bodies since it is the only human Argonaute isoform to display endonuclease activity (Liu et al., 2004a; Meister et al., 2004a; Meister et al., 2004b; Rivas et al., 2005). Further, it has been shown that these structures are a destination for miRNA-targeted localization of mRNAs (Liu et al., 2005). Thus, it is conceivable that both RNAi-dependent mRNA degradation and translational repression occur in the same cytoplasmic structure.

It is intriguing to speculate that the electron dense regions associated with Ago1 clusters are P-bodies. Although Ago1 has been shown to preferentially localize to heterochromatic foci, it was noted that there appears to be a minor, speckled distribution of Ago1 that is consistent with its association with P-bodies (Noma et al., 2004). The association of Ago1 with these cytoplasmic structures or exclusion from the nucleus is probably not dependent on the presence of siRNAs as loss of either Dcr1 or Rdp1 function did not result in a nuclear pool of Ago1. It should be noted that Ago2 association with P-bodies has been reported to be both siRNA-independent and dependent by two different groups (Liu et al., 2005; Sen and Blau, 2005). Thus, although P-bodies may be the sites of post-transcriptional gene silencing, the requirements for targeting of the RISC and trafficking of target substrates to this structure are not known.

Recent evidence suggests that Ago1, like Rdp1, also resides in a cytoplasmic and nuclear pool (Noma et al., 2004). In *D. melanogaster*, the nuclear PPD protein, Piwi, is required for heterochromatin formation through RNAi-dependent localization of heterochromatin protein 1 (HP1) (Pal-Bhadra et al., 2004). In addition the cytoplasmic proteins Ago1 and Ago2 are required for mRNA translational repression and mRNA degradation respectively (Okamura et al., 2004). The requirement for PPD proteins to be present in both the nucleus and cytoplasm to enable heterochromatin formation and mRNA degradation/translational repression implies that in *S. pombe*, Ago1 must have access to both the cytoplasm and nucleus. Although we did not detect nuclear Ago1 during active growth, upon nitrogen and glucose limiting conditions which induce mating, pools of nuclear Ago1 were observed. Indeed, in *Tetrahymena thermophila*, elimination of germ-line specific sequences during conjugation requires the methylation of DNA in a small RNA –dependent RNAi-like mechanism (Janetopoulos et al., 1999; Liu et al., 2004b; Mochizuki et al., 2002; Mochizuki and Gorovsky, 2004a; Mochizuki and Gorovsky, 2004b). In S. pombe, during conjugation the genome undergoes between 100 and 1000 times the amount of recombination to that of mitotic cells (Fox and Smith, 1998). The fact that this was the only time we observed Ago1 in the nucleus suggests that the requirement for RITS activity is increased during conjugation. Ago1 is also required for nitrogen-specific conjugation, possibly through its role in Cdc2 regulation, suggesting that there is a cell cycle-dependent convergence of RNAi-independent and dependent pathways.

Surprisingly, S-phase arrest did not result in an increase in nuclear Ago1. This result was confusing as heterochromatin formation occurs in late S-phase (Bailis and Forsburg, 2004) and may be expected to coincide with a rise in nuclear Ago1-associated RITS activity. In addition, cells treated with the DNA damaging agent CPT did not exhibit a nuclear pool of Ago1. Recently it was shown that upon DNA damage there is a redistribution of proteins required for heterochromatin formation to sites of damage, perhaps as guides for the DNA repair apparatus (Garcia-Salcedo et al., 2003; Mills et al., 1999; Shankaranarayana et al., 2003; Takeda et al., 2004). The linkage between RNAi-dependent heterochromatin formation and DNA damage response and repair is further strengthened by the observation that the DNA repair protein Ku70, associates with HP1α (Song et al., 2001). The localization of these proteins probably occurs in the same manner as RNAi-dependent localization of HP1 in *D. melanogaster* (Pal-Bhadra et al., 2004). This further supports our suggestion that convergence of these pathways is needed to maintain genome fidelity. Yet if this is the case, why did I not detect an increase in nuclear Ago1 following genotoxic insult? The dynamics of heterochromatin formation may be the key to putting these results in perspective.

The establishment of heterochromatin requires RITS-dependent recruitment of Swi6 to sites of Clr4 methylation (Hall et al., 2002; Motamedi et al., 2004; Volpe et al., 2002), but the maintenance of these established sites is not RNAi-dependent (Hall et al., 2002; Sadaie et al., 2004). It is likely that following the nucleation of heterochromatin, the spreading of heterochromatin in a Swi6-cohesin-dependent manner is also independent of RNAi (Hall et al., 2002; Sadaie et al., 2004). If this is the case, then it is possible that only a small amount of Ago1 is required for the initial nucleation event and not the propagation of heterochromatin over wide areas. Indeed, our binding assays showed that the Ago1-Rdp1 interaction in the presence of intact RNA was as robust as the Ago1-Dcr1 interaction. Thus, limiting nuclear Ago1 may be required to facilitate a rapid response when siRNAs are present. In accordance with a rapid response mechanism it has been suggested that the RITS proteins, Chp1 and Tas3, accumulate at non-centromeric loci, primed for a response upon formation of a functional RITS complex when Ago1-loaded siRNAs are encountered (Petrie et al., 2005). Since there was no detectable net movement of Ago1 from the cytoplasm to the nucleus when encountering genotoxic insults the response to genotoxins is probably independent of siRNAs. This suggests that the cell cycle response of Ago1 to genotoxins probably requires an interaction with cytoplasmic localized Cdc2-regulating factors such as 14-3-3 proteins or Cdc25.

5-4-3 *Dcr1 cytoplasmic retention is cell cycle-regulated and Ago1-dependent*

Our biochemical and fluorescence results suggest that *S. pombe* Dcr1 is primarily a cytoplasmic protein. The association between Ago1 and Dcr1 does not require intact RNA, but interestingly Ago1 is required for the retention of Dcr1 in the cytoplasm. In addition, we noted that S- or M-phase arrest by genotoxins results in a small amount of Dcr1 being detected in the nuclear compartment. It is interesting also to note that when Dcr1 is not excluded from the nucleus, a build up of the protein occurs at perinuclear sites. These results suggest that Dcr1 import into the nucleus is a regulated event. For example, regulation of Dcr1 nuclear import may occur in a similar manner to that of RNA helicase A, a protein that resides in a complex with Ku70 and Vigilin (Wang et al., 2005). The association of Ku70 with HP1α (Song et al., 2001) and the reliance of HP1 heterochromatin localization on the RNAi machinery (Pal-Bhadra et al., 2004) suggest that the accumulation of these factors at heterochromatic sites is also under the control of siRNAs. Since Ku70 is a DNA repair protein (Song et al., 2001) it is likely that the heterochromatic localization of this complex occurs in response to DNA damage.

RNA helicase A nuclear localization is regulated by arginine methylation and abrogation of this process decreases nuclear import (Smith et al., 2004). Further, upon translocation, association with PolII complexes is necessary for the nuclear retention of RNA helicase A (Fujita et al., 2005). Dcr1 contains an RGRARA motif in the RNA helicase C domain. Like RNA helicase A, it is possible that methylation of this region in Dcr1 or some other post-translational modification mediates or is necessary for translocation to the nucleus.

It should not be surprising that Dcr1 is required to function in two discrete cellular locations. By way of example, *D. melanogaster* encodes a number of Dicer homologues that display differential localizations and perform different RNAi-related functions (Han et al., 2004; Lee et al., 2003; Lee et al., 2004). For instance the nuclear protein Drosha, is required for processing pri-miRNAs into pre-miRNAs (Lee et al., 2003). The Exportin-5-dependent export of pre-mRNAs facilitates miRNA production by the cytoplasmic Dicer isoforms for translational inhibition (Lee et al., 2004; Yi et al., 2003). In *A. thaliana,* evidence exists that DCL1 is involved in nuclear processing of miRNA precursors (Papp et al., 2003). Perhaps even more telling is that vertebrates contain only one Dicer member and many of these enzymes contain putative nuclear localization signals (Bernstein et al., 2003; Wienholds et al., 2003).

The fact that Dcr1 also resides in structures that may prove to be P-bodies suggests that it may be a participant in the effector stage of mRNA degradation at these sites. Indeed, two *D. melanogaster* isoforms, DCR-1 and DCR-2, are required for siRNA-directed mRNA cleavage (Lee et al., 2004). Further, DCR-2 is required for siRNA unwinding in the context of the holo-RISC (Tomari et al., 2004), suggesting a role for Dicer family members in the effector stage of RNAi. The role of Dcr1 in formation of siRNAs is well established, yet it is not clear how Rdp1-amplified dsRNAs derived from centromeric repeats encounter Dcr1 for processing in *S. pombe*. Significantly, during S-phase arrest Dcr1 is not excluded from the nucleus. This is important as the processing of siRNAs from Rdp1-generated dsRNAs would be required at this point for DNA methylation followed by adherence of cohesin molecules in a Swi6 dependent manner (Bailis et al., 2003; Bailis and Forsburg, 2004; Bernard et al., 2001; Hall et al., 2002; Nonaka et al., 2002; Volpe et al., 2002). In addition, following DNA damage, Dcr1 was detected in the nucleus.

There is a growing body of evidence suggesting that targeting of DNA damage repair proteins occurs in association with proteins that participate in heterochromatin nucleation (Garcia-Salcedo et al., 2003; Mills et al., 1999; Shankaranarayana et al., 2003). It is quite likely that the targeting of these molecules occurs in a Dcr1-derived siRNA targeting-dependent mechanism, linking heterochromatin formation and cell cycle regulation to the detection of environmental stress for the maintenance of genome integrity.

5-4-4 *The RNAi pathway converges with cell cycle regulation*

The survival of a cell is dependent on the faithful segregation of genomic material from mother to daughter cell. It should not be surprising then that redundant systems exist to ensure genome fidelity. It appears that the stress-response, cell cycle regulatory and the RNAi pathways converge to ensure that replication and segregation of DNA occurs without defect (Carmichael et al., 2004; Degols and

Russell, 1997; Garcia-Salcedo et al., 2003; Hall et al., 2002; Janetopoulos et al., 1999; Jia et al., 2004; Kim et al., 2000; King et al., 2001; Liu et al., 2004b; Lopez-Aviles et al., 2005; Mills et al., 1999; Motamedi et al., 2004; Noma et al., 2004; Nonaka et al., 2002; Pal-Bhadra et al., 2004; Shiozaki and Russell, 1996; Song et al., 2001; Takeda et al., 2004; Volpe et al., 2002; Wang et al., 2005). I propose that the role of Ago1 and Dcr1 are both independent and dependent on the RNAi pathway. Our model (Figure 5-2) suggests that following genotoxin induced S- or M-phase arrest a pool of Dcr1 translocates to the nucleus in order to generate siRNAs that target heterochromatic effector molecules such as Swi6 or HP1 to specified genomic sequences. These molecules in association with DNA damaging sensors and/or repair proteins accumulate in an RNAi-dependent manner to sites of damage. Although we do not know how this occurs it seems likely that nucleation of these areas of damage is required for stability of repair complexes. Indeed, BRCA1 and its fission yeast homologue Cut5 are localized to nucleated chromatin following DNA damage (Harris et al., 2003; Parrilla-Castellar and Karnitz, 2003; Saka et al., 1994; Schlegel et al., 2003). This association is integral as it facilitates the recruitment of DNA damage response proteins and ultimately affects the activation of Chk1 for prolonged Cdc2 phosphorylation and inactivation (Parrilla-Castellar and Karnitz, 2003).

In addition to the RNAi response, our data suggest that Ago1 and Dcr1 are required for regulated phosphorylation of Cdc2. It is likely that this effect is mediated by the interaction of Ago1 with cytoplasmic effectors of Cdc2. This is suspected, as genotoxic insult did not cause Ago1 to redistribute to the nucleus. Thus, I suspect that Ago1 is present in limiting quantities in the nucleus whereas the bulk of Ago1 is

Figure 5-2 siRNA-dependent and independent processes are mediated by the localizations of the core RNAi proteins. Briefly, Dcr1 and Ago1 reside in P-bodies for RISC-dependent mRNA degradation. The dependence of siRNAs on Ago1 localization to P-bodies is currently a matter of controversy. RDRC is present in the cytoplasm to amplify dsRNAs. RDRC-amplified dsRNAs are transported to the P-body by an unidentified dsRNA binding protein. During normal cell cycle events, Ago1 and Rdp1 also reside in the nucleus. Dcr1 translocation to the nucleus is mediated by a post-translational modification depending on the requirement for chromatin nucleation. Nuclear Dcr1 cleaves siRNAs amplified by RDRC from centromeric repeats. The dsRNA is either produced as a hairpin formed from repeats within the nascent transcript or as a duplex of mRNA and RDRC-amplified nascent transcripts. Ago1-loaded with siRNAs binds Chp1 and Tas3 to form a functional RITS complex and targets homologous centromeric sequences. The amplification of the nascent strand requires clamping of the RDRC transcript to the mRNA through recruitment of cohesins to the methylated chromatin in a RITS-dependent manner. The Swi6/cohesin complex acts to stabilize RITS to the nascent strand. Thus, RDRC and RITS are cooperative in both the amplification and targeting steps. DNA damage or incomplete replication of DNA results in modification and release of Dcr1 from Ago1. Free Ago1 binds checkpoint induced cell cycle regulatory factor(s) for regulated phosphorylation of Cdc2 Y15 whereas Dcr1 translocates to the nucleus and participates in methylation and nucleation of heterochromatin resulting in binding of DNA damage response proteins.

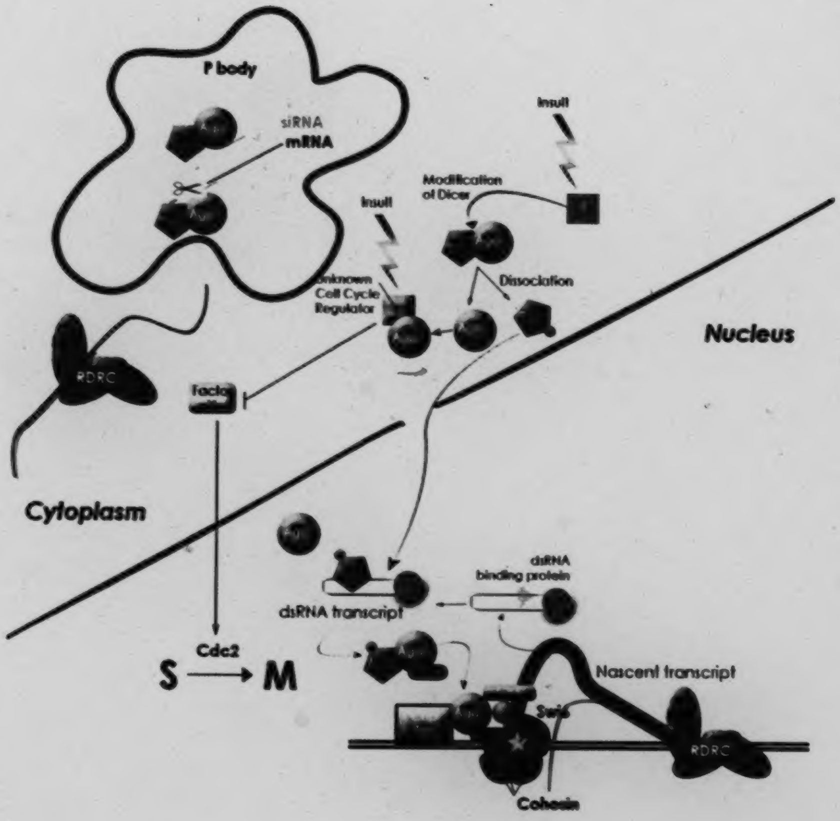
P body
siRNA
mRNA
Insult
Modification of Dicer
Insult
Unknown Cell Cycle Regulator
Dissociation
Nucleus
RDRC
Facto
Cytoplasm
dsRNA binding protein
dsRNA transcript
Cdc2
S
M
Nascent transcript
Swi6
RDRC
Cohesin

required for cytoplasmic actions such as cell cycle regulation and to a lesser extent mRNA degradation. It is possible that following insult a factor binds Ago1 causing it to release Dcr1 when DNA damage is sensed. Alternatively, post-translational modification of Dcr1 by a cell cycle regulated factor may result in the release of Ago1 and the transport of Dcr1 to the nucleus. The association of the free Ago1 with a cytoplasmic cell cycle regulator(s) results in Cdc2 phosphorylation and cell cycle arrest. Dcr1 in this scenario does not actively participate in the regulation of Cdc2 but is required for the targeting of factors to sites of DNA damage in a siRNA-dependent manner.

5-5 Concluding remarks and future directions

This work begins to address alternative roles for core RNAi proteins in siRNA-independent pathways. Although this body of work provides a basis for this assertion, it is necessary to clearly show that Ago1 and Dcr1 regulated phosphorylation of Cdc2 Y15 is indeed independent of RNAi. Thus, it will be necessary to generate mutant Dcr1 and Ago1 unable to produce siRNAs and bind siRNAs, respectively, but capable of participating in cell cycle regulation. This will enhance the argument for the divergence of these proteins from the RNAi-related pathways. Further, the identification of potential cell cycle regulatory factors that interact with Ago1 and/or Dcr1 RNAi-defective mutants will aid in providing a mechanism of action for these proteins absent of RNAi. Finally. It will be important to generate Dcr1 mutants that are not capable of localizing to the nucleus to further define the dynamic localization response this protein appears to have during genotoxic insult.

REFERENCES

Abbott, D. W., Thompson, M. E., Robinson-Benion, C., Tomlinson, G., Jensen, R. A., and Holt, J. T. (1999). BRCA1 expression restores radiation resistance in BRCA1-defective cancer cells through enhancement of transcription-coupled DNA repair. J Biol Chem *274*, 18808-18812.

al-Khodairy, F., and Carr, A. M. (1992). DNA repair mutants defining G2 checkpoint pathways in *Schizosaccharomyces pombe*. Embo J *11*, 1343-1350.

Alfa, C., Fantes, P., Hyams, J., McLeod, M., and Warbrick, E. (1993). Experiments with fission yeast: A laboratory course manual (Plainview, Cold Spring Harbor Laboratory Press).

Baber-Furnari, B. A., Rhind, N., Boddy, M. N., Shanahan, P., Lopez-Girona, A., and Russell, P. (2000). Regulation of mitotic inhibitor Mik1 helps to enforce the DNA damage checkpoint. Mol Biol Cell *11*, 1-11.

Bailis, J. M., Bernard, P., Antonelli, R., Allshire, R. C., and Forsburg, S. L. (2003). Hsk1-Dfp1 is required for heterochromatin-mediated cohesion at centromeres. Nat Cell Biol *5*, 1111-1116.

Bailis, J. M., and Forsburg, S. L. (2004). S phase assembly of centromeric heterochromatin and cohesion. Cell Cycle *3*, 416-418.

Balasubramanian, M. K., McCollum, D., and Surana, U. (2000). Tying the knot: linking cytokinesis to the nuclear cycle. J Cell Sci *113 (Pt 9)*, 1503-1513.

Barnes, E. A., Kong, M., Ollendorff, V., and Donoghue, D. J. (2001). Patched1 interacts with cyclin B1 to regulate cell cycle progression. Embo J *20*, 2214-2223.

Bashkirov, V. I., Scherthan, H., Solinger, J. A., Buerstedde, J. M., and Heyer, W. D. (1997). A mouse cytoplasmic exoribonuclease (mXRN1p) with preference for G4 tetraplex substrates. J Cell Biol *136*, 761-773.

Beltraminelli, N., Murone, M., and Simanis, V. (1999). The *S. pombe* zfs1 gene is required to prevent septation if mitotic progression is inhibited. J Cell Sci *112 Pt 18*, 3103-3114.

Bentley, N. J., Holtzman, D. A., Flaggs, G., Keegan, K. S., DeMaggio, A., Ford, J. C., Hoekstra, M., and Carr, A. M. (1996). *The Schizosaccharomyces pombe* rad3 checkpoint gene. Embo J *15*, 6641-6651.

Bernard, P., Maure, J. F., Partridge, J. F., Genier, S., Javerzat, J. P., and Allshire, R. C. (2001). Requirement of heterochromatin for cohesion at centromeres. Science *294*, 2539-2542.

Bernstein, E., Caudy, A. A., Hammond, S. M., and Hannon, G. J. (2001). Role for a bidentate ribonuclease in the initiation step of RNA interference. Nature *409*, 363-366.

Bernstein, E., Kim, S. Y., Carmell, M. A., Murchison, E. P., Alcorn, H., Li, M. Z., Mills, A. A., Elledge, S. J., Anderson, K. V., and Hannon, G. J. (2003). Dicer is essential for mouse development. Nat Genet *35*, 215-217.

Billy, E., Brondani, V., Zhang, H., Muller, U., and Filipowicz, W. (2001). Specific interference with gene expression induced by long, double-stranded RNA in mouse embryonal teratocarcinoma cell lines. Proc Natl Acad Sci U S A *98*, 14428-14433.

Bohmert, K., Camus, I., Bellini, C., Bouchez, D., Caboche, M., and Benning, C. (1998). *AGO1* defines a novel locus of *Arabidopsis* controlling leaf development. EMBO J *17*, 170-180.

Bohnsack, M. T., Czaplinski, K., and Gorlich, D. (2004). Exportin 5 is a RanGTP-dependent dsRNA-binding protein that mediates nuclear export of pre-miRNAs. Rna *10*, 185-191.

Borgne, A., and Meijer, L. (1996). Sequential dephosphorylation of p34(cdc2) on Thr-14 and Tyr-15 at the prophase/metaphase transition. J Biol Chem *271*, 27847-27854.

Boutet, S., Vazquez, F., Liu, J., Beclin, C., Fagard, M., Gratias, A., Morel, J. B., Crete, P., Chen, X., and Vaucheret, H. (2003). Arabidopsis HEN1: a genetic link between endogenous miRNA controlling development and siRNA controlling transgene silencing and virus resistance. Curr Biol *13*, 843-848.

Breeding, C. S., Hudson, J., Balasubramanian, M. K., Hemmingsen, S. M., Young, P. G., and Gould, K. L. (1998). The cdr2(+) gene encodes a regulator of G2/M progression and cytokinesis in *Schizosaccharomyces pombe*. Mol Biol Cell *9*, 3399-3415.

Carmichael, J. B., Provost, P., Ekwall, K., and Hobman, T. C. (2004). ago1 and dcr1, two core components of the RNA interference pathway, functionally diverge from rdp1 in regulating cell cycle events in *Schizosaccharomyces pombe*. Mol Biol Cell *15*, 1425-1435.

Catala, M., Lamontagne, B., Larose, S., Ghazal, G., and Elela, S. A. (2004). Cell cycle-dependent nuclear localization of yeast RNase III is required for efficient cell division. Mol Biol Cell *15*, 3015-3030.

Catalanotto, C., Azzalin, G., Macino, G., and Cogoni, C. (2002). Involvement of small RNAs and role of the qde genes in the gene silencing pathway in *Neurospora*. Genes Dev *16*, 790-795.

Catalanotto, C., Pallotta, M., ReFalo, P., Sachs, M. S., Vayssie, L., Macino, G., and Cogoni, C. (2004). Redundancy of the two dicer genes in transgene-induced posttranscriptional gene silencing in *Neurospora crassa*. Mol Cell Biol *24*, 2536-2545.

Caudy, A. A., Myers, M., Hannon, G. J., and Hammond, S. M. (2002). Fragile X-related protein and VIG associate with the RNA interference machinery. Genes Dev *16*, 2491-2496.

Cerutti, L., Mian, N., and Bateman, A. (2000). Domains in gene silencing and cell differentiation proteinsw: the novel PAZ domain and redefinition of the Piwi domain. Trends in Biochemical Sciences *25*, 481-482.

Chan, S. W., Zilberman, D., Xie, Z., Johansen, L. K., Carrington, J. C., and Jacobsen, S. E. (2004). RNA silencing genes control de novo DNA methylation. Science *303*, 1336.

Chang, E. C., Barr, M., Wang, Y., Jung, V., Xu, H. P., and Wigler, M. H. (1994). Cooperative interaction of *S. pombe* proteins required for mating and morphogenesis. Cell *79*, 131-141.

Chen, L., Liu, T. H., and Walworth, N. C. (1999). Association of Chk1 with 14-3-3 proteins is stimulated by DNA damage. Genes Dev *13*, 675-685.

Chicas, A., Cogoni, C., and Macino, G. (2004). RNAi-dependent and RNAi-independent mechanisms contribute to the silencing of RIPed sequences in *Neurospora crassa*. Nucleic Acids Res *32*, 4237-4243.

Chicas, A., Forrest, E. C., Sepich, S., Cogoni, C., and Macino, G. (2005). Small interfering RNAs that trigger posttranscriptional gene silencing are not required for the histone H3 Lys9 methylation necessary for transgenic tandem repeat stabilization in *Neurospora crassa*. Mol Cell Biol *25*, 3793-3801.

Chua, G., Lingner, C., Frazer, C., and Young, P. G. (2002). The sal3(+) gene encodes an importin-beta implicated in the nuclear import of Cdc25 in *Schizosaccharomyces pombe*. Genetics *162*, 689-703.

Ciosk, R., Zachariae, W., Michaelis, C., Shevchenko, A., Mann, M., and Nasmyth, K. (1998). An ESP1/PDS1 complex regulates loss of sister chromatid cohesion at the metaphase to anaphase transition in yeast. Cell *93*, 1067-1076.

Cogoni, C., and Macino, G. (1999). Gene silencing in *Neurospora crassa* requires a protein homologous to RNA-dependent RNA polymerase. Nature *399*, 166-169.

Cougot, N., Babajko, S., and Seraphin, B. (2004). Cytoplasmic foci are sites of mRNA decay in human cells. J Cell Biol *165*, 31-40.

Cox, D. N., Chao, A., Baker, J., Chang, L., Qiao, D., and Lin, H. (1998). A novel class of evolutionarily conserved genes defined by piwi are essential for stem cell self-renewal. Genes Dev *12*, 3715-3727.

Cox, D. N., Chao, A., and Lin, H. (2000). piwi encodes a nucleoplasmic factor whose activity modulates the number and division rate of germline stem cells. Development *127*, 503-514.

Crandall, M., Egel, R., and Mackay, V. L. (1977). Physiology of mating in three yeasts. Adv Microb Physiol *15*, 307-398.

Dalmay, T., Hamilton, A., Rudd, S., Angell, S., and Baulcombe, D. C. (2000). An RNA-dependent RNA polymerase gene in Arabidopsis is required for posttranscriptional gene silencing mediated by a transgene but not by a virus. Cell *101*, 543-553.

Degols, G., and Russell, P. (1997). Discrete roles of the Spc1 kinase and the Atf1 transcription factor in the UV response of *Schizosaccharomyces pombe*. Mol Cell Biol *17*, 3356-3363.

Degols, G., Shiozaki, K., and Russell, P. (1996). Activation and regulation of the Spc1 stress-activated protein kinase in *Schizosaccharomyces pombe*. Mol Cell Biol *16*, 2870-2877.

Denli, A. M., Tops, B. B., Plasterk, R. H., Ketting, R. F., and Hannon, G. J. (2004). Processing of primary microRNAs by the Microprocessor complex. Nature *432*, 231-235.

Doench, J. G., Petersen, C. P., and Sharp, P. A. (2003). siRNAs can function as miRNAs. Genes Dev *17*, 438-442.

Doi, N., Zenno, S., Ueda, R., Ohki-Hamazaki, H., UiTei, K., and Saigo, K. (2003). Short-Interfering-RNA-Mediated Gene Silencing in Mammalian Cells Requires Dicer and eIF2C Translation Initiation Factors. Curr Biol *13*, 41-46.

Ducommun, B., Draetta, G., Young, P., and Beach, D. (1990). Fission yeast cdc25 is a cell-cycle regulated protein. Biochem Biophys Res Commun *167*, 301-309.

Dunaway, S., Liu, H. Y., and Walworth, N. C. (2005). Interaction of 14-3-3 protein with Chk1 affects localization and checkpoint function. J Cell Sci *118*, 39-50.

Egel, R., and Egel-Mitani, M. (1974). Premeiotic DNA synthesis in fission yeast. Exp Cell Res *88*, 127-134.

Ekwall, K. (2004). The RITS complex-A direct link between small RNA and heterochromatin. Mol Cell *13*, 304-305.

Enoch, T., Carr, A. M., and Nurse, P. (1992). Fission yeast genes involved in coupling mitosis to completion of DNA replication. Genes Dev *6*, 2035-2046.

Enoch, T., and Nurse, P. (1990). Mutation of fission yeast cell cycle control genes abolishes dependence of mitosis on DNA replication. Cell *60*, 665-673.

Fagard, M., Boutet, S., Morel, J. B., Bellini, C., and Vaucheret, H. (2000). AGO1, QDE-2, and RDE-1 are related proteins required for post- transcriptional gene silencing in plants, quelling in fungi, and RNA interference in animals [In Process Citation]. Proc Natl Acad Sci U S A *97*, 11650-11654.

Fankhauser, C., Marks, J., Reymond, A., and Simanis, V. (1993). The *S. pombe* cdc16 gene is required both for maintenance of p34cdc2 kinase activity and regulation of septum formation: a link between mitosis and cytokinesis? Embo J *12*, 2697-2704.

Fankhauser, C., and Simanis, V. (1993). The *Schizosaccharomyces pombe* cdc14 gene is required for septum formation and can also inhibit nuclear division. Mol Biol Cell *4*, 531-539.

Filippov, V., Solovyev, V., Filippova, M., and Gill, S. S. (2000). A novel type of RNase III family proteins in eukaryotes. Gene *245*, 213-221.

Findley, S. D., Tamanaha, M., Clegg, N. J., and Ruohola-Baker, H. (2003). Maelstrom, a *Drosophila* spindle-class gene, encodes a protein that colocalizes with Vasa and RDE1/AGO1 homolog, Aubergine, in nuage. Development *130*, 859-871.

Fire, A., Xu, S., Montgomery, M. K., Kostas, S. A., Driver, S. E., and Mello, C. C. (1998). Potent and specific genetic interference by double-stranded RNA in *Caenorhabditis elegans*. Nature *391*, 806-811.

Fisher, D. L., and Nurse, P. (1996). A single fission yeast mitotic cyclin B p34cdc2 kinase promotes both S- phase and mitosis in the absence of G1 cyclins. Embo J *15*, 850-860.

Ford, J. C., al-Khodairy, F., Fotou, E., Sheldrick, K. S., Griffiths, D. J., and Carr, A. M. (1994). 14-3-3 protein homologs required for the DNA damage checkpoint in fission yeast. Science *265*, 533-535.

Forstemann, K., Tomari, Y., Du, T., Vagin, V. V., Denli, A. M., Bratu, D. P., Klattenhoff, C., Theurkauf, W. E., and Zamore, P. D. (2005). Normal microRNA Maturation and Germ-Line Stem Cell Maintenance Requires Loquacious, a Double-Stranded RNA-Binding Domain Protein. PLoS Biol *3*, e236.

Fortin, K. R., Nicholson, R. H., and Nicholson, A. W. (2002). Mouse ribonuclease III. cDNA structure, expression analysis, and chromosomal location. BMC Genomics *3*, 26.

Fox, M. E., and Smith, G. R. (1998). Control of meiotic recombination in *Schizosaccharomyces pombe*. Prog Nucleic Acid Res Mol Biol *61*, 345-378.

Francesconi, S., Smeets, M., Grenon, M., Tillit, J., Blaisonneau, J., and Baldacci, G. (2002). Fission yeast *chk1* mutants show distinct responses to different types of DNA damaging treatments. Genes Cells *7*, 663-673.

Fujita, H., Ohshima, T., Oishi, T., Aratani, S., Fujii, R., Fukamizu, A., and Nakajima, T. (2005). Relevance of nuclear localization and functions of RNA helicase A. Int J Mol Med *15*, 555-560.

Fukagawa, T., Nogami, M., Yoshikawa, M., Ikeno, M., Okazaki, T., Takami, Y., Nakayama, T., and Oshimura, M. (2004). Dicer is essential for formation of the heterochromatin structure in vertebrate cells. Nat Cell Biol *6*, 784-791.

Furnari, B., Rhind, N., and Russell, P. (1997). Cdc25 mitotic inducer targeted by chk1 DNA damage checkpoint kinase. Science *277*, 1495-1497.

Gaits, F., Degols, G., Shiozaki, K., and Russell, P. (1998). Phosphorylation and association with the transcription factor Atf1 regulate localization of Spc1/Sty1 stress-activated kinase in fission yeast. Genes Dev *12*, 1464-1473.

Garcia-Salcedo, J. A., Gijon, P., Nolan, D. P., Tebabi, P., and Pays, E. (2003). A chromosomal SIR2 homologue with both histone NAD-dependent ADP-ribosyltransferase and deacetylase activities is involved in DNA repair in *Trypanosoma brucei*. Embo J *22*, 5851-5862.

Gould, K. L., and Nurse, P. (1989). Tyrosine phosphorylation of the fission yeast cdc2+ protein kinase regulates entry into mitosis. Nature *342*, 39-45.

Grewal, S. I., and Elgin, S. C. (2002). Heterochromatin: new possibilities for the inheritance of structure. Curr Opin Genet Dev *12*, 178-187.

Griffith, J. D., Lindsey-Boltz, L. A., and Sancar, A. (2002). Structures of the human Rad17-replication factor C and checkpoint Rad 9-1-1 complexes visualized by glycerol spray/low voltage microscopy. J Biol Chem *277*, 15233-15236.

Grishok, A., Pasquinelli, A. E., Conte, D., Li, N., Parrish, S., Ha, I., Baillie, D. L., Fire, A., Ruvkun, G., and Mello, C. C. (2001). Genes and mechanisms related to RNA interference regulate expression of the small temporal RNAs that control *C. elegans* developmental timing. Cell *106*, 23-34.

Grishok, A., Tabara, H., and Mello, C. C. (2000). Genetic requirements for inheritance of RNAi in C. elegans. Science *287*, 2494-2497.

Guacci, V., Koshland, D., and Strunnikov, A. (1997). A direct link between sister chromatid cohesion and chromosome condensation revealed through the analysis of MCD1 in *S. cerevisiae*. Cell *91*, 47-57.

Guertin, D. A., Chang, L., Irshad, F., Gould, K. L., and McCollum, D. (2000). The role of the sid1p kinase and cdc14p in regulating the onset of cytokinesis in fission yeast. Embo J *19*, 1803-1815.

Gupta, S., Campbell, D., Derijard, B., and Davis, R. J. (1995). Transcription factor ATF2 regulation by the JNK signal transduction pathway. Science *267*, 389-393.

Hall, I., Noma, K., and Grewal, S. I. (2003). RNA interference machinery regulates chromosome dynamics during mitosis and meiosis in fission yeast. Proc Natl Acad Sci U S A *100*, 193-198.

Hall, I. M., Shankaranarayana, G. D., Noma, K., Ayoub, N., Cohen, A., and Grewal, S. I. (2002). Establishment and maintenance of a heterochromatin domain. Science *297*, 2232-2237.

Hamilton, A., Voinnet, O., Chappell, L., and Baulcombe, D. (2002). Two classes of short interfering RNA in RNA silencing. Embo J *21*, 4671-4679.

Hamilton, A. J., and Baulcombe, D. C. (1999). A species of small antisense RNA in posttranscriptional gene silencing in plants. Science *286*, 950-952.

Hammond, S. M., Bernstein, E., Beach, D., and Hannon, G. J. (2000). An RNA-directed nuclease mediates post-transcriptional gene silencing in Drosophila cells. Nature *404*, 293-296.

Hammond, S. M., Boettcher, S., Caudy, A. A., Kobayashi, R., and Hannon, G. J. (2001). Argonaute2, a link between genetic and biochemical analyses of RNAi. Science *293*, 1146-1150.

Han, J., Lee, Y., Yeom, K. H., Kim, Y. K., Jin, H., and Kim, V. N. (2004). The Drosha-DGCR8 complex in primary microRNA processing. Genes Dev *18*, 3016-3027.

Hannon, G. J. (2002). RNA interference. Nature *418*, 244-251.

Hansen, K. R., Burns, G., Mata, J., Volpe, T. A., Martienssen, R. A., Bahler, J., and Thon, G. (2005). Global effects on gene expression in fission yeast by silencing and RNA interference machineries. Mol Cell Biol *25*, 590-601

Harris, S., Kemplen, C., Caspari, T., Chan, C., Lindsay, H. D., Poitelea, M., Carr, A. M., and Price, C. (2003). Delineating the position of rad4+/cut5+ within the DNA-structure checkpoint pathways in *Schizosaccharomyces pombe*. J Cell Sci *116*, 3519-3529.

Hatfield, S. D., Shcherbata, H. R., Fischer, K. A., Nakahara, K., Carthew, R. W., and Ruohola-Baker, H. (2005). Stem cell division is regulated by the microRNA pathway. Nature.

He, X., Patterson, T. E., and Sazer, S. (1997). The *Schizosaccharomyces pombe* spindle checkpoint protein mad2p blocks anaphase and genetically interacts with the anaphase-promoting complex. Proc Natl Acad Sci U S A *94*, 7965-7970.

Houvras, Y., Benezra, M., Zhang, H., Manfredi, J. J., Weber, B. L., and Licht, J. D. (2000). BRCA1 physically and functionally interacts with ATF1. J Biol Chem *275*, 36230-36237.

Hutvagner, G., McLachlan, J., Pasquinelli, A. E., Balint, E., Tuschl, T., and Zamore, P. D. (2001). A cellular function for the RNA-interference enzyme Dicer in the maturation of the let-7 small temporal RNA. Science *293*, 834-838.

Hutvagner, G., and Zamore, P. D. (2002). A microRNA in a multiple-turnover RNAi enzyme complex. Science *297*, 2056-2060.

Ishizuka, A., Siomi, M. C., and Siomi, H. (2002). A *Drosophila* fragile X protein interacts with components of RNAi and ribosomal proteins. Genes Dev *16*, 2497-2508.

Janetopoulos, C., Cole, E., Smothers, J. F., Allis, C. D., and Aufderheide, K. J. (1999). The conjusome: a novel structure in *Tetrahymena* found only during sexual reorganization. J Cell Sci *112 (Pt 7)*, 1003-1011.

Jia, S., Noma, K., and Grewal, S. I. (2004). RNAi-independent heterochromatin nucleation by the stress-activated ATF/CREB family proteins. Science *304*, 1971-1976.

Jimenez, G., Yucel, J., Rowley, R., and Subramani, S. (1992). The rad3+ gene of *Schizosaccharomyces pombe* is involved in multiple checkpoint functions and in DNA repair. Proc Natl Acad Sci U S A *89*, 4952-4956.

Kanoh, J., Watanabe, Y., Ohsugi, M., Iino, Y., and Yamamoto, M. (1996). *Schizosaccharomyces pombe* gad7+ encodes a phosphoprotein with a bZIP domain, which is required for proper G1 arrest and gene expression under nitrogen starvation. Genes Cells *1*, 391-408.

Kanter-Smoler, G., Knudsen, K. E., Jimenez, G., Sunnerhagen, P., and Subramani, S. (1995). Separation of phenotypes in mutant alleles of the *Schizosaccharomyces pombe* cell-cycle checkpoint gene rad1+. Mol Biol Cell *6*, 1793-1805.

Kataoka, Y., Takeichi, M., and Uemura, T. (2001). Developmental roles and molecular characterization of a Drosophila homologue of *Arabidopsis* Argonaute1, the founder of a novel gene superfamily. Genes Cells *6*, 313-325.

Kato, T., Jr., Okazaki, K., Murakami, H., Stettler, S., Fantes, P. A., and Okayama, H. (1996). Stress signal, mediated by a Hog1-like MAP kinase, controls sexual development in fission yeast. FEBS Lett *378*, 207-212.

Kay, B. K., Williamson, M. P., and Sudol, M. (2000). The importance of being proline: the interaction of proline-rich motifs in signaling proteins with their cognate domains. Faseb J *14*, 231-241.

Ketting, R. F., Fischer, S. E., Bernstein, E., Sijen, T., Hannon, G. J., and Plasterk, R. H. (2001). Dicer functions in RNA interference and in synthesis of small RNA involved in developmental timing in *C. elegans*. Genes Dev *15*, 2654-2659.

Kim, M., Lee, W., Park, J., Kim, J. B., Jang, Y. K., Seong, R. H., Choe, S. Y., and Park, S. D. (2000). The stress-activated MAP kinase Sty1/Spc1 and a 3'-regulatory element mediate UV-induced expression of the uvi15(+) gene at the post-transcriptional level. Nucleic Acids Res *28*, 3392-3402.

King, F. J., Szakmary, A., Cox, D. N., and Lin, H. (2001). Yb modulates the divisions of both germline and somatic stem cells through piwi- and hh-mediated mechanisms in the *Drosophila* ovary. Mol Cell *7*, 497-508.

Knight, S. W., and Bass, B. L. (2001). A role for the RNase III enzyme DCR-1 in RNA interference and germ line development in *Caenorhabditis elegans*. Science *293*, 2269-2271.

Kumagai, A., and Dunphy, W. G. (1999). Binding of 14-3-3 proteins and nuclear export control the intracellular localization of the mitotic inducer Cdc25. Genes Dev *13*, 1067-1072.

Kumagai, A., Guo, Z., Emami, K. H., Wang, S. X., and Dunphy, W. G. (1998). The *Xenopus* Chk1 protein kinase mediates a caffeine-sensitive pathway of checkpoint control in cell-free extracts. J Cell Biol *142*, 1559-1569.

Kuramochi-Miyagawa, S., Kimura, T., Yomogida, K., Kuroiwa, A., Tadokoro, Y., Fujita, Y., Sato, M., Matsuda, Y., and Nakano, T. (2001). Two mouse piwi-related genes: miwi and mili. Mech Dev *108*, 121-133.

Kyriakis, J. M., Banerjee, P., Nikolakaki, E., Dai, T., Rubie, E. A., Ahmad, M. F., Avruch, J., and Woodgett, J. R. (1994). The stress-activated protein kinase subfamily of c-Jun kinases. Nature *369*, 156-160.

Lagos-Quintana, M., Rauhut, R., Lendeckel, W., and Tuschl, T. (2001). Identification of novel genes coding for small expressed RNAs. Science *294*, 853-858.

Lamontagne, B., Larose, S., Boulanger, J., and Elela, S. A. (2001). The RNase III family: a conserved structure and expanding functions in eukaryotic dsRNA metabolism. Curr Issues Mol Biol *3*, 71-78.

Lau, N. C., Lim, L. P., Weinstein, E. G., and Bartel, D. P. (2001). An abundant class of tiny RNAs with probable regulatory roles in *Caenorhabditis elegans*. Science *294*, 858-862.

Le Goff, X., Utzig, S., and Simanis, V. (1999). Controlling septation in fission yeast: finding the middle, and timing it right. Curr Genet *35*, 571-584.

Lee, J. Y., and Orr-Weaver, T. L. (2001). The molecular basis of sister-chromatid cohesion. Annu Rev Cell Dev Biol *17*, 753-777.

Lee, M. S., Enoch, T., and Piwnica-Worms, H. (1994). mik1+ encodes a tyrosine kinase that phosphorylates p34cdc2 on tyrosine 15. J Biol Chem *269*, 30530-30537.

Lee, R. C., and Ambros, V. (2001). An extensive class of small RNAs in *Caenorhabditis elegans*. Science *294*, 862-864.

Lee, S. E., Moore, J. K., Holmes, A., Umezu, K., Kolodner, R. D., and Haber, J. E. (1998). *Saccharomyces* Ku70, mre11/rad50 and RPA proteins regulate adaptation to G2/M arrest after DNA damage. Cell *94*, 399-409.

Lee, S. E., Paques, F., Sylvan, J., and Haber, J. E. (1999). Role of yeast SIR genes and mating type in directing DNA double-strand breaks to homologous and non-homologous repair paths. Curr Biol *9*, 767-770.

Lee, Y., Ahn, C., Han, J., Choi, H., Kim, J., Yim, J., Lee, J., Provost, P., Radmark, O., Kim, S., and Kim, V. N. (2003). The nuclear RNase III Drosha initiates microRNA processing. Nature *425*, 415-419.

Lee, Y. S., Nakahara, K., Pham, J. W., Kim, K., He, Z., Sontheimer, E. J., and Carthew, R. W. (2004). Distinct roles for *Drosophila* Dicer-1 and Dicer-2 in the siRNA/miRNA silencing pathways. Cell *117*, 69-81.

Liu, J., Carmell, M. A., Rivas, F. V., Marsden, C. G., Thomson, J. M., Song, J. J., Hammond, S. M., Joshua-Tor, L., and Hannon, G. J. (2004a). Argonaute2 Is the Catalytic Engine of Mammalian RNAi. Science.

Liu, J., Valencia-Sanchez, M. A., Hannon, G. J., and Parker, R. (2005). MicroRNA-dependent localization of targeted mRNAs to mammalian P-bodies. Nat Cell Biol.

Liu, Q., Rand, T. A., Kalidas, S., Du, F., Kim, H. E., Smith, D. P., and Wang, X. (2003). R2D2, a bridge between the initiation and effector steps of the *Drosophila* RNAi pathway. Science *301*, 1921-1925.

Liu, Y., Mochizuki, K., and Gorovsky, M. A. (2004b). Histone H3 lysine 9 methylation is required for DNA elimination in developing macronuclei in *Tetrahymena*. Proc Natl Acad Sci U S A *101*, 1679-1684.

Lopez-Aviles, S., Grande, M., Gonzalez, M., Helgesen, A. L., Alemany, V., Sanchez-Piris, M., Bachs, O., Millar, J. B., and Aligue, R. (2005). Inactivation of the Cdc25 phosphatase by the stress-activated Srk1 kinase in fission yeast. Mol Cell *17*, 49-59.

Lopez-Girona, A., Furnari, B., Mondesert, O., and Russell, P. (1999). Nuclear localization of Cdc25 is regulated by DNA damage and a 14-3-3 protein. Nature *397*, 172-175.

Lopez-Girona, A., Kanoh, J., and Russell, P. (2001a). Nuclear exclusion of Cdc25 is not required for the DNA damage checkpoint in fission yeast. Curr Biol *11*, 50-54.

Lopez-Girona, A., Tanaka, K., Chen, X. B., Baber, B. A., McGowan, C. H., and Russell, P. (2001b). Serine-345 is required for Rad3-dependent phosphorylation and function of checkpoint kinase Chk1 in fission yeast. Proc Natl Acad Sci U S A *98*, 11289-11294.

Lundgren, K., Walworth, N., Booher, R., Dembski, M., Kirschner, M., and Beach, D. (1991). mik1 and wee1 cooperate in the inhibitory tyrosine phosphorylation of cdc2. Cell *64*, 1111-1122.

Lynn, K., Fernandez, A., Aida, M., Sedbrook, J., Tasaka, M., Masson, P., and Barton, M. K. (1999). The PINHEAD/ZWILLE gene acts pleiotropically in *Arabidopsis* development and has overlapping functions with the ARGONAUTE1 gene. Development *126*, 469-481.

Ma, J. B., Ye, K., and Patel, D. J. (2004). Structural basis for overhang-specific small interfering RNA recognition by the PAZ domain. Nature *429*, 318-322.

Majka, J., and Burgers, P. M. (2003). Yeast Rad17/Mec3/Ddc1: a sliding clamp for the DNA damage checkpoint. Proc Natl Acad Sci U S A *100*, 2249-2254.

Makeyev, E. V., and Bamford, D. H. (2002). Cellular RNA-dependent RNA polymerase involved in posttranscriptional gene silencing has two distinct activity modes. Mol Cell *10*, 1417-1427.

Marks, J., Fankhauser, C., and Simanis, V. (1992). Genetic interactions in the control of septation in *Schizosaccharomyces pombe*. J Cell Sci *101 (Pt 4)*, 801-808.

Martin, S. G., Laroche, T., Suka, N., Grunstein, M., and Gasser, S. M. (1999). Relocalization of telomeric Ku and SIR proteins in response to DNA strand breaks in yeast. Cell *97*, 621-633.

Martin-Castellanos, C., Labib, K., and Moreno, S. (1996). B-type cyclins regulate G1 progression in fission yeast in opposition to the p25rum1 cdk inhibitor. Embo J *15*, 839-849.

Martinez, J., Patkaniowska, A., Urlaub, H., Luhrmann, R., and Tuschl, T. (2002). Single-stranded antisense siRNAs guide target RNA cleavage in RNAi. Cell *110*, 563-574.

McCollum, D., and Gould, K. L. (2001). Timing is everything: regulation of mitotic exit and cytokinesis by the MEN and SIN. Trends Cell Biol *11*, 89-95.

Meister, G., Landthaler, M., Dorsett, Y., and Tuschl, T. (2004a). Sequence-specific inhibition of microRNA- and siRNA-induced RNA silencing. Rna *10*, 544-550.

Meister, G., Landthaler, M., Patkaniowska, A., Dorsett, Y., Teng, G., and Tuschl, T. (2004b). Human Argonaute2 mediates RNA cleavage targeted by miRNAs and siRNAs. Mol Cell *15*, 185-197.

Michaelis, C., Ciosk, R., and Nasmyth, K. (1997). Cohesins: chromosomal proteins that prevent premature separation of sister chromatids. Cell *91*, 35-45.

Millar, J. B., Buck, V., and Wilkinson, M. G. (1995). Pyp1 and Pyp2 PTPases dephosphorylate an osmosensing MAP kinase controlling cell size at division in fission yeast. Genes Dev *9*, 2117-2130.

Millar, J. B., McGowan, C. H., Lenaers, G., Jones, R., and Russell, P. (1991). p80cdc25 mitotic inducer is the tyrosine phosphatase that activates p34cdc2 kinase in fission yeast. Embo J *10*, 4301-4309.

Mills, K. D., Sinclair, D. A., and Guarente, L. (1999). MEC1-dependent redistribution of the Sir3 silencing protein from telomeres to DNA double-strand breaks. Cell *97*, 609-620.

Mochizuki, K., Fine, N. A., Fujisawa, T., and Gorovsky, M. A. (2002). Analysis of a piwi-related gene implicates small RNAs in genome rearrangement in *tetrahymena*. Cell *110*, 689-699.

Mochizuki, K., and Gorovsky, M. A. (2004a). Conjugation-specific small RNAs in *Tetrahymena* have predicted properties of scan (scn) RNAs involved in genome rearrangement. Genes Dev *18*, 2068-2073.

Mochizuki, K., and Gorovsky, M. A. (2004b). Small RNAs in genome rearrangement in *Tetrahymena*. Curr Opin Genet Dev *14*, 181-187.

Morel, J. B., Godon, C., Mourrain, P., Beclin, C., Boutet, S., Feuerbach, F., Proux, F., and Vaucheret, H. (2002). Fertile hypomorphic ARGONAUTE (ago1) mutants impaired in post- transcriptional gene silencing and virus resistance. Plant Cell *14*, 629-639.

Motamedi, M. R., Verdel, A., Colmenares, S. U., Gerber, S. A., Gygi, S. P., and Moazed, D. (2004). Two RNAi Complexes, RITS and RDRC, Physically Interact and Localize to Noncoding Centromeric RNAs. Cell *119*, 789-802.

Mourelatos, Z., Dostie, J., Paushkin, S., Sharma, A., Charroux, B., Abel, L., Rappsilber, J., Mann, M., and Dreyfuss, G. (2002). miRNPs: a novel class of ribonucleoproteins containing numerous microRNAs. Genes Dev *16*, 720-728.

Mourrain, P., Beclin, C., Elmayan, T., Feuerbach, F., Godon, C., Morel, J. B., Jouette, D., Lacombe, A. M., Nikic, S., Picault, N., *et al.* (2000). *Arabidopsis* SGS2 and SGS3 genes are required for posttranscriptional gene silencing andnatural virus resistance. Cell *101*, 533-542.

Moussian, B., Schoof, H., Haecker, A., Juergens, G., and Laux, T. (1998). Role of the ZWILLE gene in the regulation of central shoot meristem cell fate during *Arabidopsis* embryogenesis. EMBO J *17*, 1799-1809.

Murone, M., and Simanis, V. (1996). The fission yeast dma1 gene is a component of the spindle assembly checkpoint, required to prevent septum formation and premature exit from mitosis if spindle function is compromised. Embo J *15*, 6605-6616.

Muslin, A. J., Tanner, J. W., Allen, P. M., and Shaw, A. S. (1996). Interaction of 14-3-3 with signaling proteins is mediated by the recognition of phosphoserine. Cell *84*, 889-897.

Naito, T., Matsuura, A., and Ishikawa, F. (1998). Circular chromosome formation in a fission yeast mutant defective in two ATM homologues. Nat Genet *20*, 203-206.

Nelson, P. T., Hatzigeorgiou, A. G., and Mourelatos, Z. (2004). miRNP:mRNA association in polyribosomes in a human neuronal cell line. Rna *10*, 387-394.

Nguyen, A. N., Ikner, A. D., Shiozaki, M., Warren, S. M., and Shiozaki, K. (2002). Cytoplasmic localization of Wis1 MAPKK by nuclear export signal is important for nuclear targeting of Spc1/Sty1 MAPK in fission yeast. Mol Biol Cell *13*, 2651-2663.

Nicholson, A. W. (1999). Function, mechanism and regulation of bacterial ribonucleases. FEMS Microbiol Rev *23*, 371-390.

Nishi, K., Yoshida, M., Fujiwara, D., Nishikawa, M., Horinouchi, S., and Beppu, T. (1994). Leptomycin B targets a regulatory cascade of crm1, a fission yeast nuclear protein, involved in control of higher order chromosome structure and gene expression. J Biol Chem *269*, 6320-6324.

Nishikawa, T., Aiba, H., and Mizuno, T. (1999). The cta3+ gene that encodes a cation-transporting P-type ATPase is induced by salt stress under control of the Wis1-Sty1 MAPKK-MAPK cascade in fission yeast. FEBS Lett *455*, 183-187.

Nolan, T., Braccini, L., Azzalin, G., De Toni, A., Macino, G., and Cogoni, C. (2005). The post-transcriptional gene silencing machinery functions independently of DNA methylation to repress a LINE1-like retrotransposon in *Neurospora crassa*. Nucleic Acids Res *33*, 1564-1573.

Noma, K. I., Sugiyama, T., Cam, H., Verdel, A., Zofall, M., Jia, S., Moazed, D., and Grewal, S. I. (2004). RITS acts in cis to promote RNA interference-mediated transcriptional and post-transcriptional silencing. Nat Genet.

Nonaka, N., Kitajima, T., Yokobayashi, S., Xiao, G., Yamamoto, M., Grewal, S. I., and Watanabe, Y. (2002). Recruitment of cohesin to heterochromatic regions by Swi6/HP1 in fission yeast. Nat Cell Biol *4*, 89-93.

Nurse, P. (1990). Universal control mechanism regulating onset of M-phase. Nature *344*, 503-508.

Nurse, P., and Bissett, Y. (1981). Gene required in G1 for commitment to cell cycle and in G2 for control of mitosis in fission yeast. Nature *292*, 558-560.

Nurse, P., and Thuriaux, P. (1980). Regulatory genes controlling mitosis in the fission yeast *Schizosaccharomyces pombe*. Genetics *96*, 627-637.

Nykanen, A., Haley, B., and Zamore, P. D. (2001). ATP requirements and small interfering RNA structure in the RNA interference pathway. Cell *107*, 309-321.

O'Connell, M. J., Raleigh, J. M., Verkade, H. M., and Nurse, P. (1997). Chk1 is a wee1 kinase in the G2 DNA damage checkpoint inhibiting cdc2 by Y15 phosphorylation. Embo J *16*, 545-554.

Okamura, K., Ishizuka, A., Siomi, H., and Siomi, M. C. (2004). Distinct roles for Argonaute proteins in small RNA-directed RNA cleavage pathways. Genes Dev *18*, 1655-1666.

Okazaki, N., Okazaki, K., Watanabe, Y., Kato-Hayashi, M., Yamamoto, M., and Okayama, H. (1998). Novel factor highly conserved among eukaryotes controls sexual development in fission yeast. Mol Cell Biol *18*, 887-895.

Ouyang, H., Nussenzweig, A., Kurimasa, A., Soares, V. C., Li, X., Cordon-Cardo, C., Li, W., Cheong, N., Nussenzweig, M., Iliakis, G., *et al.* (1997). Ku70 is required for DNA repair but not for T cell antigen receptor gene recombination In vivo. J Exp Med *186*, 921-929.

Pal-Bhadra, M., Bhadra, U., and Birchler, J. A. (2002). RNAi related mechanisms affect both transcriptional and posttranscriptional transgene silencing in *Drosophila*. Mol Cell *9*, 315-327.

Pal-Bhadra, M., Leibovitch, B. A., Gandhi, S. G., Rao, M., Bhadra, U., Birchler, J. A., and Elgin, S. C. (2004). Heterochromatic silencing and HP1 localization in *Drosophila* are dependent on the RNAi machinery. Science *303*, 669-672.

Papp, I., Mette, M. F., Aufsatz, W., Daxinger, L., Schauer, S. E., Ray, A., van der Winden, J., Matzke, M., and Matzke, A. J. (2003). Evidence for nuclear processing of plant micro RNA and short interfering RNA precursors. Plant Physiol *132*, 1382-1390.

Park, W., Li, J., Song, R., Messing, J., and Chen, X. (2002). CARPEL FACTORY, a Dicer homolog, and HEN1, a novel protein, act in microRNA metabolism in *Arabidopsis thaliana*. Curr Biol *12*, 1484-1495.

Parker, J. S., Roe, S. M., and Barford, D. (2004). Crystal structure of a PIWI protein suggests mechanisms for siRNA recognition and slicer activity. Embo J *23*, 4727-4737.

Parrilla-Castellar, E. R., and Karnitz, L. M. (2003). Cut5 is required for the binding of Atr and DNA polymerase alpha to genotoxin-damaged chromatin. J Biol Chem *278*, 45507-45511.

Parrish, S., and Fire, A. (2001). Distinct roles for RDE-1 and RDE-4 during RNA interference in *Caenorhabditis elegans*. Rna *7*, 1397-1402.

Paull, T. T., Rogakou, E. P., Yamazaki, V., Kirchgessner, C. U., Gellert, M., and Bonner, W. M. (2000). A critical role for histone H2AX in recruitment of repair factors to nuclear foci after DNA damage. Curr Biol *10*, 886-895.

Peng, H., Zheng, L., Lee, W. H., Rux, J. J., and Rauscher, F. J., 3rd (2002). A common DNA-binding site for SZF1 and the BRCA1-associated zinc finger protein, ZBRK1. Cancer Res *62*, 3773-3781.

Petrie, V. J., Wuitschick, J. D., Givens, C. D., Kosinski, A. M., and Partridge, J. F. (2005). RNA interference (RNAi)-dependent and RNAi-independent association of the Chp1 chromodomain protein with distinct heterochromatic loci in fission yeast. Mol Cell Biol *25*, 2331-2346.

Pham, J. W., Pellino, J. L., Lee, Y. S., Carthew, R. W., and Sontheimer, E. J. (2004). A Dicer-2-dependent 80s complex cleaves targeted mRNAs during RNAi in Drosophila. Cell *117*, 83-94.

Pillai, R. S., Artus, C. G., and Filipowicz, W. (2004). Tethering of human Ago proteins to mRNA mimics the miRNA-mediated repression of protein synthesis. Rna *10*, 1518-1525.

Provost, P., Dishart, D., Doucet, J., Frendewey, D., Samuelsson, B., and Radmark, O. (2002a). Ribonuclease activity and RNA binding of recombinant human Dicer. EMBO J *21*, 5864-5874.

Provost, P., Samuelsson, B., and Radmark, O. (1999). Interaction of 5-lipoxygenase with cellular proteins. Proc Natl Acad Sci U S A *96*, 1881-1885.

Provost, P., Silverstein, R., Dishart, D., Walfridsson, J., Djupedal, I., Kniola, B., Wright, A., Samuelsson, B., Radmark, O., and Ekwall, K. (2002b). Dicer is required for chromosome segregation and gene silencing in fission yeast cells. Proc Natl Acad Sci U S A *(in press)*.

Raleigh, J. M., and O'Connell, M. J. (2000). The G(2) DNA damage checkpoint targets both Wee1 and Cdc25. J Cell Sci *113 (Pt 10)*, 1727-1736.

Rand, T. A., Ginalski, K., Grishin, N. V., and Wang, X. (2004). Biochemical identification of Argonaute 2 as the sole protein required for RNA-induced silencing complex activity. Proc Natl Acad Sci U S A *101*, 14385-14389.

Rauen, M., Burtelow, M. A., Dufault, V. M., and Karnitz, L. M. (2000). The human checkpoint protein hRad17 interacts with the PCNA-like proteins hRad1, hHus1, and hRad9. J Biol Chem *275*, 29767-29771.

Reinhart, B. J., and Bartel, D. P. (2002). Small RNAs correspond to centromere heterochromatic repeats. Science *297*, 1831.

Reinhart, B. J., Weinstein, E. G., Rhoades, M. W., Bartel, B., and Bartel, D. P. (2002). MicroRNAs in plants. Genes Dev *16*, 1616-1626.

Rhind, N., Furnari, B., and Russell, P. (1997). Cdc2 tyrosine phosphorylation is required for the DNA damage checkpoint in fission yeast. Genes Dev *11*, 504-511.

Rhind, N., and Russell, P. (1998a). Mitotic DNA damage and replication checkpoints in yeast. Curr Opin Cell Biol *10*, 749-758.

Rhind, N., and Russell, P. (1998b). Tyrosine phosphorylation of cdc2 is required for the replication checkpoint in *Schizosaccharomyces pombe*. Mol Cell Biol *18*, 3782-3787.

Rhoades, M. W., Reinhart, B. J., Lim, L. P., Burge, C. B., Bartel, B., and Bartel, D. P. (2002). Prediction of plant microRNA targets. Cell *110*, 513-520.

Rivas, F. V., Tolia, N. H., Song, J. J., Aragon, J. P., Liu, J., Hannon, G. J., and Joshua-Tor, L. (2005). Purified Argonaute2 and an siRNA form recombinant human RISC. Nat Struct Mol Biol *12*, 340-349.

Robb, G. B., Brown, K. M., Khurana, J., and Rana, T. M. (2005). Specific and potent RNAi in the nucleus of human cells. Nat Struct Mol Biol *12*, 133-137.

Roos-Mattjus, P., Hopkins, K. M., Oestreich, A. J., Vroman, B. T., Johnson, K. L., Naylor, S., Lieberman, H. B., and Karnitz, L. M. (2003). Phosphorylation of human Rad9 is required for genotoxin-activated checkpoint signaling. J Biol Chem *278*, 24428-24437.

Rouse, J., Cohen, P., Trigon, S., Morange, M., Alonso-Llamazares, A., Zamanillo, D., Hunt, T., and Nebreda, A. R. (1994). A novel kinase cascade triggered by stress and heat shock that stimulates MAPKAP kinase-2 and phosphorylation of the small heat shock proteins. Cell *78*, 1027-1037.

Rowley, R., Subramani, S., and Young, P. G. (1992). Checkpoint controls in *Schizosaccharomyces pombe*: rad1. Embo J *11*, 1335-1342.

Roy, S., and Ingham, P. W. (2002). Hedgehogs tryst with the cell cycle. J Cell Sci *115*, 4393-4397.

Sadaie, M., Iida, T., Urano, T., and Nakayama, J. (2004). A chromodomain protein, Chp1, is required for the establishment of heterochromatin in fission yeast. Embo J *23*, 3825-3835.

Saito, K., Ishizuka, A., Siomi, H., and Siomi, M. C. (2005). Processing of Pre-microRNAs by the Dicer-1-Loquacious Complex in *Drosophila* Cells. PLoS Biol *3*, e235.

Saka, Y., Fantes, P., Sutani, T., McInerny, C., Creanor, J., and Yanagida, M. (1994a). Fission yeast cut5 links nuclear chromatin and M phase regulator in the replication checkpoint control. Embo J *13*, 5319-5329.

Saka, Y., Fantes, P., and Yanagida, M. (1994b). Coupling of DNA replication and mitosis by fission yeast rad4/cut5. J Cell Sci Suppl *18*, 57-61.

Samejima, I., Mackie, S., Warbrick, E., Weisman, R., and Fantes, P. A. (1998). The fission yeast mitotic regulator win1+ encodes an MAP kinase kinase kinase that phosphorylates and activates Wis1 MAP kinase kinase in response to high osmolarity. Mol Biol Cell *9*, 2325-2335.

Sarot, E., Payen-Groschene, G., Bucheton, A., and Pelisson, A. (2004). Evidence for a piwi-dependent RNA silencing of the gypsy endogenous retrovirus by the *Drosophila melanogaster* flamenco gene. Genetics *166*, 1313-1321.

Schauer, S. E., Jacobsen, S. E., Meinke, D. W., and Ray, A. (2002). DICER-LIKE1: blind men and elephants in Arabidopsis development. Trends Plant Sci *7*, 487-491.

Schlegel, B. P., Starita, L. M., and Parvin, J. D. (2003). Overexpression of a protein fragment of RNA helicase A causes inhibition of endogenous BRCA1 function and defects in ploidy and cytokinesis in mammary epithelial cells. Oncogene *22*, 983-991.

Schwarz, D. S., Hutvagner, G., Du, T., Xu, Z., Aronin, N., and Zamore, P. D. (2003). Asymmetry in the assembly of the RNAi enzyme complex. Cell *115*, 199-208.

Schwarz, D. S., Hutvagner, G., Haley, B., and Zamore, P. D. (2002). Evidence that siRNAs function as guides, not primers, in the *Drosophila* and human RNAi pathways. Mol Cell *10*, 537-548.

Sen, G. L., and Blau, H. M. (2005). Argonaute 2/RISC resides in sites of mammalian mRNA decay known as cytoplasmic bodies. Nat Cell Biol *7*, 633-636.

Shankaranarayana, G. D., Motamedi, M. R., Moazed, D., and Grewal, S. I. (2003). Sir2 regulates histone H3 lysine 9 methylation and heterochromatin assembly in fission yeast. Curr Biol *13*, 1240-1246.

Sharma, A. K., Nelson, M. C., Brandt, J. E., Wessman, M., Mahmud, N., Weller, K. P., and Hoffman, R. (2001). Human CD34(+) stem cells express the hiwi gene, a human homologue of the *Drosophila* gene piwi. Blood *97*, 426-434.

Shieh, J. C., Wilkinson, M. G., Buck, V., Morgan, B. A., Makino, K., and Millar, J. B. (1997). The Mcs4 response regulator coordinately controls the stress-activated Wak1-Wis1-Sty1 MAP kinase pathway and fission yeast cell cycle. Genes Dev *11*, 1008-1022.

Shieh, J. C., Wilkinson, M. G., and Millar, J. B. (1998). The Win1 mitotic regulator is a component of the fission yeast stress- activated Sty1 MAPK pathway. Mol Biol Cell *9*, 311-322.

Shiomi, Y., Shinozaki, A., Nakada, D., Sugimoto, K., Usukura, J., Obuse, C., and Tsurimoto, T. (2002). Clamp and clamp loader structures of the human checkpoint protein complexes, Rad9-1-1 and Rad17-RFC. Genes Cells *7*, 861-868.

Shiozaki, K., and Russell, P. (1995). Cell-cycle control linked to extracellular environment by MAP kinase pathway in fission yeast. Nature *378*, 739-743.

Shiozaki, K., and Russell, P. (1996). Conjugation, meiosis, and the osmotic stress response are regulated by Spc1 kinase through Atf1 transcription factor in fission yeast. Genes Dev *10*, 2276-2288.

Sigova, A., Rhind, N., and Zamore, P. D. (2004). A single Argonaute protein mediates both transcriptional and posttranscriptional silencing in *Schizosaccharomyces pombe*. Genes Dev.

Sijen, T., Fleenor, J., Simmer, F., Thijssen, K. L., Parrish, S., Timmons, L., Plasterk, R. H., and Fire, A. (2001). On the role of RNA amplification in dsRNA-triggered gene silencing. Cell *107*, 465-476.

Smardon, A., Spoerke, J. M., Stacey, S. C., Klein, M. E., Mackin, N., and Maine, E. M. (2000). EGO-1 is related to RNA-directed RNA polymerase and functions in germ-line development and RNA interference in *C. elegans*. Curr Biol *10*, 169-178.

Smith, D. A., Toone, W. M., Chen, D., Bahler, J., Jones, N., Morgan, B. A., and Quinn, J. (2002). The Srk1 protein kinase is a target for the Sty1 stress-activated MAPK in fission yeast. J Biol Chem *277*, 33411-33421.

Smith, W. A., Schurter, B. T., Wong-Staal, F., and David, M. (2004). Arginine methylation of RNA helicase a determines its subcellular localization. J Biol Chem *279*, 22795-22798.

Song, J. J., Smith, S. K., Hannon, G. J., and Joshua-Tor, L. (2004). Crystal Structure of Argonaute and Its Implications for RISC Slicer Activity. Science.

Song, K., Jung, Y., Jung, D., and Lee, I. (2001). Human Ku70 interacts with heterochromatin protein 1alpha. J Biol Chem *276*, 8321-8327.

Stein, P., Svoboda, P., Anger, M., and Schultz, R. M. (2003). RNAi: mammalian oocytes do it without RNA-dependent RNA polymerase. Rna *9*, 187-192.

Stern, B., and Nurse, P. (1998). Cyclin B proteolysis and the cyclin-dependent kinase inhibitor rum1p are required for pheromone-induced G1 arrest in fission yeast. Mol Biol Cell *9*, 1309-1321.

Su, S. S., Tanaka, Y., Samejima, I., Tanaka, K., and Yanagida, M. (1996). A nitrogen starvation-induced dormant G0 state in fission yeast: the establishment from uncommitted G1 state and its delay for return to proliferation. J Cell Sci *109*, 1347-1357.

Sugiyama, T., Cam, H., Verdel, A., Moazed, D., and Grewal, S. I. (2005). RNA-dependent RNA polymerase is an essential component of a self-enforcing loop coupling heterochromatin assembly to siRNA production. Proc Natl Acad Sci U S A *102*, 152-157.

Tabara, H., Sarkissian, M., Kelly, W. G., Fleenor, J., Grishok, A., Timmons, L., Fire, A., and Mello, C. C. (1999). The rde-1 gene, RNA interference, and transposon silencing in *C. elegans*. Cell *99*, 123-132.

Tabara, H., Yigit, E., Siomi, H., and Mello, C. C. (2002). The dsRNA binding protein RDE-4 interacts with RDE-1, DCR-1, and a DExH-box helicase to direct RNAi in *C. elegans*. Cell *109*, 861-871.

Tabata, T., and Kornberg, T. B. (1994). Hedgehog is a signaling protein with a key role in patterning *Drosophila* imaginal discs. Cell *76*, 89-102.

Tahbaz, N., Carmichael, J. B., and Hobman, T. C. (2001). GERp95 belongs to a family of signal-transducing proteins and requires Hsp90 activity for stability and Golgi localization. J Biol Chem *276*, 43294-43299.

Tahbaz, N., Kolb, F. A., Zhang, H., Jaronczyk, K., Filipowicz, W., and Hobman, T. C. (2004). Characterization of the interactions between mammalian PAZ PIWI domain proteins and Dicer. EMBO Rep *5*, 189-194.

Takeda, S., Tadele, Z., Hofmann, I., Probst, A. V., Angelis, K. J., Kaya, H., Araki, T., Mengiste, T., Scheid, O. M., Shibahara, K., *et al.* (2004). BRU1, a novel link between responses to DNA damage and epigenetic gene silencing in *Arabidopsis*. Genes Dev *18*, 782-793.

Tanaka, K., Boddy, M. N., Chen, X. B., McGowan, C. H., and Russell, P. (2001). Threonine-11, phosphorylated by Rad3 and atm in vitro, is required for activation of fission yeast checkpoint kinase Cds1. Mol Cell Biol *21*, 3398-3404.

Tanaka, K., and Russell, P. (2004). Cds1 phosphorylation by Rad3-Rad26 kinase is mediated by forkhead-associated domain interaction with Mrc1. J Biol Chem *279*, 32079-32086.

Taricani, L., Feilotter, H. E., Weaver, C., and Young, P. G. (2001). Expression of hsp16 in response to nucleotide depletion is regulated via the spc1 MAPK pathway in *Schizosaccharomyces pombe*. Nucleic Acids Res *29*, 3030-3040.

Thon, G., Cohen, A., and Klar, A. J. (1994). Three additional linkage groups that repress transcription and meiotic recombination in the mating-type region of *Schizosaccharomyces pombe*. Genetics *138*, 29-38.

Tijsterman, M., Okihara, K. L., Thijssen, K., and Plasterk, R. H. (2002). PPW-1, a PAZ/PIWI protein required for efficient germline RNAi, is defective in a natural isolate of *C. elegans*. Curr Biol *12*, 1535-1540.

Tomari, Y., Matranga, C., Haley, B., Martinez, N., and Zamore, P. D. (2004). A protein sensor for siRNA asymmetry. Science *306*, 1377-1380.

Toueille, M., El-Andaloussi, N., Frouin, I., Freire, R., Funk, D., Shevelev, I., Friedrich-Heineken, E., Villani, G., Hottiger, M. O., and Hubscher, U. (2004). The human Rad9/Rad1/Hus1 damage sensor clamp interacts with DNA polymerase beta and increases its DNA substrate utilisation efficiency: implications for DNA repair. Nucleic Acids Res *32*, 3316-3324.

Tsukahara, K., Yamamoto, H., and Okayama, H. (1998). An RNA binding protein negatively controlling differentiation in fission yeast. Mol Cell Biol *18*, 4488-4498.

Tuschl, T., Zamore, P. D., Lehmann, R., Bartel, D. P., and Sharp, P. A. (1999). Targeted mRNA degradation by double-stranded RNA in vitro. Genes Dev *13*, 3191-3197.

Vaistij, F. E., Jones, L., and Baulcombe, D. C. (2002). Spreading of RNA targeting and DNA methylation in RNA silencing requires transcription of the target gene and a putative RNA-dependent RNA polymerase. Plant Cell *14*, 857-867.

Vaucheret, H., Vazquez, F., Crete, P., and Bartel, D. P. (2004). The action of ARGONAUTE1 in the miRNA pathway and its regulation by the miRNA pathway are crucial for plant development. Genes Dev *18*, 1187-1197.

Vazquez, F., Gasciolli, V., Crete, P., and Vaucheret, H. (2004). The nuclear dsRNA binding protein HYL1 is required for microRNA accumulation and plant development, but not posttranscriptional transgene silencing. Curr Biol *14*, 346-351.

Venclovas, C., and Thelen, M. P. (2000). Structure-based predictions of Rad1, Rad9, Hus1 and Rad17 participation in sliding clamp and clamp-loading complexes. Nucleic Acids Res *28*, 2481-2493.

Verdel, A., Jia, S., Gerber, S., Sugiyama, T., Gygi, S., Grewal, S. I., and Moazed, D. (2004). RNAi-mediated targeting of heterochromatin by the RITS complex. Science *303*, 672-676.

Volpe, T., Schramke, V., Hamilton, G. L., White, S. A., Teng, G., Martienssen, R. A., and Allshire, R. C. (2003). RNA interference is required for normal centromere function in fission yeast. Chromosome Res *11*, 137-146.

Volpe, T. A., Kidner, C., Hall, I. M., Teng, G., Grewal, S. I., and Martienssen, R. A. (2002). Regulation of heterochromatic silencing and histone H3 lysine-9 methylation by RNAi. Science *297*, 1833-1837.

Wang, J. F., Zhou, H., Chen, Y. Q., Luo, Q. J., and Qu, L. H. (2004). Identification of 20 microRNAs from Oryza sativa. Nucleic Acids Res *32*, 1688-1695.

Wang, Q., Zhang, Z., Blackwell, K., and Carmichael, G. G. (2005). Vigilins bind to promiscuously A-to-I-edited RNAs and are involved in the formation of heterochromatin. Curr Biol *15*, 384-391.

Warbrick, E., and Fantes, P. A. (1991). The wis1 protein kinase is a dosage-dependent regulator of mitosis in *Schizosaccharomyces pombe*. Embo J *10*, 4291-4299.

Weiss, R. S., Matsuoka, S., Elledge, S. J., and Leder, P. (2002). Hus1 acts upstream of chk1 in a mammalian DNA damage response pathway. Curr Biol *12*, 73-77.

Wienholds, E., Koudijs, M. J., van Eeden, F. J., Cuppen, E., and Plasterk, R. H. (2003). The microRNA-producing enzyme Dicer1 is essential for zebrafish development. Nat Genet *35*, 217-218.

Wu, H., Xu, H., Miraglia, L. J., and Crooke, S. T. (2000). Human RNase III is a 160-kDa protein involved in preribosomal RNA processing. J Biol Chem *275*, 36957-36965.

Wu, L., and Russell, P. (1997). Roles of Wee1 and Nim1 protein kinases in regulating the switch from mitotic division to sexual development in *Schizosaccharomyces pombe*. Mol Cell Biol *17*, 10-17.

Xie, Z., Johansen, L. K., Gustafson, A. M., Kasschau, K. D., Lellis, A. D., Zilberman, D., Jacobsen, S. E., and Carrington, J. C. (2004). Genetic and functional diversification of small RNA pathways in plants. PLoS Biol *2*, E104.

Xie, Z., Kasschau, K. D., and Carrington, J. C. (2003). Negative feedback regulation of Dicer-Like1 in *Arabidopsis* by microRNA-guided mRNA degradation. Curr Biol *13*, 784-789.

Yamamoto, R. R., Axton, J. M., Yamamoto, Y., Saunders, R. D., Glover, D. M., and Henderson, D. S. (2000). The Drosophila mus101 gene, which links DNA repair, replication and condensation of heterochromatin in mitosis, encodes a protein with seven BRCA1 C-terminus domains. Genetics *156*, 711-721.

Yarden, R. I., and Brody, L. C. (1999). BRCA1 interacts with components of the histone deacetylase complex. Proc Natl Acad Sci U S A *96*, 4983-4988.

Yarden, R. I., Pardo-Reoyo, S., Sgagias, M., Cowan, K. H., and Brody, L. C. (2002). BRCA1 regulates the G2/M checkpoint by activating Chk1 kinase upon DNA damage. Nat Genet *30*, 285-289.

Yi, R., Qin, Y., Macara, I. G., and Cullen, B. R. (2003). Exportin-5 mediates the nuclear export of pre-microRNAs and short hairpin RNAs. Genes Dev *17*, 3011-3016.

Zamore, P. D., Tuschl, T., Sharp, P. A., and Bartel, D. P. (2000). RNAi: double-stranded RNA directs the ATP-dependent cleavage of mRNA at 21 to 23 nucleotide intervals. Cell *101*, 25-33.

Zeng, Y., and Cullen, B. R. (2002). RNA interference in human cells is restricted to the cytoplasm. Rna *8*, 855-860.

Zeng, Y., and Piwnica-Worms, H. (1999). DNA damage and replication checkpoints in fission yeast require nuclear exclusion of the Cdc25 phosphatase via 14-3-3 binding. Mol Cell Biol *19*, 7410-7419.

Zeng, Y., Yi, R., and Cullen, B. R. (2003). MicroRNAs and small interfering RNAs can inhibit mRNA expression by similar mechanisms. Proc Natl Acad Sci U S A *100*, 9779-9784.

Zhang, H., Kolb, F., Brondani, V., Billy, E., and Filipowicz, W. (2002). Human Dicer preferentially cleaves dsRNAs at their termini without a requirement for ATP. EMBO J *21*, 5875-5885.

Zilberman, D., Cao, X., and Jacobsen, S. E. (2003). ARGONAUTE4 control of locus-specific siRNA accumulation and DNA and histone methylation. Science *299*, 716-719.

Zilberman, D., Cao, X., Johansen, L. K., Xie, Z., Carrington, J. C., and Jacobsen, S. E. (2004). Role of *Arabidopsis* ARGONAUTE4 in RNA-directed DNA methylation triggered by inverted repeats. Curr Biol *14*, 1214-1220.